The Effect of Tibiofemoral Bony Morphological Risk Factors for ACL Injury on Knee Mechanics

by

Sene Kenneti Polamalu

Applied Mathematics, Millersville University, 2016

Submitted to the Graduate Faculty of the

Swanson School of Engineering in partial fulfillment

of the requirements for the degree of

Doctor of Philosophy

University of Pittsburgh

2022

UNIVERSITY OF PITTSBURGH

SWANSON SCHOOL OF ENGINEERING

This dissertation was presented

by

Sene Kenneti Polamalu

It was defended on

June 10, 2022

and approved by

Adam Popchak, DPT PhD, Associate Professor,
Department of Physical Therapy

Steven Abramowitch, PhD Professor,
Departments of Bioengineering and Clinical and Translational Science Institute

Spandan Maiti, PhD, Associate Professor,
Departments of Bioengineering, Mechanical Engineering, and Materials Science

Volker Musahl, MD, Professor,
Departments of Orthopaedic Surgery and Bioengineering

Dissertation Director: Richard Debski, Professor,
Departments of Bioengineering and Orthopaedic Surgery

The Effect of Tibiofemoral Bony Morphological Risk Factors for ACL Injury on Knee Mechanics

Sene Polamalu, PhD

University of Pittsburgh, 2022

Anterior cruciate ligament (ACL) tears have a high rate of occurrence, debilitating symptoms, arduous recovery process, and economic impact that necessitate improved injury prevention programs and clinical treatment. Patient-specific care has improved clinical outcomes and additional individualized measures are needed. Tibiofemoral bony morphology impacts knee mechanics by influencing knee motion through bone-to-bone articulation. Therefore, determining tibiofemoral bony morphological risk factors for ACL injuries and their influence on knee mechanics would provide clinicians with parameters to individualize injury prevention and treatment. The objective of this dissertation is to provide a better understanding of tibiofemoral bony morphological risk factors for ACL injury and their effect on knee mechanics before and after injury and treatment.

Using statistical shape modeling, a smaller anterior-posterior length of the tibial plateau, a greater angle between the femoral long axis and femoral condylar axis, and a more lateral mechanical axis of the distal femur were determined to associate with ACL injuries compared to uninjured subjects. No differences were determined between the ACL injured knee and the contralateral knee of the ACL injured subject demonstrating their knees are at equal risk for injury. A computational model of the knee used this data to predict that smaller anterior posterior length of the tibial plateau and more lateral mechanical axis resulted in greater force in the ACL in response to an anterior drawer at 30° and 60° of flexion. Functional bracing was also found to provide additional rotatory stability to the knee and decreased the force in the ACL in response to

a simulated pivot shift at lower flexion angles using a cadaveric model. These findings demonstrate that functional braces can reduce ACL injury risk. Tibiofemoral bony morphological features were also correlated with knee kinematics and kinetics before and after application of a brace and lateral extraarticular tenodesis demonstrating that certain morphological features influence the impact of each treatment option. Overall, tibiofemoral bony morphological features are risk factors for ACL injury, influence knee mechanics differently after injury and treatment, and impact biomechanical behavior of the knee. Implementing individualized programs that account for these morphological features may result in better clinical outcomes.

Table of Contents

List of Tables

List of Figures

1.0 Introduction and Background

The tibiofemoral joint is often described as a hinge synovial joint comprised of the articulation between the tibia and femur. Injuries about the tibiofemoral joint are one of the most common patterns preventing athletes from participation in their respective sport. Ligamentous injuries, more specifically anterior cruciate ligament (ACL) rupture, are common, especially in the young, active population. Annually, there are up to 400,000 ACL injuries with a national economic impact at $25.3 billion per year (Bradley, Klimkiewicz, Rytel, & Powell, 2002; L. Y. Griffin et al., 2006; Hewett, Torg, & Boden, 2009; Luc, Gribble, & Pietrosimone, 2014; Mather et al., 2013; Sousa et al., 2017; J. M. Uhorchak et al., 2003). Subsequent knee instability after ACL rupture increases abnormal loading on surrounding tissues, which can lead to further injury to these structures (Nicholls, Ingvarsson, & Briem, 2021; O'Connor, Laughlin, & Woods, 2005). Furthermore, due to low vascularity, the healing capacity of the ACL is poor, especially in cases of mid-substance rupture (Ihara & Kawano, 2017; Murray, Martin, Martin, & Spector, 2000). Treatment modalities of ACL injury have progressed significantly in the last forty years. Once complicated by an 80% rate of failure (Kannus & Järvinen, 1987), management now includes utilization of surgical reconstruction with soft tissue grafts (Jung, Fisher, & Woo, 2009). However, 25% of ACL injured subjects still have unsatisfactory outcomes (Jung et al., 2009). Long-term studies have shown ACL injured subjects were at an increased risk for development of knee OA, and that even with ACL reconstruction, studies have shown that up to 90% of patients with an ACL reconstruction had a worse grade of OA in their injured knee compared to their contralateral (Selmi, Fithian, & Neyret, 2006).

As technology progresses, new treatment approaches may be developed to reduce failure rates. One method of improving treatment is through a better understanding of the risk factors for injury. ACL injury occurs after internal and valgus torquing; thus determining factors that influence these rotational motions may increase knowledge on ACL injury prevention and treatment (Boden, Dean, Feagin, & Garrett, 2000; Krosshaug et al., 2007; Matsumoto, 1990). A key contributor of knee motion is the tibiofemoral bony morphology through the articulation of the tibial plateau and femoral condyles (Hoshino, Wang, Lorenz, Fu, & Tashman, 2012a; D. Lansdown & Ma, 2018; van Diek, Wolf, Murawski, van Eck, & Fu, 2014). Tibiofemoral bony morphological features may exist that influence knee kinematics causing greater internal and valgus torques and thus be risk factors for ACL injury. Therefore, the focus of this dissertation is understanding the effect of tibiofemoral bony morphology risk factors on knee mechanics before and after ACL treatment.

1.1 Tibiofemoral Joint Anatomy and ACL Function

The tibiofemoral joint is a load bearing joint that consists primarily of the tibia, femur, articular cartilage, capsule, menisci, collateral ligaments, and cruciate ligaments (Figure 1.1). The knee joint is dynamically stabilized mainly through the quadriceps and hamstring muscles. The knee joint acts as a hinge joint in the sagittal plane allowing knee flexion-extension through hamstring and quadriceps activation. Internal and external tibial rotation occurs in the transverse plane and a small range of motion occurs in the coronal plane as varus and valgus rotations.

The ACL functions as the primary restraint to anterior tibial translation with respect to the femur and contributes to rotatory stability (Branch, Siebold, Freedberg, & Jacobs, 2011; Giesche, Niederer, Banzer, & Vogt, 2020; Kohn, Rembeck, & Rauch, 2020). Physiologically, the ACL has been shown to have two bundles: the anteromedial (AM) and posterolateral (PL) bundles (Starman et al., 2007). The two bundles have been described to stabilize the knee at different positions where the AM bundle provides more stability at greater flexion angles and the PL bundle provides more stability near full extension. Furthermore, the AM bundle has been shown to have higher modulus and ultimate stress compared to the PL bundle (D. L. Butler et al., 1992).

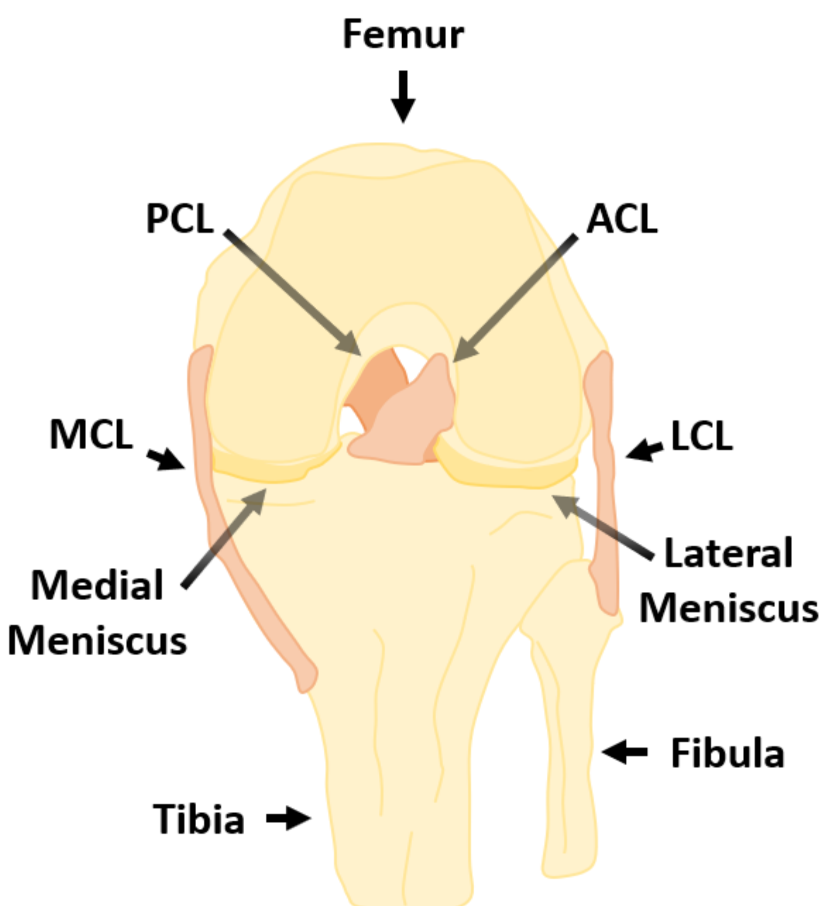

Figure 1.1: Depiction of the knee joint showing the femur, tibia, fibula, collateral ligaments, cruciate ligaments, and menisci from an anterior view of the knee in 90° of flexion

1.2 ACL Injuries

Up to 400,000 ACL injuries occur annually, and approximately 70% of these injuries are the result of non-contact mechanisms (Boden et al., 2000; Racine & Aaron, 2014). Patient reported outcomes and video analyses have shown that non-contact ACL injuries most often occur during deceleration or landing from jumping (Krosshaug et al., 2007; Renstrom et al., 2008). These injury mechanics typically occur near full extension and induce internal rotation and valgus torques which can lead to valgus collapse (Figure 1.2) (Boden et al., 2000; Krosshaug et al., 2007; Matsumoto, 1990; Renstrom et al., 2008). Due to limited vascularity, the ACL has low propensity to spontaneously heal, and without ACL reconstruction leaves the knee vulnerable to instability and damage to surrounding anatomic structures(Ihara & Kawano, 2017; Murray et al., 2000; Nicholls et al., 2021; O'Connor et al., 2005). Furthermore, damage to the other structures of the knee frequently occur concomitantly with ACL injuries (Hagino et al., 2015; Musahl et al., 2017; Shelbourne & Porter, 1992). Specifically, anterolateral capsule injury has been shown in up to 90% of ACL injury (Andrea Ferretti, Monaco, Fabbri, Maestri, & De Carli, 2017). OA has also been shown to develop in 90% of individuals after ACL injury (Selmi et al., 2006).

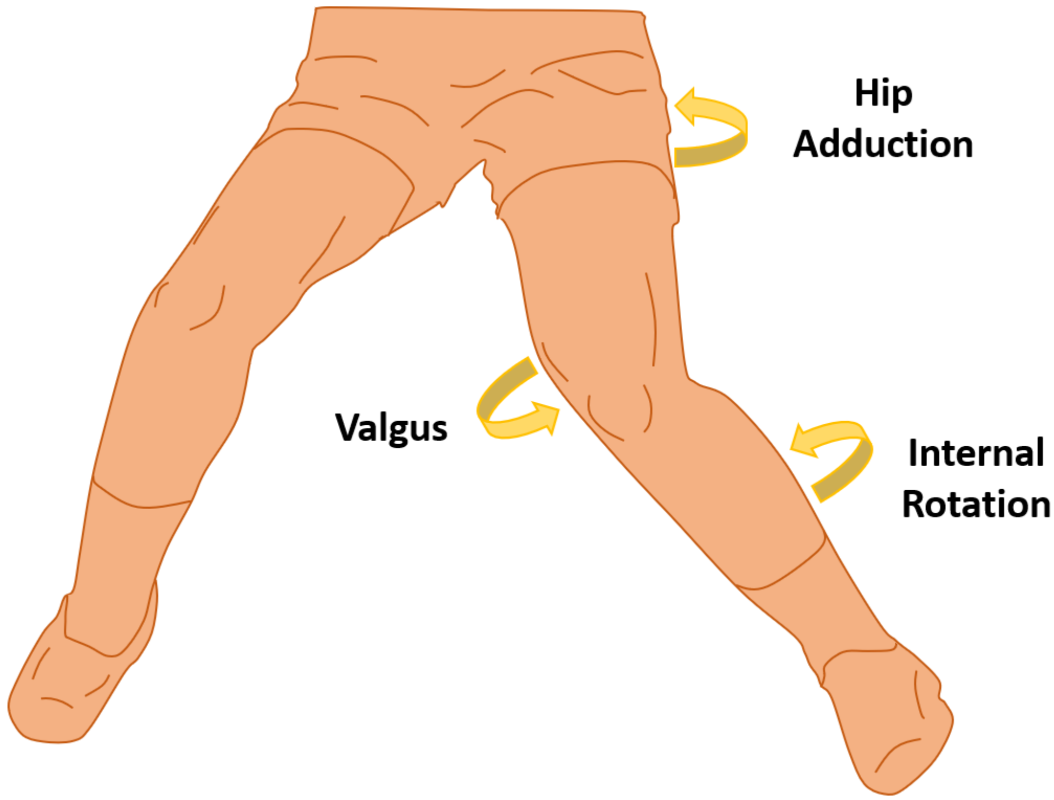

Figure 1.2: Depiction of a valgus collapse that is a combination of a valgus and internal rotation and is a mechanism for ACL injury.

1.3 ACL Injury Treatment Options

ACL rupture is more commonly managed operatively, especially in younger patients, given better restoration of rotational stability. Non-operative options revolve around physical therapy strengthening the dynamic stabilizers, adjustments to functional activity, and inclusion of protective bracing (Paterno, 2017). Non-operative treatment has been showed to be more effective on sedentary, less active individuals compared to their physically active counterparts (van der List, Hagemans, Hofstee, & Jonkers, 2020).

While operative treatments for ACL injury have been shown to have greater rates of positive outcomes compared to non-operative treatment, limitations still exist. The most common operative treatment is an ACL reconstruction using a soft tissue graft (Figure 1.3). The most prevalent grafts utilized are the bone-patellar-tendon-bone (BTB), semitendinosus tendon, and quadriceps tendon. While ACL reconstruction has shown to improve stability in the knee, post-operative complications still persist in up to 25% patients and have been described as graft site pain, arthrofibrosis and limited flexion-extension range of motion (Mohtadi, Webster-Bogaert, & Fowler, 1991; Niki et al., 2012; Skutek et al., 2004). Furthermore, patients after ACL reconstruction still have much higher rates of developing OA (A Ferretti, Conteduca, De Carli, Fontana, & Mariani, 1991; Kessler et al., 2008).

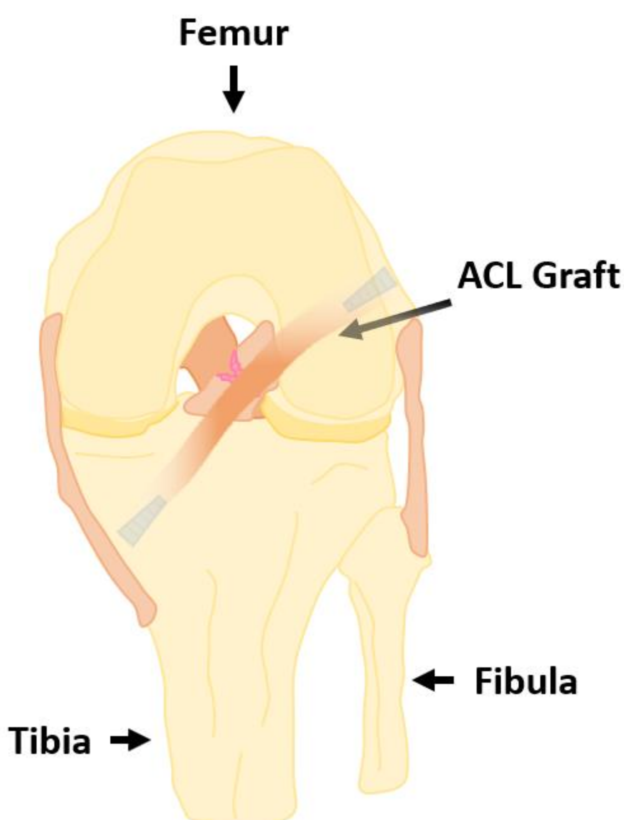

Figure 1.3: Depiction of ACL reconstruction using a soft tissue graft

Although ACL reconstruction has been shown to improve patient outcomes, rotatory instability still persists in a number of patients (Biau et al., 2009). Many clinicians attribute this persistent rotatory instability to unaddressed concomitant injury to the anterolateral capsule that has been described as frequently concomitant with ACL injuries (Golan et al., 2019; Kernkamp, van de Velde, Bakker, & van Arkel, 2015). However, the biomechanical behavior of the anterolateral capsule is disputed as some research has described an anterolateral ligament existing through the same region of the knee (Claes et al., 2013; Kennedy et al., 2015), while other research has described the anterolateral capsule as a sheet of tissue (Guenther, Rahnemai-Azar, et al., 2017). An operative treatment that was popular before ACL reconstructions, known as a lateral extraarticular tenodesis (LET), has recently resurfaced as an augmentation to ACL reconstructions (Duthon, Magnussen, Servien, & Neyret, 2013; Hewison et al., 2015; Slette et al., 2016). An LET is an operative procedure in which a soft tissue graft is added to the lateral aspect of the knee to address the persistent rotatory instability (Figure 1.4). While ACL reconstruction augmented with LET has been shown to improve outcomes on rotatory stability, some clinicians have concern that LET has no anatomical analogue and may overly constrain internal rotation, increasing contact pressure and thus increased risk for OA (Marom et al., 2021; Novaretti, Arner, et al., 2020).

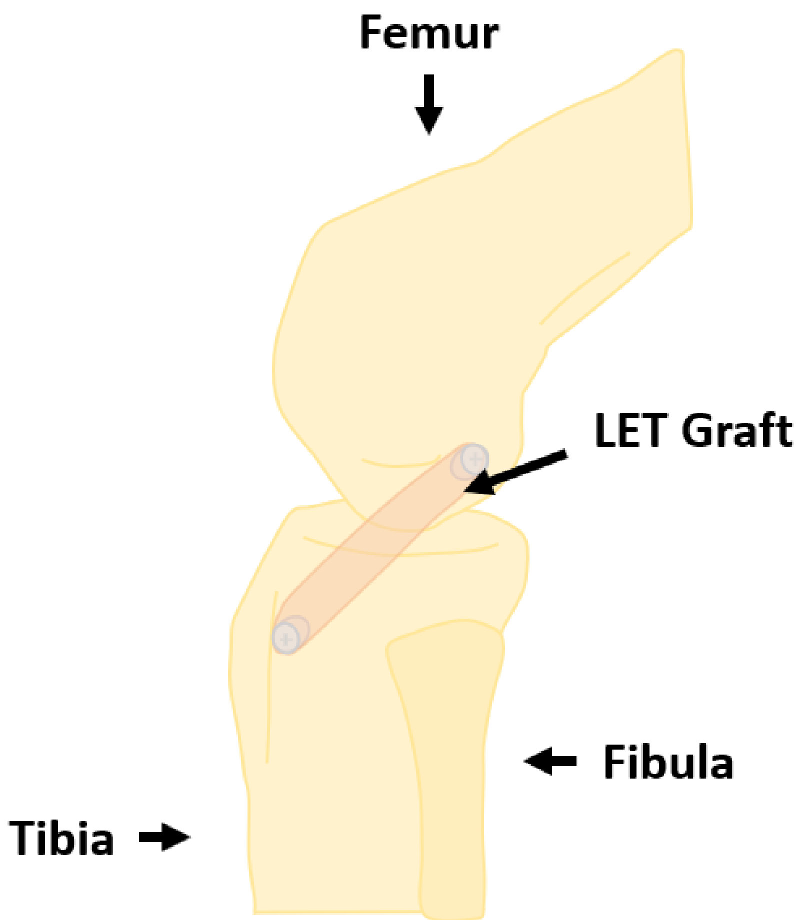

Figure 1.4: Depiction of a lateral extraarticular tenodesis that is performed to augment an ACL reconstruction and address persistent rotatory instability

Non-operative treatment options to ACL reconstruction are also common in clinical practice. Strengthening of the hamstrings muscles have been shown to improve treatment outcomes as quadriceps dominance has been shown to predispose individuals to a second ACL injury (Dedinsky, Baker, Imbus, Bowman, & Murray, 2017; Myer, Ford, & Hewett, 2006). By increasing the strength of the hamstrings muscles, dynamic stability improves and prevents the quadriceps from causing harmful increased anterior translation. Another non-operative augmentation to ACL reconstruction is inclusion of functional knee bracing (N. E. Marshall, Keller, Dines, Bush-Joseph, & Limpisvasti, 2019; Moon, Kim, Lee, & Panday, 2018) (Figure 1.5). Functional knee bracing is commonly prescribed to individuals after ACL reconstruction to improve knee stability and for increased protection against internal and valgus torques (Hanzlíková, Richards, Hébert-Losier, & Smékal, 2019).

Figure 1.5: Depiction of the functional knee bracing applied to a knee to provide additional stability and protection to the soft tissue structures

Functional knee bracing is frequently prescribed after ACL injury or ACL reconstruction as a means of returning near normal stability or reducing range of motion and forces at the knee (Cawley, France, & Paulos, 1989; Gentile et al., 2021; Marois et al., 2021; Rishiraj et al., 2009). Clinicians have recommended functional bracing for ACL injuries with concomitant grade I-II MCL injuries (Guenther et al., 2021). This treatment option has been shown to have good postoperative outcome in both short term and long-term follow up investigations (Blanke et al., 2017; Lucidi et al., 2022). Functional bracing has also been prescribed to intact knees for conservative treatment and preventative measures (Marois et al., 2021). However, the effectiveness of functional knee bracing in response to external loads requires further investigation. Furthermore, conflicting evidence has been shown on the effectiveness of functional knee brace to prevent ACL injury as no systematic review has shown knee bracing to reduce risk of ACL injury. Furthermore a previous study found that braced players trended towards having a lower injury rate for non-skill players in football while braced players at skill positions exhibited higher rate of injury compared to unbraced (Albright et al., 1994).

1.4 Robotic Testing System

Six degree-of freedom robotic testing systems are frequently used to perform biomechanical research to examine joint mechanics. Robotic testing systems originally applied external loading conditions to the joint at discrete flexion angles and recording the positions and forces in the joint using a force/moment sensor. The force in a soft tissue structure in response to the external loads can be determined by cutting the structure and repeating the recorded motion. The change in force recorded by the force/moment sensor can be attributed to the cut structure (Bell et al., 2015; Fujie, Livesay, Woo, Kashiwaguchi, & Blomstrom, 1995; Woo, Debski, Wong, Yagi, & Tarinelli, 1999). The loading conditions that are applied to the joint are commonly chosen to replicate clinical exams such as an anterior drawer (Kanamori et al., 2000; Leblanc et al., 2015). Loading at discrete flexion angles has drawbacks of an inability to apply dynamic loads and can lead to lengthy experiments. Therefore, researchers developed robotic testing systems that apply continuous loads through flexion (Bell et al., 2015).

Researchers utilize these 6 degree-of-freedom robotic testing system to test the effect of dynamic loads on joints before and after various injuries and treatments (Naendrup et al., 2019; Novaretti, Arner, et al., 2020; Novaretti et al., 2019; Patel et al., 2020; Thomas Rudolf Pfeiffer et al., 2018). The implications drawn from the research performed in these studies can improve clinical practice by informing clinicians of the impacts of the injuries and how well the treatments address those impacts.

The research performed in this dissertation will utilize a unique robotic testing system (Technology Service Ltd., Model FRS2010, Chino, Japan) that is repeatable to less than ±0.015 mm and ±0.01° (Figure 1.6). The long bones of the distal femur and proximal tibia is potted with an epoxy compound (Bondo, Atlanta, GA) and then secured to the lower plate and upper end effector of the system, respectively. The knee joint coordinate system is then defined to calculate knee kinematics (Grood & Suntay, 1983). The motion through flexion that resulted in minimized forces and moments in all degrees of freedom is found and called the passive path. The passive path is repeated to eliminate the viscoelastic effects of the soft tissue at the knee joint. Relevant dynamic loading conditions are then applied at approximately 1°/s with the kinematics and kinetics recorded. The forces in the soft tissue structure are then determined using the principal of superposition as previously mentioned. This robotic testing system and protocol was used for the research laid out in this dissertation to ascertain the effect of additional treatment options for ACL injury.

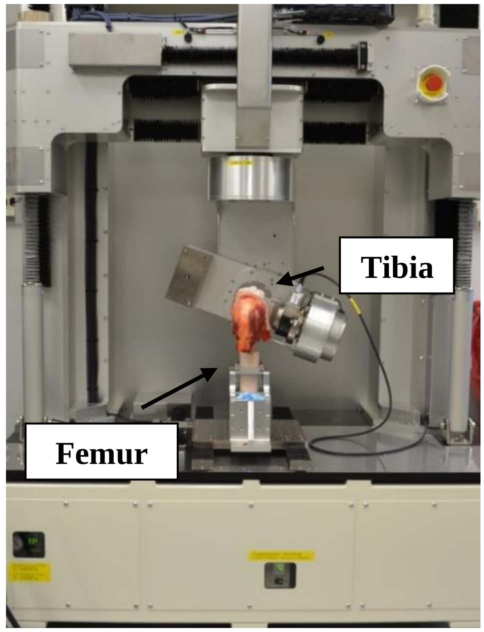

Figure 1.6: Six degree of freedom robotic testing system utilizing a UFS with a knee mounted at 90° of flexion imaged from an anterior view.

1.5 ACL Injury Risk Factors

Risk factors for non-contact ACL injury include age, sex, ethnicity, and level of activity (J. M. Uhorchak et al., 2003). Females have been shown to have up to eight times higher incidence rate of ACL injury per athletic exposure compared to males (Clarke & Buckley, 1980; Sutton & Bullock, 2013). During athletic activities and situations associated with ACL injuries, females have been shown to have greater variability in internal-external and varus-valgus motions (Arendt & Dick, 1995). Furthermore, quadriceps dominance relative to the hamstrings has been shown to be a risk factor for ACL injury, affecting females more commonly (Dedinsky et al., 2017).

Given the impact that the tibiofemoral bony morphology has on the impact of the bone-to-bone articulation at the knee, knee bony morphology became of interest as a possible risk factor for ACL injury. Using gross measurements and x-rays, 2-dimensional measurements of the knee were studied and certain morphological features were found to associate with ACL injury (Anderson, Lipscomb, Liudahl, & Addlestone, 1987; John M Uhorchak et al., 2003). Smaller femoral notch widths have been observed in ACL injured knees compared to control knees (Figure 7A) (Andrade et al., 2016; Görmeli et al., 2015; D. C. Whitney et al., 2014), and posterior tibial slope has been shown to be greater in ACL injured knees compared to control knees (Figure 7B) (Todd, Lalliss, Garcia, DeBerardino, & Cameron, 2010; Zeng et al., 2016). Recently, bony morphological studies have expanded to examine 3-dimensional bone shape at the knee utilizing statistical shape modeling (Pedoia et al., 2015) and these studies have further confirmed femoral notch width and posterior tibial slope as risk factors for ACL injury. However, additional bony morphological features that are difficult to capture 2-dimensionally may still exist. Furthermore, the effect of these tibiofemoral bony morphological features on knee kinematics have not been examined.

A)

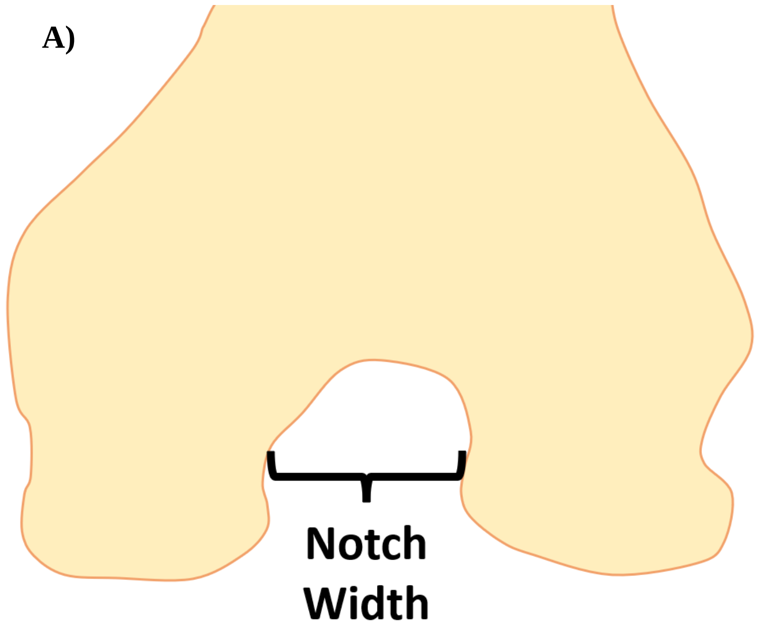

B)

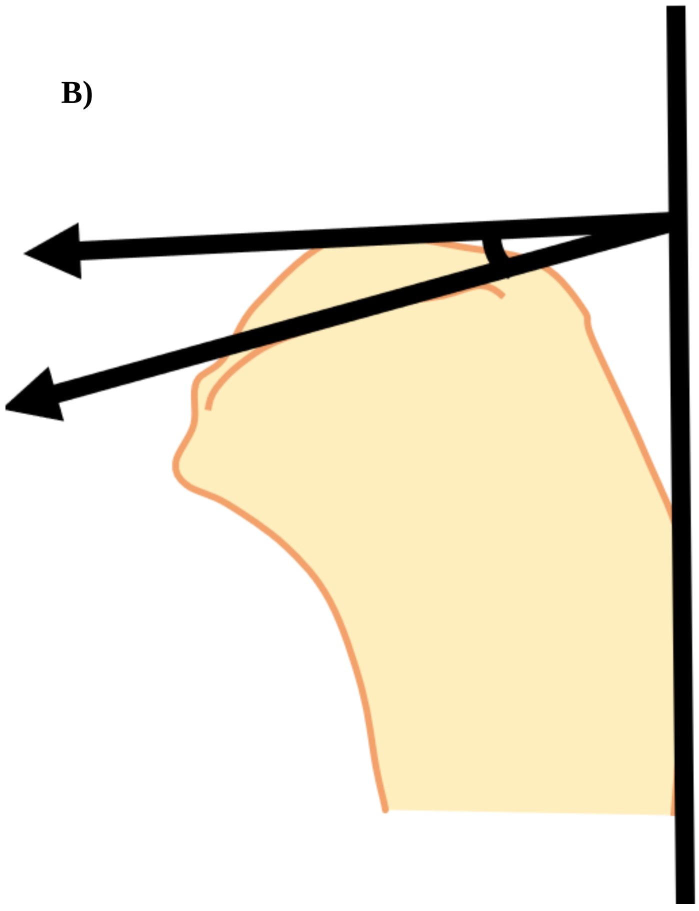

Figure 1.7: Bony morphological risk factors for ACL injury: A) Femoral notch width, B) Posterior tibial slope.

1.6 Evaluation of Bony Morphology Using Statistical Shape Modeling

Statistical shape modeling has been developed to analyze morphologic variation that direct linear measurements cannot properly capture. Researchers employed statistical shape modeling to analyze the curved surfaces of bones imaged in radiographic images to be able to quantify features those traditional measurements did not properly capture. Recently, the use of statistical shape modeling has expanded to analyze bony morphology 3-dimensionally captured with MRIs and CTs (Heimann & Meinzer, 2009). Another benefit of recently developed statistical shape modeling is analyses can be performed automatically removing human biases and errors that can occur with direct measurements or previously used landmark-based statistical shape modeling. However, interpretation of the results of statistical shape modeling analyses are difficult due to this bias free nature of the analysis that prevents targeting specific 2-dimensional features.

Three-dimensional statistical shape modeling quantifies shape variation through a correspondence-based methodology and the research in this dissertation uses Shapeworks (https://www.sci.utah.edu/software/shapeworks.html). Correspondence points are automatically placed on the surfaces of the inputted geometries in a manner that equally distributes them across the surface such that the points that correspond with each other are located similarly on different surface (Atkins et al., 2017; Cates, Elhabian, & Whitaker, 2017; Cates, Fletcher, Styner, Shenton, & Whitaker, 2007) A principal component analysis is then performed to reduce the high dimensionality of the corresponding point clouds into the directions of maximum variance(Abdi & Williams, 2010). The directions of maximum variance correspond with variations in shape in the input geometry and, in the case of the work in this dissertation, bony morphology. Each bone surface has a scalar value for each direction of maximum variance called PCA loading values which can then be used to associate bony morphology with groupings (i.e., ACL injured or uninjured).

Furthermore, the mechanical effect of morphological features determined using statistical shape models is something that can examined, but little research has done to this end. Research examining the influence of tibiofemoral bony morphology on knee mechanics is limited. Previous studies have examined the connection between certain 2-dimensional measurements at the knee with various kinematic parameters (Hoshino et al., 2012a; D. Lansdown & Ma, 2018), but expanding this work flow to 3-dimensional measures and furthering it to connect these 3-dimensional features with kinetic and arthrokinematic parameters are novel approaches.

1.7 Computational Modeling

The use of computational modeling is an alluring approach to determining the effect of pathologies and treatment options on joint behavior. Models with subject specific geometry driven by their joint kinematics lead to a better understanding of the joint behavior during motions or loading conditions of interest. This framework is popular as the inputs match with an existing clinical environment of a patient’s morphology and accompanying motion. However, subject-specific geometry may result in joint mechanics that do not apply to individuals with different bony morphology. A research protocol that incorporates varying bony morphology that are a risk factor for injury into a computational model allows for researchers and clinicians to have a better grasp on how those morphological features influence mechanics. Part of this dissertation aims to do just that by creating a computational model with inputs from the results of a statistical shape model that delineates risk factors for ACL injury.

The biomechanical behavior of ligamentous structures have been modeled using various computational methods (Galbusera et al., 2014; Limbert, Middleton, & Taylor, 2004; C.-H. Yu, Walker, & Dewar, 2001). These computational methods have been used to predict the effect of external loads on tissue and the interaction of various pathologies and treatment options. Common types of computational analyses model ligaments as either finite element models or springs. Finite element analyses have the advantage of analyzing the response at any location in the structure but can be more computationally intensive. Analyzing the ligaments as springs, non-linear springs more specifically, benefit from their simplicity while being able to model the response in soft tissue and only depend on slack length, elongation, toe region stiffness coefficient, and linear region stiffness as input parameters. Slack length is determined based on the difference between the insertion sites on the tibia and femur in the reference position of full extension which can be affected by the bony morphology. The research in part of this dissertation utilizes non-linear springs as their simplicity allows for scenarios that isolate the effect of the varying bony morphology on the forces in the ACL by not including superfluous parameters that may detract from the comparison to be made.

1.8 Motivation

Anterior cruciate ligament tears are a common injury among the young, athletic population and have a significant impact on the patient due to debilitating symptoms and on the health care system due to the economic impact from reconstructions, physical therapy, and treatments of OA down the line (Bradley et al., 2002; L. Y. Griffin et al., 2006; Luc et al., 2014; Sousa et al., 2017). Determining risk factors for ACL injury and their impact on knee mechanics would improve clinician's ability to individualize patient care and could help improve preventative measures for the at-risk athletes. Currently known risk factors include sex, age, level of activity, and tibiofemoral bony morphology (J. M. Uhorchak et al., 2003). Sex, age, and level of activity are already accounted for in training regimens when trying to reduce risk of ACL injury, but tibiofemoral bony morphology is often unaccounted for in these injury risk reduction efforts.

Determining the 3-dimensional bony morphological risk factors for ACL injury at the tibiofemoral joint and their impact on joint behavior before and after injury and treatment would allow clinicians and physical therapists to tailor treatment of individuals who are at greater risk for injury. Combining the use of statistical shape modeling to determine risk factors for ACL injury with computational modeling would allow researchers to determine the effect of tibiofemoral bony morphological features that associate with ACL injury on the force in the ACL. Furthermore, combining the use of statistical shape modeling with 6 degree-of-freedom robotic testing would allow researchers to determine the effect of tibiofemoral bony morphology on knee kinematics and kinetics before and after injury and treatment.

Overall, the goal of this dissertation is to establish tibiofemoral bony morphological risk factors for ACL injury (Aim 1), their impact on the forces in the ACL (Aim 2), and their influence on knee mechanics after injury and treatment (Aim 3). This dissertation will take a multifaceted approach to this goal utilizing a combination of 6 degree-of-freedom robotic testing, 3-dimensional statistical shape modeling, and computational modeling.

2.0 Specific Aims

The specific objective of this dissertation is to better understand the effect of tibiofemoral bony morphology on knee mechanics before and after ACL injury and ACL injury treatment. Three specific aims were accomplished to meet the specific objectives of this dissertation:

2.1.1 Specific Aim 1

Utilize a 3-dimensional statistical shape analysis to establish bony morphological features of the tibiofemoral joint that are associated with ACL injuries and sex.

It was hypothesized that ACL injury would associate with bony morphological features that may increase internal and valgus torques as those are the mechanisms for ACL injury.

2.1.2 Specific Aim 2

Determine the effect of bony morphology that associates with ACL injury determined in Aim 1 on ACL force in response to anterior displacement by modeling the ACL with non-linear springs.

It was hypothesized that the bony morphological features that associated with ACL injury will have greater force in the ACL.

2.1.3 Specific Aim 3

<u>Specific Aim 3a</u>

It was hypothesized that 1) functional knee brace would reduce tibial rotation and valgus rotation compared to the unbraced states and 2) functional bracing will reduce the in-situ force in the ACL in response to combined 5Nm internal and valgus torque.

<u>Specific Aim 3b</u>

Analyze the effect of bony morphology with and without functional bracing.

It was hypothesized that bony morphological risk factors for ACL injury would correlate with greater differences between braced and unbraced kinematics and ACL forces in response to external loads.

<u>Specific Aim 3c</u>

Analyze the effect of bony morphology on knee kinematics, contact pressures, and contact areas in response to external loads before and after anterolateral capsule injury and a type of LET.

It was hypothesized that bony morphologic risk factors for ACL injury would correlate with increased knee kinematics and contact pressures and decreased contact areas in response to external loads.

3.0 Aim 1: Tibiofemoral Bony Morphological Risk Factors for ACL Injury

3.1 Statistical Shape Analysis of Tibiofemoral Joint of ACL Injured Subjects

3.1.1 Introduction

Anterior cruciate ligament (ACL) injuries are one of the most common and traumatic ligamentous injuries among the active population (Letha Y Griffin et al., 2006; Hewett et al., 2009). Even after reconstruction, individuals who have previously experienced ACL injury are at high risk for a second ACL injury in either the same knee or the contralateral knee (Kamath et al., 2014; Webster & Feller, 2016). Multiple studies have shown that some individuals are at more risk for injury than others (Eduard Alentorn-Geli et al., 2009; Dai, Herman, Liu, Garrett, & Yu, 2012; Kaeding et al., 2015; McLean, Huang, & Van Den Bogert, 2005; Myer et al., 2006). Therefore, identifying risk factors for ACL injury would be crucial for developing preventative action.

Risk factors for non-contact ACL injury include level of activity, sex, age, and bony morphology (Boden, Sheehan, Torg, & Hewett, 2010; J. M. Uhorchak et al., 2003). Bony morphology of the knee dictates arthrokinematics according to bone-to-bone articulation. This articulation then dictates function of the ACL and is thus a risk factor for ACL injury as the shape of the bones affects articulation guiding joint motion (Zantop, Herbort, Raschke, Fu, & Petersen, 2007). As internal and valgus torques are the mechanisms for ACL injury (Matsumoto, 1990), many clinicians are interested in determining bony morphology that affect these rotational degrees of freedom.

Even though males experience ACL injury due to their higher numbers participating in sports, women are up to eight times more likely to sustain ACL injury then men during athletic activity (Clarke & Buckley, 1980; Sutton & Bullock, 2013). Women are at greater risk for ACL injury for a multitude of reasons including their pelvic variation that causes increased valgus angles at the knee (Ireland, 2002). Women have also been found to have greater joint laxity than men and have been associated with bony morphological features that predispose individuals for ACL injury such as a smaller femoral notch width (Branch et al., 2011; Shelbourne & Kerr, 2001).

Statistical shape modeling has been employed to analyze shape characteristics of the femur and tibia in 2D radiographs and 3D shapes for a more complete shape analysis (Baldwin, Langenderfer, Rullkoetter, & Laz, 2010; Pedoia et al., 2015; Rao et al., 2013). Differences in bony morphology have been found between sexes as well as ACL injured and control knees, however most analyses have only compared the 2-dimensional geometry of the femur and tibia (Baldwin et al., 2010; Pedoia et al., 2015; Rao et al., 2013; Shelbourne, Davis, & Klootwyk, 1998; Todd et al., 2010). Previous 3-dimensional bony morphology studies of the tibiofemoral joint examining the effects on ACL injuries only analyzed distinct predetermined features, utilized methods with a priori assumptions on shape, did not include the long axes of the tibia or femur in their analysis, or did not analyze the effect of sex on ACL injury risk with bony morphology (Muneta, Takakuda, & Yamamoto, 1997; Simon, Everhart, Nagaraja, & Chaudhari, 2010; van Diek et al., 2014). Therefore, the objective of this study is to utilize a 3-dimensional statistical shape analysis to establish bony morphological features of the tibiofemoral joint that are associated with ACL injuries and sex. It was hypothesized that ACL injury would associate with bony morphological features that may increase internal and valgus torques as those are the mechanisms for ACL injury (Eduard Alentorn-Geli et al., 2009; McLean et al., 2005).

3.1.2 Methods

Subjects

Bilateral computed-tomography (CT) scans of the lower extremity (1 mm slice thickness, 1 mm spacing, 512 x 512 acquisition matrix size, 300 mA at 120 kV, GE LightSpeed 16) were captured for 20 patients with complete ACL injuries 6 months after ACL reconstruction including a mix of acute and delayed ACL procedures (age = 22.4 ± 8.5, 10 female) and 20 control subjects with no history of knee injuries (age = 30.4 ± 6.7, 10 females). Bilateral CT scans allow for capture of the contralateral knees of the ACL injured subjects to provide the third group for analysis. The study received approval from the institutional review board at the University of Pittsburgh.

Preprocessing

The distal femurs and proximal tibiae were semi-automatically segmented to include a uniform amount of their long axis using Mimics 21 (Materialise NV, Leuven, Belgium). The distal femurs were segmented so that the largest medial-lateral dimension is equal to the distance from the inferior most point to the cut on the long axis of the femur (Figure 3.1). The proximal tibiae were segmented from the most proximal point to a point distally along the long axis 90% of the largest medial-lateral dimension of the tibial plateau. Including the entire long axis of the tibia would add unwanted variability into the statistical shape model and shift the focus of the analysis. Utilizing Mimics 21 Automatic 3D Calculation function, 3-Dimensional surface models of the distal femur and proximal tibia were created. Anti-aliasing was then performed utilizing a Laplacian filter with a smoothing factor of 0.7 for three iterations. The 3-dimensional models were then exported to 3D Slicer (3D Slicer, 4.10.2, slicer.org). The femur surface models were rotated so the distal most points were in the same plane for alignment purposes of the bounding boxes. The femur and tibia surface models were then exported as binary segmentations to Seg3D (Seg3D

2.2.1, https://www.sci.utah.edu/cibc-software/seg3d.html) to create uniform bounding boxes. Lastly all right femurs and tibiae were reflected as left femurs and tibiae for uniformity.

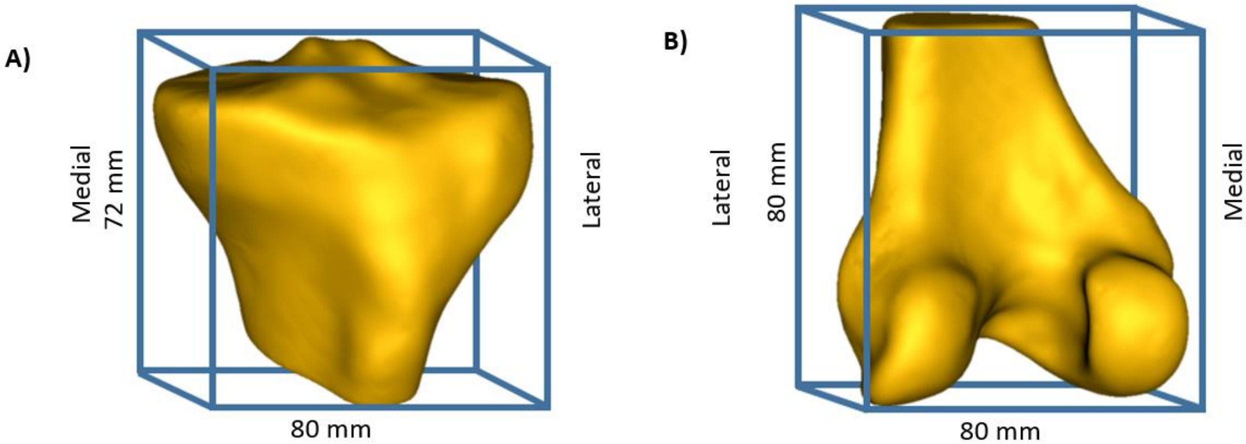

Figure 3.1: A) Uniform dimensions of the tibia were maintained by trimming the inferior-superior dimension to 90% of the medial lateral dimension (Anterior View). B) Uniform dimensions of the femur were maintained by trimming the inferior-superior dimension to 100% of the medial lateral dimension (Posterior View).

Statistical Shape Analysis

Two statistical shape models were developed to analyze the variability in shape: one for the femurs and one for the tibiae. The 3-dimensional surface models were imported into Shapeworks (https://www.sci.utah.edu/cibc-software/shapeworks.html) which employs a correspondence method to analyze the variation in 3-dimensional shape (Hoshino et al., 2012a; Hoshino, Wang, Lorenz, Fu, & Tashman, 2012b). One difficulty of statistical shape modeling is limiting the bias when using bony landmarks to determine particle placement (Atkins et al., 2017; Cates et al., 2007; Chan, Farnsworth, Koziol, Hosalkar, & Sah, 2013). This limitation is avoided through an automatic particle placement using a splitting strategy that randomly chooses a surface location for the first particle which is then split into two particles and repel each other along the surface until a steady state is achieved (Atkins et al., 2017). This splitting process was repeated until 2,048 particles were uniformly placed on each bone in the analysis. The uniformity was optimally achieved using a gradient descent approach with a cost function while simultaneously creating a compact distribution of the correspondence of particles on the surface models (Atkins et al., 2017; Cates et al., 2007). A generalized Procrustes analysis was performed throughout to optimize alignment and normalize with respect to scale (Gower, 1975).

The shape configurations were divided into three groups: knees of control subjects, knees with ACL injury, and uninjured contralateral knees of ACL injured subjects A principal component analysis (PCA) was performed to analyze the variability of the correspondence particle placement in each configuration. The PCA reduces the dimensionality of the correspondence of particles to orthogonal descriptions of the data set while extracting information about independent bony morphological features that describe the cohort of bone shapes. From the PCA, bony morphological features can be projected or mapped onto shape variability spectrums called principal components or modes of variation. This mapping called PCA loading values provides a quantitative assessment of the distal femur or proximal tibiae configurations onto each mode of variation. Each mode of variation represents an independent shape feature. The total variation in the data set is described by combining each mode of variation. The largest modes of variation that additively describe 80% of the variation among all the distal femurs or proximal tibiae were analyzed for statistical significance between injury states and sex.

The modes of variation can be visualized by modeling the movement of each particle from one end of the spectrum to the other (±2 SD) as vectors on top of the mean distal femur or proximal tibia surface models (Figure 3.2). Two orthopaedic sports medicine fellows performed an independent analysis to examine these 3-D models and interpret physical representations which were then reviewed by the researchers of this study. Two dimensional parameters matching the bony morphological feature interpreted by the orthopaedic surgery fellows were then measured and analyzed for statistical differences.

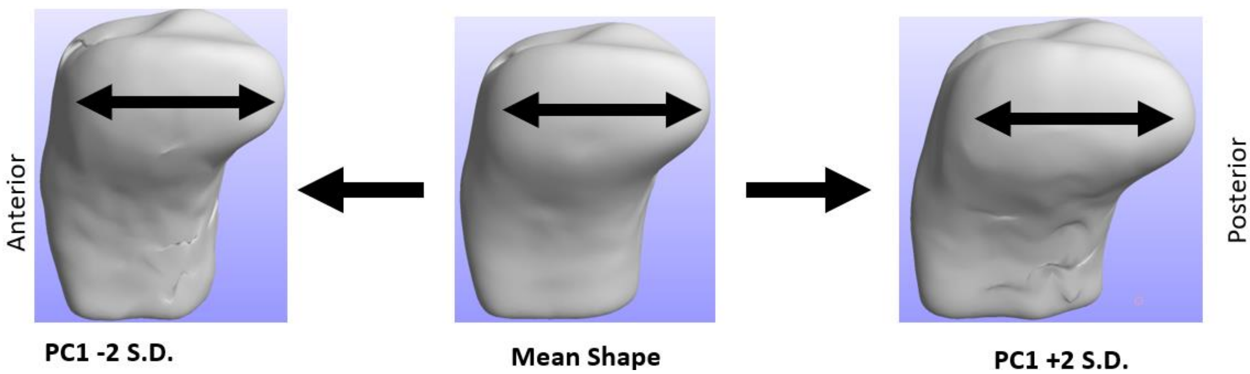

Figure 3.2: Visualization from a medial view demonstrating the variation of the second tibial principal component from -2 S.D. to +2 S.D. with the mean shape in the middle.

Direct Measurement Analysis

The anatomical axis was defined as the line between two centroids of the long axis of the femur (Cherian et al., 2014).The anatomical axis was extended inferiorly to the point halfway between the distal most points on the femoral condyles. The anatomical axis was then rotated 6° about the distal most point in the coronal plane to form the mechanical axis (Cherian et al., 2014) (Figure 3.3). The superficial MCL insertion site was visually identified on each knee by an orthopaedic surgeon on the 3-dimensional surface models created from the segmentations of the CT scans. The perceived center of the LCL insertion site was identified based on Blumensaat's line determined in the sagittal view on the CT scans because it was found to be a more accurate determination (Thomas R Pfeiffer et al., 2018). The orthogonal distance between the established insertion sites and mechanical axis were calculated and then normalized by the largest medial lateral width in an axial plane of the respective femur. The directional components of each orthogonal distance between the mechanical axis and the insertion sites were calculated and normalized by their respective widths (i.e., the anterior-posterior component scaled by the anterior-posterior width).

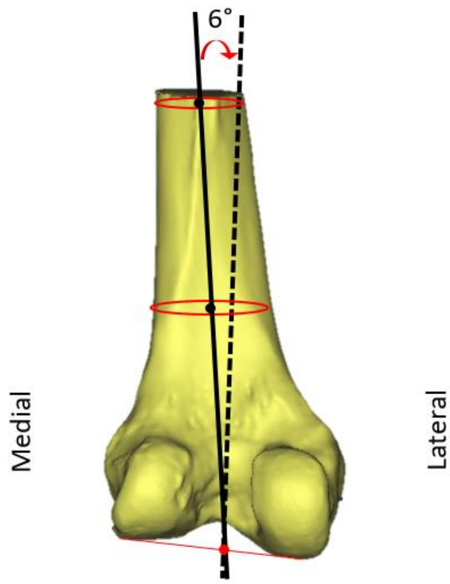

Figure 3.3: Centroids of the femoral long axis are determined in the coronal plane and denoted by the black points inside the red ovals. The anatomical axis is determined by the line connecting those two points. To determine the mechanical axis (dotted line), the anatomical axis is rotated 6° about the distal most point (red dot).

Statistical Analysis

Normality was assessed using a Shapiro Wilk W Test. The standard deviations (S.D.) of the modes of variation for each group were determined not be different to establish homoscedasticity. Two-way analysis of variance (ANOVA) was performed to compare the PCA loading values of shape between ACL injured and control knees as well as ACL injured knees and contralateral knees with sex being the other main factor in both analyses. Two-way ANOVAs were then performed on the 2D measurements that match the physical representations determined. Significance was set at $p < 0.05$.

3.1.3 Results

The ACL injured group consisted of ten males and ten females with an average age of 22.4 years while the uninjured control group consisted of ten males and ten females with an average age of 30.4 years. The first modes of variation that describe over 80% of the total variation were included in our analysis (Figure 3.4). The first five principal components represented 85% of the variation among the data set of distal femurs.

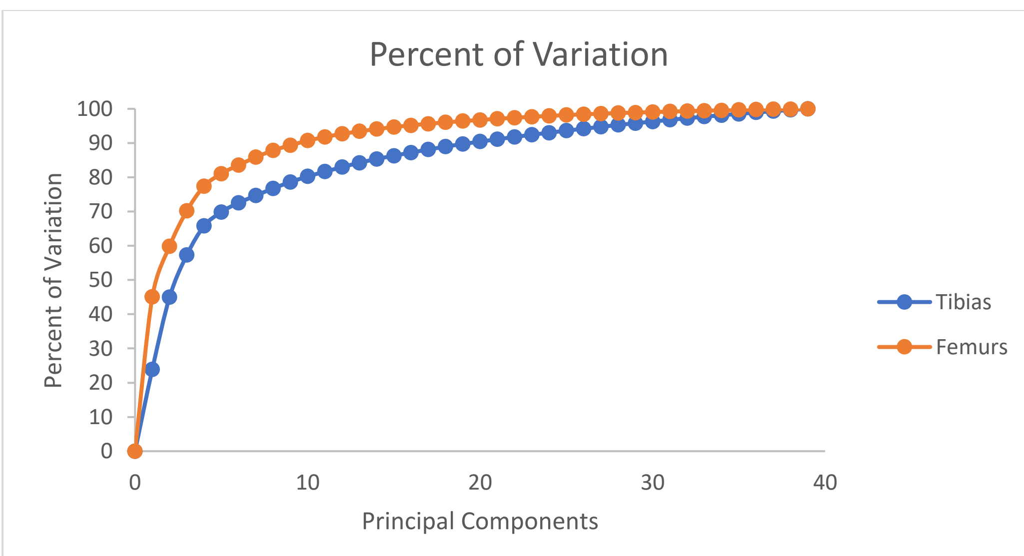

Figure 3.4: Cumulative percent of variation encompassed in the tibial and femoral principal components.

The two-way ANOVA demonstrated statistically significant differences between male and female knees in the second and third femoral principal components. The 3D models were created for modes of variation that were determined to be different between ACL injured knees and control knees and between male and female knees (Figures 3.5-3.7). The second femoral principal component demonstrated males having a more anterior medial trochlear ridge (Figure 3.5), and the third mode of variation demonstrated that female knees have a more lateral mechanical axis than male knees (Table 1). Significant differences between the distal femurs of ACL injured and control knees were found in the first and third femoral principal components. The ACL injured knees demonstrated a smaller angle between the long axis and the condylar axis of the femur (Figure 3.6a and 3.6b) and a more lateral femoral mechanical axis than the control knees (Figure 3.6c and 3.6d). No statistically significant differences were found in the bony morphology between the ACL injured and contralateral knees.

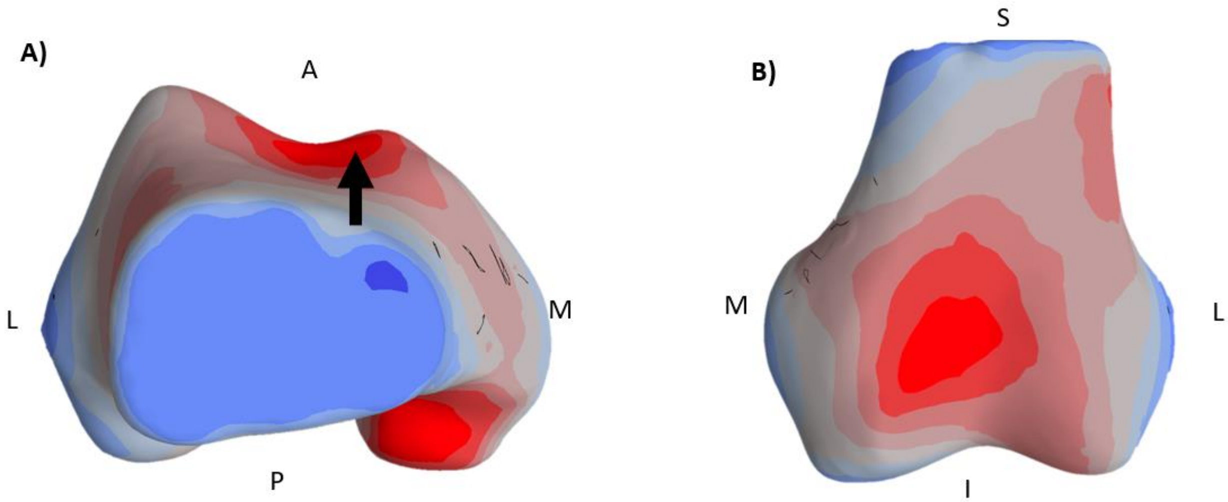

Figure 3.5: Visualizations of second principal component of the distal femurs utilizing 3D distance topography plots imaging the distance between +2 SD and -2 SD of the second principal component where red represents outward distance and blue represents inward distance. A) Superior view and B) anterior view showing males having a more anterior medial trochlear ridge than females where males had significantly greater PC1 loading values. (M: Medial, L: Lateral, P: Posterior, A: Anterior, I: Inferior, S: Superior).

Table 1: Distances from the mechanical axis to the MCL and LCL and the directional components scaled by the directional widths of their respective knee. Three-dimensional distances are scaled by the medial-lateral widths. (* $p<0.05$) (Mean ± S.D.)

	ACL Injured Knees	**Control Knees**	**p value**
1. Distance from Mechanical Axis to MCL	47 ± 2%	43 ± 3%	p = 0.0004
a. Medial-lateral component	45.4 ± 2%	42.5 ± 3%	p = 0.01
b. Anterior-posterior component	14 ± 5%	7 ± 5%	p = 0.007
2. Distance from Mechanical Axis to LCL	55 ± 2%	55 ± 3%	p = 0.90
a. Medial-lateral component	50 ± 3%	50 ± 3%	p = 0.85
b. Anterior-posterior component	26 ± 4%	26 ± 7%	p = 0.79

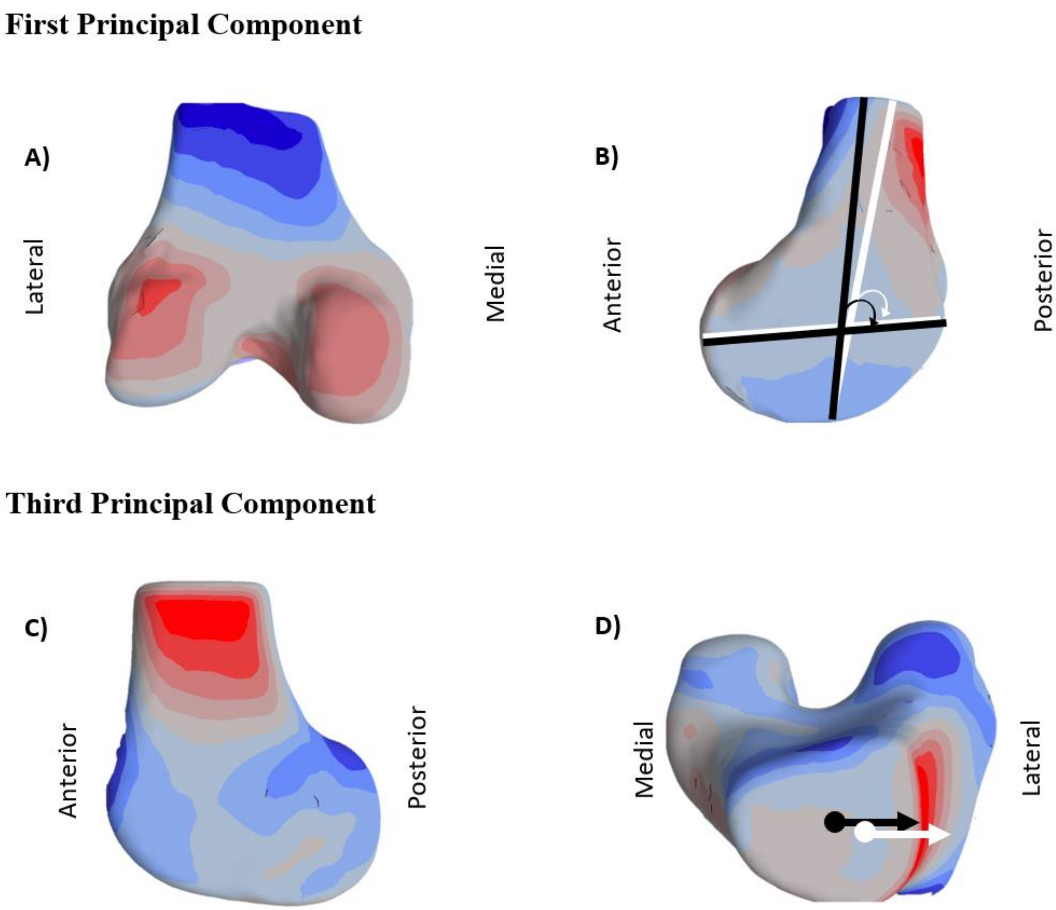

Figure 3.6: Visualizations of first and third principal components of the distal femurs utilizing 3D distance topography plots imaging the distance between +2 SD and -2 SD of the first and third principal components where red represents outward distance and blue represents inward distance. A) Posterior view and B) medial view showing view showing control knees have a smaller angle between the long axis and the condylar axis than ACL injured knees as ACL injured knees have significantly greater PC0 Loading values. C) Lateral view and D) Superior view demonstrating a more lateral mechanical axis among ACL injured knees and female knees compared to control knees male knees, respectively as ACL injured and female knees had significantly greater PC2 loading values.

The first ten modes of variation represented 80% of the variation among the data set of proximal tibiae. The two-way ANOVA demonstrated statistically significant differences in the second tibial principal component between ACL injured and control knees as well as male and female knees. The ACL injured and female tibiae were found to have a smaller anteroposterior dimension of the lateral tibial plateau compared to control and male tibiae (Figure 3.7).

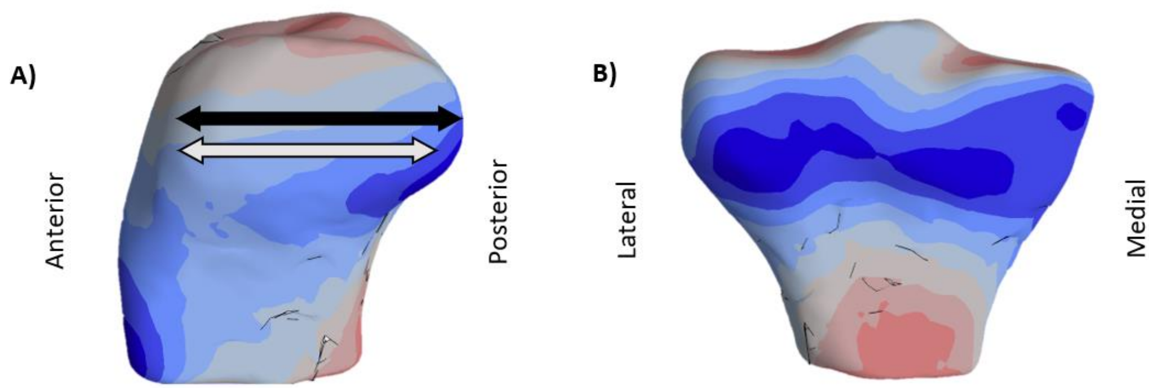

Figure 3.7: Visualizations of first and third principal components of the distal femurs utilizing 3D distance topography plots imaging the distance between +2SD and −2SD of the first and third principal components where red represents outward distance and blue represents inward distance. (A) Lateral view and (B) posterior view showing ACL injured and female knees have a smaller anterior-posterior aspect of the tibial plateau compared to control and male knees.

<u>Mechanical Axis Analysis</u>

The distance from the MCL insertion sites to the mechanical axis was found to be statistically significantly different between the ACL injured group and the control group as the ACL injured knees had MCL insertion sites of the injured knees were 4% further away from the mechanical axis than the MCL insertion sites of the control knee and 3% more lateral (p=0.0004 and p=0.01). The post hoc analysis determined a significant interaction effect exists between injury state and sex in the measurement between the mechanical axis and the MCL insertion site. The MCL insertion site of the injured knees were 7% more anterior than that of the control knees when referenced to the mechanical axis (p=0.03). No significance differences existed between the ACL injured and control knees with regard to the distance from the mechanical axis to the LCL nor any of the directional components.

3.1.4 Discussion

Statistical shape modeling was used to determine modes of variation that were interpreted as bony morphological features associated with ACL injuries when compared to control knees. Significant differences were determined between distal femurs of male and female knees in the second and third modes of variation (anterior medial trochlear ridge and mechanical axis location), and between the distal femurs of ACL injured and control knees in the first and third modes of variation (angle between long axis and condylar axis and mechanical axis location). The first mode of variation demonstrated that ACL injured knees have a greater angle between the long axis and the condylar axis compared to control knees. Variation in this angle may affect the area of articulation between the femoral condyles and tibial plateau. A smaller angle between the long axis and the condylar axis may allow for a larger contact area between the femur and tibia as the condylar axis is more parallel with the tibial plateau. A larger contact area would thus allow for greater stability and a decreased risk for ACL injury. Furthermore, a greater angle may result in hyperextension of the knee and increased laxity which is a risk factor for ACL injury.

Female knees had a less anterior medial trochlear ridge than male knees. This less anterior ridge may allow for greater Q angles as the patella can be aligned more laterally. This finding is similar to a previous study that found female knees have greater Q angles than male knees (Medina McKeon & Hertel, 2009).

The MCL insertion sites on the distal femurs of the ACL injured knees and female knees were further away from the mechanical axis than that of the control knees and male knees. Thus, the location of the mechanical axis was identified as more lateral on the ACL injured and female knees compared to control and male knees. However, this assumes that the tibial plateau is parallel to the ground. If the tibial plateau is angled such that the lateral plateau was elevated differently than the medial plateau so that the tibial plateau is not parallel to the ground, the variation in mechanical axis may have implications in valgus angles and moments. However, one limitation of our mechanical axis analysis is the assumed 6° difference between the anatomical axis and mechanical axis as 6° is based on an average of femurs from the published literature. The mechanical axis was estimated instead utilizing the anatomical axis as it is more clinically relevant for the mechanical effect of the bony morphology on the knee. The MCL insertion site was also found to be more anterior on the ACL injured distal femurs. A more posterior mechanical axis may put more force on the posterior horn of the medial meniscus which may be why medial meniscus injuries are more common with chronically ACL deficiency (Hagino et al., 2015). A more lateral mechanical axis may cause more force to be exerted on the lateral tibial plateau during axial compression. This difference in force location may predispose knees to ACL injuries due to increased valgus and internal rotations near full extension, which is a mechanism for ACL injury (Matsumoto, 1990). Moreover, variation in the orthogonal distances between the mechanical axis and the insertion sites of the secondary stabilizers would change their moment arms possibly affecting load sharing. A more anterior MCL insertion site may result in less load sharing between the MCL and ACL in response to an internal torque causing the ACL to experience larger forces.

However, the interpretation that this bony morphological feature affects load sharing between the ACL and MCL is affected by multiple factors including limb alignment, dynamic stability, and joint loading. Therefore, further research must be performed to assess the effect of these factors.

ACL injured and female knees were found to have a smaller anterior-posterior dimension in the lateral tibial plateau compared to control and male knees, respectively. A smaller anterior-posterior dimension of the lateral tibial plateau would decrease the amount of articulation between the distal femur and proximal tibia. This decreased articulation may decrease stability, increasing risk for ACL injury. Furthermore, a smaller anterior-posterior dimension may cause ACL injured knees to be at greater risk for subluxation and thus ACL injuries and other concomitant knee injuries.

No differences were found between the ACL injured and contralateral knees suggesting that both knees of individuals predisposed to ACL injury are at equal risk of injury due to their bony morphology. This is supported by previous findings that suggest a high occurrence rate of a second ACL injury in the same knee or contralateral knee (Kamath et al., 2014; Webster & Feller, 2016). Furthermore, no difference was found between the left and right knees of the ACL injured subjects.

Determining bony morphological features that are associated with ACL injuries would be invaluable to clinicians, physical therapists, and athletic trainers as it would assist with the development of individualized prevention and treatment protocols for ACL injury. These individualized protocols would be able to reduce ACL injury risk by increasing dynamic stabilizations through quadriceps and hamstring strengthening. Furthermore, orthopaedic surgeons can account for individualized bony morphological parameters to improve injury recovery rates.

An interaction effect between injury state and sex was found during the post hoc analysis of the distance between the MCL insertion site and the mechanical axis. This may be due to female knees having naturally greater valgus angles (Ireland, 2002). A main limitation of our study is collection of control knees, which were comprised of individuals who have never had an ACL injury. However, they could still be at risk for ACL injury. Another limitation is that the CT scans were 6 months after reconstruction where some were delayed procedures so bony remodeling could have occurred before or after surgery prior to the CT scans. In our study, distal femurs and proximal tibiae were analyzed independently for bony morphological differences leading to many future directions. The distal femurs and proximal tibiae can be analyzed together for paired differences between ACL injured and control knees. Furthermore, most bony morphological features are considered to be innate shapes that do not change. However, data exist showing that repeated loading from training and sport or after ACL reconstruction can cause bone remodeling (Crockett et al., 2002). In the future, bony morphological differences will be analyzed between athletes in different types of sports.

In conclusion, more bony morphological differences exist between ACL injured and control knees than described in previous literature. Specifically, ACL injured knees have a more lateral mechanical axis of the femur resulting in greater genu valgum possibly altering the forces in the soft tissue structures at the knee demonstrating a reason for it be a risk factor for ACL injury (Brophy, Silvers, & Mandelbaum, 2010). Furthermore, a smaller anterior-posterior dimension of the lateral tibial plateau increasing the risk of subluxation. Furthermore, female knees have similar bony morphology as ACL injured knees. This information would be valuable to clinicians and patients to understand their increased risk, treatment options, and injury prevention strategies. Variation between males and females was found supporting previous studies while describing new differences. The framework of this study can be applied to future research investigating bony morphological risk factors for ACL injury at the knee as well as other injuries for different joints.

4.0 Aim 2: The Effect of Tibiofemoral Bony Morphological Risk Factors for ACL Injury on ACL Forces

4.1 Non-Linear Spring Model of ACL of Tibiofemoral Bony Morphological Risk Factors for ACL Injury

4.1.1 Introduction

Anterior cruciate ligament (ACL) injuries are prevalent in the young athletic population (Mather et al., 2013). These injuries are immediately debilitating with long term effects including early onset posttraumatic osteoarthritis (Kessler et al., 2008) and require an arduous recovery even if treated surgically (A Ferretti et al., 1991; Friel & Chu, 2013; Racine & Aaron, 2014; Selmi et al., 2006). The primary function of the ACL is to prevent anterior tibial translation with respect to the femur so an anterior drawer is often performed to assess the state of the ACL (J. Marshall, Wang, Furman, Girgis, & Warren, 1975; Takeda, Xerogeanes, Livesay, Fu, & Woo, 1994). Furthermore, second ACL injury, contralateral or ipsilateral, after ACL reconstruction has been found to be 15 times greater than control subjects (Paterno, Rauh, Schmitt, Ford, & Hewett, 2012). While ACL injury treatment has progressed significantly over the last few decades, individualized treatment options can still be improved.

The biomechanical behavior of the ACL has been modeled previously through a various computational methods (Checa, Taylor, & New, 2008; Galbusera et al., 2014; C.-H. Yu et al., 2001). The use of modeling has become common to predict the effect of various pathologies and treatment options as it allows researchers to control the inputs of a research question and adjust those inputs in a manner that in-vivo or in-situ experiments do not allow. However little research has been shown on the effect of risk factors for pathology even though certain risk factors could be a part of those controlled inputs.

Determining risk factors for ACL injuries is a critical step for improving patient care on an individualized basis as studies have shown that some people are at greater risk of ACL injury than others. Known risk factors for ACL injury include sex, age, level of activity, and bony morphology. The results from Aim 1 show that 3-dimensional bony morphological features of the tibia and femur associate with ACL injury. These features being a smaller anterior-posterior length of the tibial plateau, a greater angle between the femoral long axis and the femoral condylar axis, and a more lateral mechanical axis of the distal femur (S. K. Polamalu, Musahl, & Debski, 2020).

Certain bony morphological features such as posterior tibial slope and femoral notch shape have been shown to associate with ACL injury and have been shown to influence knee kinematics (D. Lansdown & Ma, 2018). Bony morphology dictates the function of the ACL by influencing knee motion through the tibiofemoral arthrokinematics. Furthermore, this motion in combination with the bony morphology determine the force in the ACL. However, the effect of bony morphological risk factors for ACL injury on the force in the ACL in response to knee motion has not been shown. Therefore, the objective of this study is to determine the effect of bony morphology that associates with ACL injury determined in Aim 1 on ACL force in response to anterior displacement by modeling the ACL with non-linear springs.

4.1.2 Methods

Two 3-dimensional statistical shape models, one for the femoral bony morphology and one for tibial morphology, were created from CT scans of the knees of 20 ACL injured subjects and twenty control subjects with no history of new injury as described in Aim 1. The proximal tibia and the distal femur were segmented for each subject from each CT scan and 3-dimensional surface models were created for each bone. Correspondence particles were automatically and optimally place on the bone surface models. Utilizing a principal component analysis, the independent, orthogonal axes of variation in the high-dimensional space called principal components were determined that corresponded with shape features the describe the cohort of surfaces. This process was performed using ShapeWorks (https://www.sci.utah.edu/software/shapeworks.html). The outcomes of the statistical shape model were surface models ±2 standard deviations along the principal components that significantly differed between ACL injured and control subjects (Figure 3.2).

Two femoral bony morphological features and one tibial bony morphological feature associated with ACL injury: a greater angle between the femoral long axis and the femoral condylar axis, a more lateral mechanical axis of the distal femur, and a smaller anterior-posterior length of the tibial plateau. Eight 3-dimensional models were created from the statistical shape model: the mean femur, the mean tibia, the femur model that associated with ACL injury with the greater angle between the femoral long axis and the femoral condylar axis, the femur model that associated with uninjured subjects with the smaller angle between the femoral long axis and the femoral condylar axis, the femoral model that associated with ACL injury with a more lateral mechanical axis, the femur model that associated with control subjects with the less lateral mechanical axis, the tibia model that associated with ACL injury with a smaller anterior-posterior length of the tibial plateau, and the tibia model that associated with control subjects with a longer anterior-posterior length of the tibial plateau (Figure 4.1). The femurs from the femoral principal components were paired with the mean tibia and the tibias from the tibial principal components were paired with the mean femur.

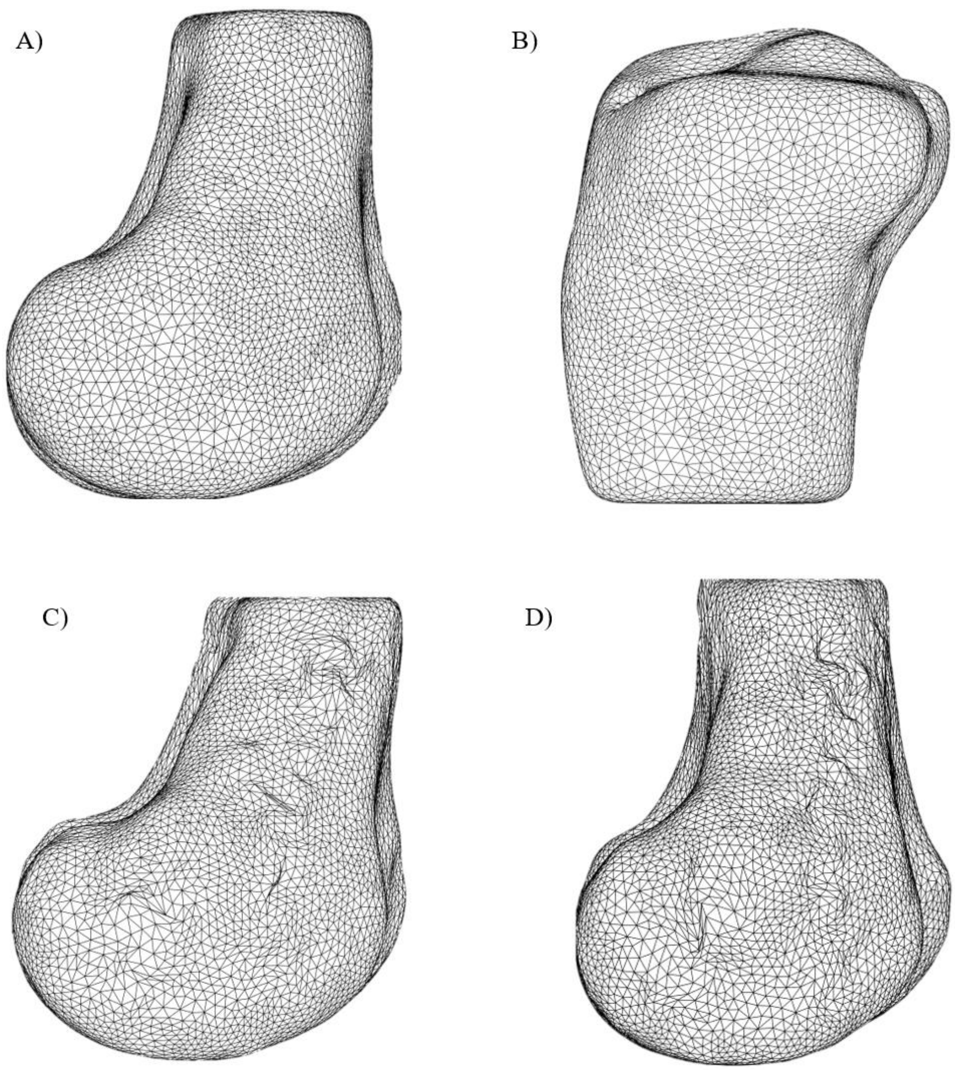

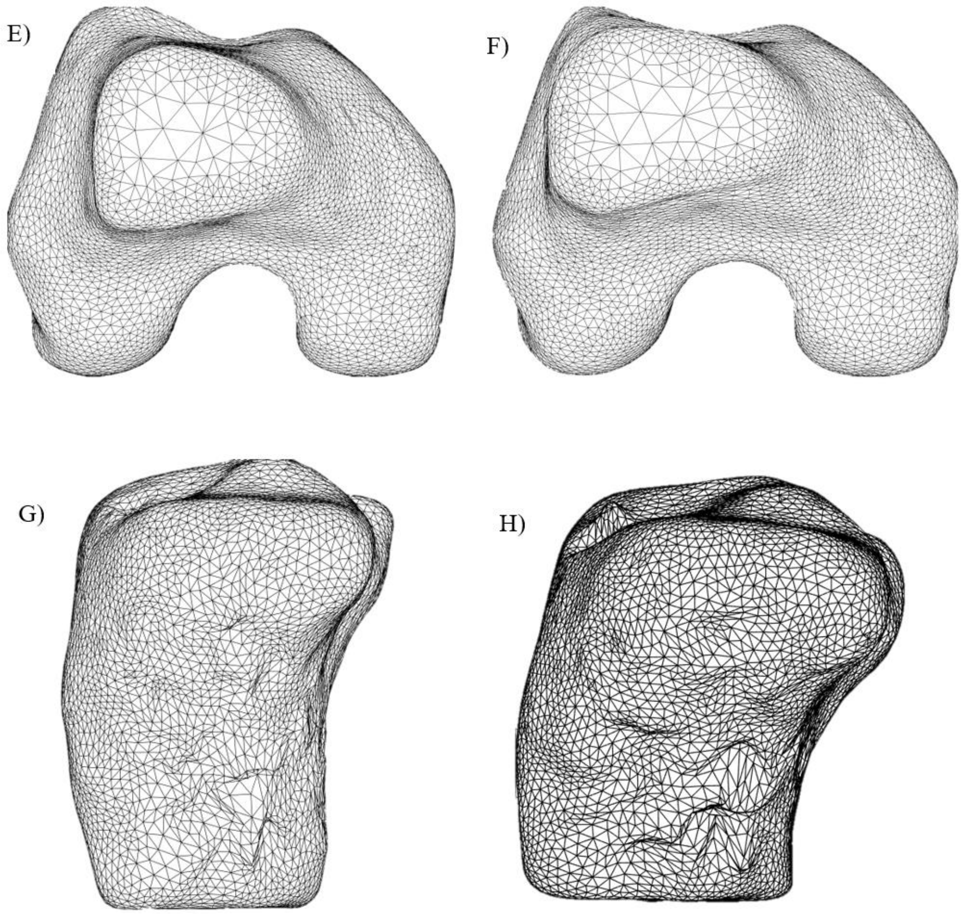

Figure 4.1: A) medial view of the mean femur, B) lateral view of the mean tibia, C) medial view of the femur with a greater angle between the femoral long axis and the femoral condylar axis that associates with ACL injured subjects, D) medial view of the femur with a smaller angle between the femoral long axis and the femoral condylar axis that associates with uninjured subjects, E) medial view of the femur with a more lateral mechanical axis that associates with ACL injured subjects, F) medial view of the femur with a less lateral mechanical axis that associates with uninjured subjects, G) lateral view of the tibia with a smaller anterior-posterior length that associates with ACL injured subjects, and H) lateral view of the tibia with a longer anterior-posterior length that associates with uninjured subjects. Note that the unsmooth areas on the bone models are due to noise captured within the correspondence of the statistical shape model.

Utilizing a custom Matlab code, the anteromedial (AM) and posterolateral (PL) bundles of the ACL were modeled as non-linear springs using the following equation (Checa et al., 2008; C.-H. Yu et al., 2001):

$$F = \begin{cases} 0 & where\ \varepsilon \leq 0 \\ K_1\ (L - L_0)^2 & where\ 0 \leq \varepsilon \leq 2\varepsilon_1 \\ K_2(L - (1 + \varepsilon_1)L_0 & where\ \varepsilon \geq 2\varepsilon_1 \end{cases}$$

where ε represents ACL bundle strain, ε_1 represents the non-linear strain parameter for the amount of strain that transitions from the toe region to the linear region, K_1 represents the stiffness coefficient for the toe region, K_2 represents the linear region stiffness coefficient, L represents the length of the ACL bundle, and L_0 represents the slack length. The slack length is determined by the following equation:

$$\varepsilon_r = \frac{L_r - L_0}{L_0}$$

where ε_r is the reference strain and L_r is the length of the ACL bundle at the reference position which is determined at full extension. The non-linear strain parameter, stiffness coefficients, and reference strain were obtained from previous studies (Checa et al., 2008; C.-H. Yu et al., 2001) (Table 2).

Table 2: Input parameters for non-linear spring models.

Bundle	ε_1 (%)	K1 (N/mm^2)	K2 (N/mm)	ε_r (%)
AM	3	22.48	83.15	0
PL	3	26.27	83.15	5.1

The insertion sites of the ACL bundles were determined based on bony landmarks with the help of an orthopaedic surgery resident (Petersen & Zantop, 2007; Zantop, Petersen, & Fu, 2005). Each ACL bundle was modeled as eleven non-linear springs from the selected insertion site vertex on the one bone surface model to the other selected insertion site vertex on the other bone surface model and the next closest five vertices (Figure 4.2). The different insertion sites accounted for the possible variation in forces due to location within insertion site footprint. The forces from the AM and PL bundles in the mean knee at full extension varied within 5% (Table 3).

Table 3: Forces in the AM bundle at different points in the insertion site footprints. The first row refers to vary position of the insertion site on the femur and the second row refers to the tibial insertion site. The first force is the force in the spring at both initially selected insertion sites (N).

<table>
<tr><td>Femur Insertion Site</td><td rowspan="2">144.3</td><td>147.1</td><td>142.4</td><td>138.2</td><td>145.0</td><td>150.8</td></tr>
<tr><td>Tibial Insertion Site</td><td>150.9</td><td>145.6</td><td>158.5</td><td>145.0</td><td>153.2</td></tr>
</table>

A)

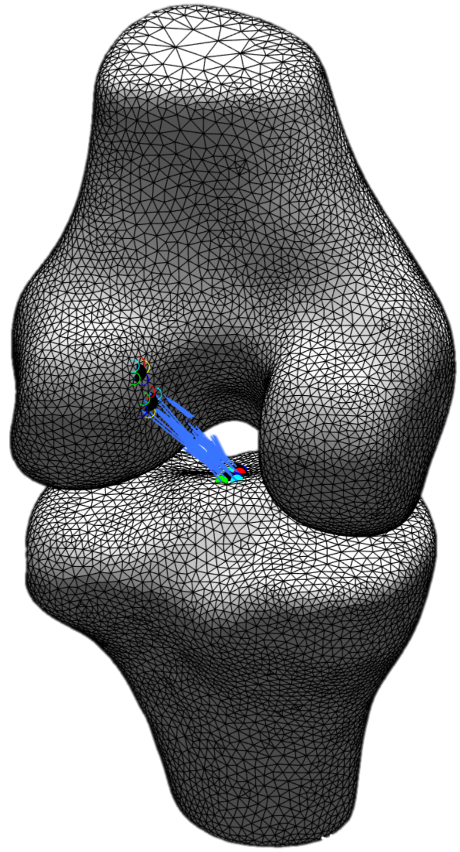

B)

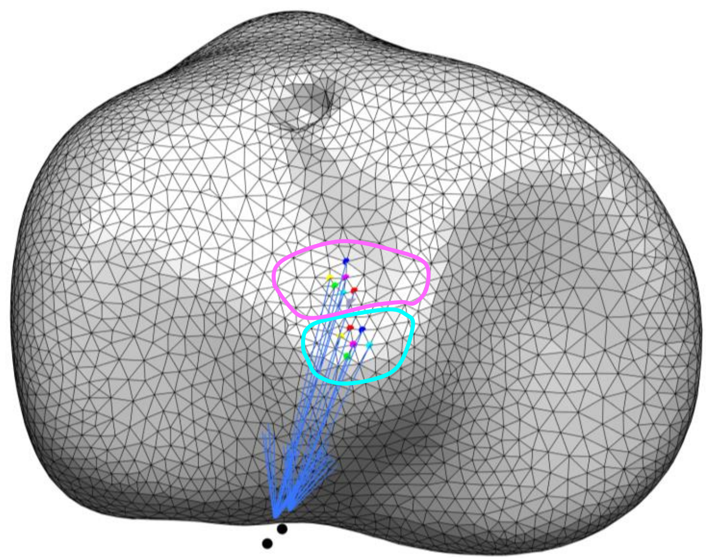

Figure 4.2: A) Posteriorly oblique view of the nonlinear springs, B) superior view of the ACL insetion on the tibial plateau within the bundle footprints outlined (magneta for the AM bundle and cyan for the PL bundle).

The reference position was determined by aligning the distal femur and proximal tibia with short film x-rays of knees at full extension (Figure 4.3). The femur was consistently aligned proximally from the tibial plateau by the average meniscal width. Local coordinate systems for the tibia and femur were defined to establish a joint coordinate system (Grood & Suntay, 1983). Translations and rotations in response to an anterior load were prescribed to the knee at full extension, 30°, 60°, and 90° (Gabriel, Wong, Woo, Yagi, & Debski, 2004). Passive motion of the tibiofemoral joint through flexion was included before translations and rotations according to a previous study (Wilson, Feikes, Zavatsky, & O'connor, 2000). Passive motion was included so that the knee models were in the position seen clinically whereas not including these motions would have the relative prescribed displacement, but not be the tibia would not be in the correct place with regard to the femur affecting the distance between the insertion sites.

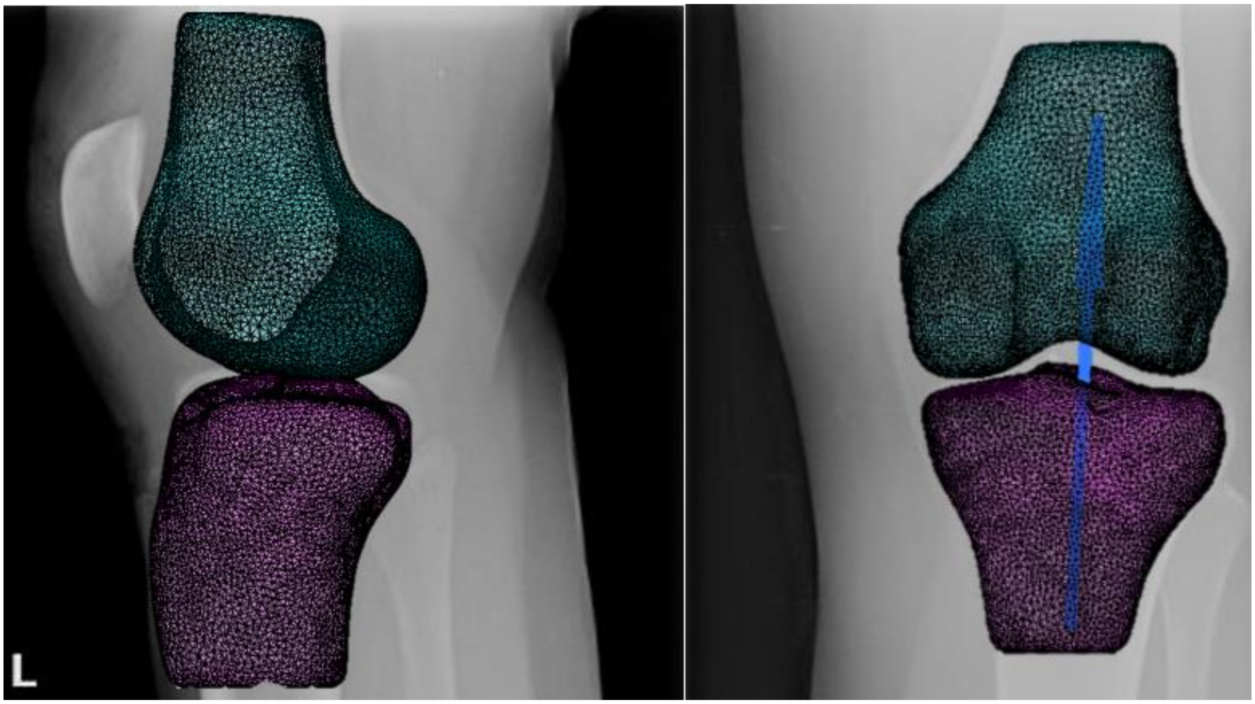

Figure 4.3: Lateral and anterior view of a femur and tibia aligned with a short film x-ray of a knee in full extension.

4.1.3 Results

Forces in the AM and PL bundles of the ACL varied in response to the displacements and rotations due to a 134N anterior load for varying bony morphology (Table 4-9). No differences were found in the forces in either bundle of the ACL for the bony morphologies at full extension. Smaller anterior-posterior length in the tibial plateau, which associated with ACL injured subjects, resulted in over 43% greater force in the AM bundle and over 76% greater force in the PL bundle at 30°, 60°, and 90° compared to the larger anterior-posterior length of the tibial plateau, which associated with uninjured subjects. The AM and PL bundle forces of the tibia with the smaller anterior-posterior length of the tibial plateau increased 30° and 60° compared to full extension whereas the tibia with the longer anterior-posterior length of the tibial plateau had the forces decrease through flexion.

Table 4: Forces in the AM bundle in response to the displacements and rotations due to a 134N anterior load in tibial bony morphology with varying anterior-posterior lengths.

	ACL Injured	Mean	Uninjured
Full extension	150	147	146
30°	185	108	104
60°	177	121	82
90°	28	12	7

Table 5: Forces in the PL bundle in response to the displacements and rotations due to a 134N anterior load in tibial bony morphology with varying anterior-posterior lengths.

	ACL Injured	Mean	Uninjured
Full extension	199	193	189
30°	141	67	33
60°	120	80	18
90°	73	66	11

A smaller angle between the femoral long axis and the femoral condylar axis, which associated with uninjured subjects, resulted in over 32% greater force in the AM bundle and over 53% greater force in the PL bundle at 30°, 60°, and 90° compared to the greater angle between the femoral long axis and the femoral condylar axis, which associated with ACL injured subjects. The joint with the femur with a smaller angle between the femoral long axis and the femoral condylar axis had the forces in the AM bundle increase through 60° of flexion. The AM and PL bundle forces of the joint with smaller angle between the femoral long axis and the femoral condylar axis decrease through flexion.

Table 6: Forces in the AM bundle in response to the displacements and rotations due to a 134N anterior load in femoral bony morphology with varying angles between the femoral long axis and the femoral condylar axis.

	ACL Injured	Mean	Uninjured
Full extension	148	147	152
30°	122	108	180
60°	123	121	189
90°	20	12	34

Table 7: Forces in the PL bundle in response to the displacements and rotations due to a 134N anterior load in femoral bony morphology with varying angles between the femoral long axis and the femoral condylar axis.

	ACL Injured	Mean	Uninjured
Full extension	194	193	191
30°	74	67	160
60°	79	80	197
90°	83	66	162

A more lateral mechanical axis, which associated with ACL injured subjects, resulted in over 34% greater force in the AM bundle at 60° and 90° and resulted in over 42% greater force in the PL bundle at 30°, 60°, and 90° compared to the less lateral mechanical axis, which associated with uninjured subjects. The force of the AM bundle of femur with the more lateral mechanical axis increases at 60° of flexion while the force in the PL bundle decreases through flexion.

Table 8: Forces in the AM bundle in response to the displacements and rotations due to a 134N anterior load in femoral bony morphology with varying mechanical axis location.

	ACL Injured	Mean	Uninjured
Full extension	139	147	133
30°	152	108	137
60°	201	121	131
90°	106	12	5

Table 9: Forces in the PL bundle in response to the displacements and rotations due to a 134N anterior load in femoral bony morphology with varying mechanical axis location.

	ACL Injured	Mean	Uninjured
Full extension	201	201	188
30°	98	98	56
60°	80	80	21
90°	77	77	0

4.1.4 Discussion

Seven computational models of knees with varying bony morphology were created from a statistical shape model that differentiated features of ACL injured subjects and uninjured subjects. The displacements and rotations due to a 134N anterior load of an intact knee were prescribed to these models and the force in the ACL was determined by modeling the AM and PL bundles as non-linear springs. The bony morphological parameters that associated with ACL injury differed at 30°, 60°, and 90°, however no differences were found at full extension. From 30° to 90° of flexion, the forces in the ACL were greater for two of the bony morphological features that associated with ACL injury and greater for one of the bony morphological features that associated with uninjured knees.

A smaller anterior-posterior length of the tibial plateau, risk factor for ACL injury, resulted in a greater force in this model compared to a longer anterior-posterior length. This greater force in the ACL in this bony morphological feature supports the findings of Aim 1 that it is a risk factor for ACL injury. However, the force was not found to be greater at full extension where knees are at greatest risk for ACL injury (Boden et al., 2010). A smaller anterior posterior length may also increase risks of instability due to the decreased area of potential bony contact as well increased risk of anterior subluxation which occurs during ACL injury.

A more lateral mechanical axis of the femur resulted in greater forces in the ACL in this model compared to the knee with less lateral mechanical axis supporting the findings of Aim 1. Like the anterior-posterior length, no difference was found at full extension. The more lateral mechanical axis might also have a greater effect on knee kinematics in response to external loads based on the possibly shifted center of pressure which could occur as the mechanical axis is more lateral and thus the force of body weight through the femur shifts laterally. This model does not consider that lateral shift of the force of the body weight which might add additional influence on knee mechanics.

A greater angle between the femoral long axis and the femoral condylar axis resulted in greater forces in this model compared to the knees with a smaller angle between the femoral long axis and the femoral condylar axis. This differs from the other results and our hypothesis as a smaller angle between the femoral long axis and the femoral condylar axis is a risk factor for ACL injury. One possible explanation for this result is that the bony morphological feature may be at a possible risk for hyperextension that is not shown in the model due to the alignment process of the long axes. This risk of hyperextension would because of the possibility of the femur rolling forward based on the difference in angle between the femoral condylar axis and the tibial slope. Furthermore, the decreased area of contact due to the difference between the angle between the femoral condylar axis and the tibial slope may also increase risk of instability.

Several limitations of this study exist. This model was displacement driven based on the intact kinematics in response to 134N anterior load instead of a force driven model. This choice was made to simplify the model and allow comparisons between conditions. Comparing the forces in the ACL when the knees are in the same position would allow a comparative assessment of the forces whereas a force driven model could be more accurate kinematically, but it would be a more apt assessment of differences in displacements than the forces in the ACL. Another limitation is that this model does not accurately represent the previously described relationship between the AM and PL bundle at 90° of flexion where the AM bundle should take up more of the force (Gabriel et al., 2004). This might adequately be explained by the lack of inclusion of the interaction between the condylar bone and the ACL where the ACL is described as wrapping around the condyle at higher flexion angles (Song, Debski, Musahl, Thomas, & Woo, 2004). Overall, these limitations are within reason when considering that this model is designed to be purely comparative between the independent bony morphological features.

The overall magnitude of the forces determined in our model is reasonable compared to previous studies even with the stated limitations (Galbusera et al., 2014; Song et al., 2004). Furthermore, the strength of this research is its demonstration of how a bony morphological feature that associates with ACL injury can influence the force in the ACL when all other factors are equal. As a purely comparative model, this research shows that a smaller anterior-posterior length of the tibial plateau and a more lateral mechanical axis result in greater force in the ACL when in the same position as a longer anterior-posterior length of the tibial plateau and a less lateral mechanical axis.

Overall, two bony morphological risk factors for ACL injury resulted in increased ACL force when modeled as a non-linear spring in response to the displacements and rotations due to a 134N anterior load while one femoral bony morphological risk factor did not. These models show that bony morphology can play a role in the force borne in the ACL in response to external loads but does not completely capture the multifaceted nature of what makes the bony morphological features risk factors for ACL injury. One future direction of this research is a force driven model instead of a displacement driven model to see the effect of isolated tibiofemoral bony morphological features on knee motion. Another future direction of this research would be to model the bundles of the ACL as continuum elements instead of springs to determine the stresses throughout different regions of the ACL.

5.0 Aim 3: The Effect of Tibiofemoral Bony Morphology on Additional ACL Injury Treatment Options

5.1 Aim 3a: The Effect of Functional Knee Bracing on Knee Mechanics

5.1.1 Introduction

Anterior cruciate ligament injuries are very common among the athletic population and various treatment options and preventative measures are prescribed in order to address or reduce the risk of these injuries (Bradley et al., 2002; Mather et al., 2013; Nessler, Denney, & Sampley, 2017; Rishiraj et al., 2009). In addition to ACL reconstruction or repair, operative and non-operative options are often prescribed. These options include an additional exterior graft to reduce rotatory instability (lateral extraarticular tenodesis), strengthening of the dynamic stabilizers at the knee, and knee bracing. Knee bracing is of particular interest as there is conflicting evidence of its effectiveness as biomechanically, functional bracing has been shown to reduce valgus angulation in uninjured knees and increase flexion during jumping in ACL reconstructed knees, but no systematic review has shown a reduction in injuries clinically (E. Alentorn-Geli et al., 2014; R. J. Butler, Dai, Garrett, & Queen, 2014; Gentile et al., 2021; Marois et al., 2021; Negrin, Uribe-Echevarria, & Reyes, 2017; Perrone et al., 2019).

Functional knee bracing is often prescribed after ACL injury and reconstruction but is also prescribed as a preventative measure to provide added protection and often to prevent reinjury (Gentile et al., 2021; Guenther et al., 2021). Functional knee bracing has been shown to provide additional stability and return to ACL-deficient and ACL reconstructed to near normal knee kinematics (Marois et al., 2021; Rishiraj et al., 2009). These knee braces are designed to protect the other soft tissue structures or the graft by limiting range of motion (Cawley et al., 1989). The purpose of using the functional bracing method during conservative treatment is to provide additional stability as much as possible against rotational and translational loads on the knee joint (Guenther et al., 2021).

Previous biomechanical studies examined the effect of bracing on knee mechanics and showed that hinged-knee braces, which are the most used functional bracing method, reduce dynamic valgus angulation in the knees of healthy individuals (Gentile et al., 2021). Other studies have shown conflicting effect of knee bracing in athletic activities (Focke et al., 2020; B. Yu et al., 2004). Furthermore a lack of evidence exists on the effectiveness of knee bracing to reduce injury risk in a clinical setting (Rishiraj et al., 2009; Silvers & Mandelbaum, 2011). Therefore, the effect of functional bracing as preventative measure and a conservative treatment option for ACL injury against these external loads is of interest.

The aim of this study is to determine the effect of functional knee bracing on knee kinematics and in situ forces in the ACL. It was hypothesized that 1) functional knee brace would reduce tibial rotation and valgus rotation compared to the unbraced states and 2) functional bracing will reduce the in-situ force in the ACL in response to combined 5Nm internal and valgus torque but not in response to the anterior load or combined external and valgus torque.

5.1.2 Methods

The study used eight fresh-frozen cadaveric knees (mean age of 66.4 years; four females, four males). Each specimen was examined by a fellowship-trained sports medicine orthopaedic surgeon to exclude specimens with (1) any bony deformities, (2) any ligamentous injuries, (3) any meniscal injuries, (4) osteoarthritis greater than grade 2 as determined by the Kellgren-Lawrence grading scale (Katakura et al., 2019; Novaretti, Herbst, Chan, Debski, & Musahl, 2021), or (5) chondral injuries greater than grade 2 according to the International Cartilage Repair Society grading system. The femur and the tibia were cut 20 cm from the joint line, and the fibula was fixed to the tibia using a bicortical screw to maintain its anatomic position to allow proper function of the lateral collateral ligament during testing. The femur and the tibia were potted in an epoxy compound (Bondo; 3M, St Paul, MN) and secured within custom-made aluminum clamps.

A 6 degree-of-freedom robotic testing system that was designed for assessment of knee joint biomechanics (MJT model FRS2010) applied loads to the knee during continuous flexion and allowed unconstrained knee motion (Figure 5.1). To provide feedback to the controller, a universal force-moment sensor (UFS) (ATI Delta IP60, SI-660-60) was used. A LabView Program (Technology Services Inc) was used to control the robotic testing system. The position repeatability of the robotic manipulator was determined to be less than ±0.015 mm and ±0.01°, whereas the measurement uncertainty of the UFS was approximately 1% of full scale (accuracy) (Bell et al., 2015).

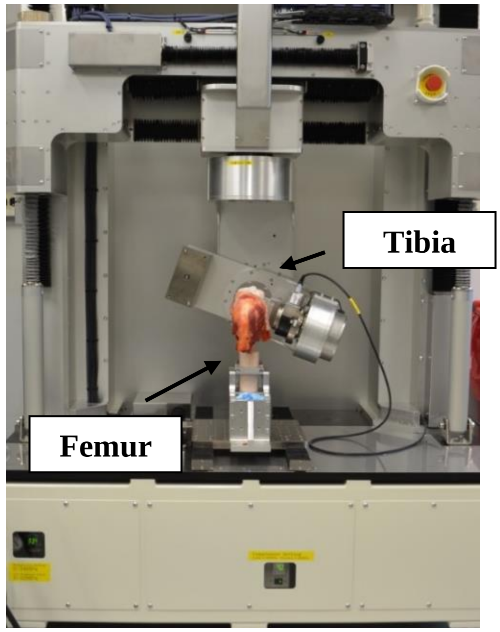

Figure 5.1: Six degree-of-freedom robotic testing system utilizing a universal force/moment sensor viewing the mounted knee flexed to 90° of flexion from an anterior view.

The knees were mounted in the robotic testing system and the path of passive flexion–extension of the intact knee was then determined from full extension to 90° of flexion while the forces and moments were continuously minimized. This passive path was then repeated five times to precondition the knee prior mechanical loading (Bell et al., 2015). Three loading conditions were applied to each knee at full extension, 30°, 60°, and 90° of flexion and the resulting kinematics which were defined using the Grood-Suntay joint coordinate system were recorded (Grood & Suntay, 1983). The three loading conditions were (1) 134-N of anterior tibial load, to simulate and anterior drawer, (2) 5-Nm internal tibial torque combined with 5-Nm of valgus torque, to simulate a pivot shift, and (3) 5-Nm external tibial torque combined with 5-Nm valgus torque at rates of 1.5 mm/s or 1.5 deg/s. To remove the viscoelastic effects of the soft tissue, the specimens were cycled through the loads five times and the fifth cycle was used for the analysis.

The knees were tested at the native state and with a functional brace. The ACL was transected arthroscopically so that the in-situ force of the ACL was determined in each state using the principal of superposition.

Brace Attachment

A DonJoy Playmaker II was modified for use within the constraints of the robotic testing system for this research. The main constraining factor was the distance between the inferior edge of the femoral clamp and the superior edge of the tibial clamp. Since the length of the brace was less than the distance between the clamps the brace arms were cut and modified to allow for a rigid attachment between the brace arms and the robotic clamps which rigidly clamped to the knee (Figure 5.2). This attachment methodology replicated an "ideal" functional knee brace as a rigid connection between the brace and the leg would be the optimal function of a knee brace according to the collaborating physical therapists and orthotic specialists. The flexion axis of the functional knee brace was aligned with the flexion axis of the knee to replicate the way the braces were implemented clinically with the help of orthotists and a physical therapist. To achieve this the femoral insertion sites of the MCL and the LCL were marked and the center of the hinges of the braced were set to the same height.

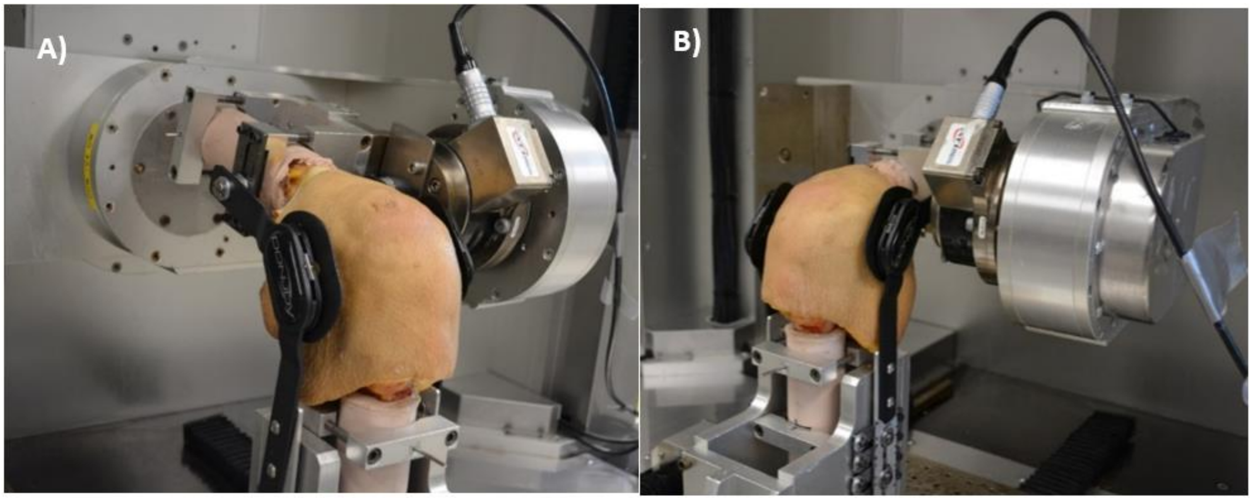

Figure 5.2: A) lateral and B) medial oblique views of the modified functional knee brace rigidly connected to the robotic clamps simulating the "ideal" knee brace.

Misalignment of the flexion axis of the knee brace with the flexion of the axis has been shown to not detrimentally alter gait mechanics (Singer & Lamontagne, 2008). However, to make conclusions from results of this study, the repeatability of the brace placement and the effect of possible misalignment is important to determine. A preliminary analysis was performed to assess the effect of the inferior-superior alignment of the knee flexion axis with the knee brace flexion axis. The alignment of the knee brace was set in three configurations: in line with the knee flexion axis, 5 mm superior of the knee flexion axis, and 5 mm inferior of the knee flexion axis. The alteration distance was chosen from a repeatability analysis on the placement of the knee brace on the experimental set up where the maximum deviation from one set position to another was 5 mm when trying to align the brace with the flexion axis of the knee. An isolated 5-Nm valgus torque was applied to the three configurations to determine the effect of the misalignment on knee kinematics.

Statistical Analysis

Shapiro-Wilk normality tests were performed to each distribution of data to test for normality which found that the distributions were not normal and thus non-parametric statistical analyses were required. Wilcoxon sign-ranked tests were performed at each flexion angle to compare kinematic outcomes and in-situ force in the ACL in response to the external load between the native, unbraced state and the braced state.

5.1.3 Results

Alignment Analysis

In response to the isolated 5-Nm valgus torque, the root mean squared deviations of the kinematic curves of the correctly applied brace to kinematic curves of the misaligned brace were less than 1 mm and less than 1 degree (Table 10).

Table 10: The root mean squared deviations from the kinematic response of the configuration with the knee brace in line and the configurations with the knee brace misaligned in each degree of freedom in response to an isolated 5-Nm valgus torque.

Root Mean Squared Deviation		
Degree of Freedom	**Misaligned Superior 5 mm**	**Misaligned Inferior 5 mm**
ML	0.1	0.1
VV	0.3	0.1
AP	0.9	0.5
IE	0.8	0.3

Effect of Brace Analysis

The application of a functional brace significantly increased the resultant anterior translation in the native knee at full extension by 0.9 mm ($p < 0.05$) (Figure 5.3a). At 60° of flexion, the application of a functional knee brace significantly decreased anterior translation by 1.0 mm ($p < 0.05$). The functional brace had no significant effect on lateral translation in response to the 134-N anterior load (Figure 5.3b). No significant effect of functional bracing was found in the internal and varus/valgus rotations (Figure 5.3c and 5.3d). Furthermore, no significant differences were found in the in-situ ACL force in response to the 134-N anterior load between the braced state and the braced state (Figure 5.4).

A)

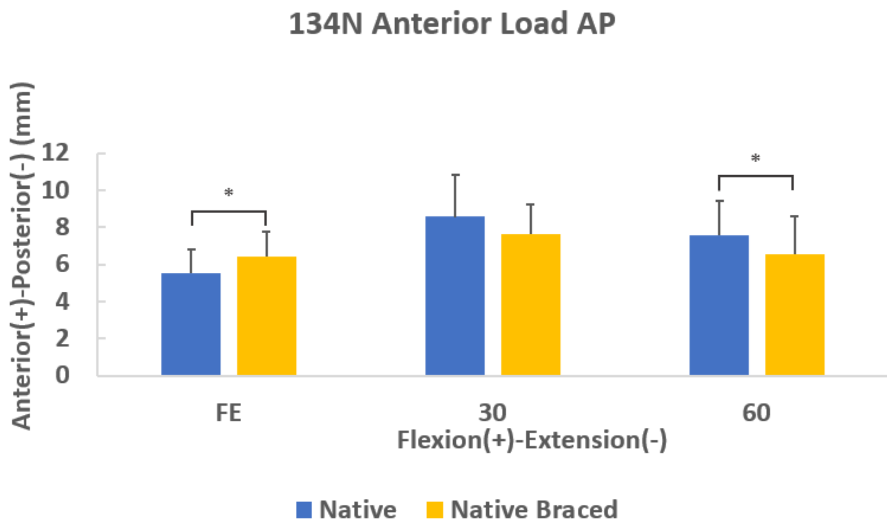
134N Anterior Load AP
Anterior(+)-Posterior(-) (mm)
12
10
8
6
4
2
0
*
*
FE
30
60
Flexion(+)-Extension(-)
Native
Native Braced

B)

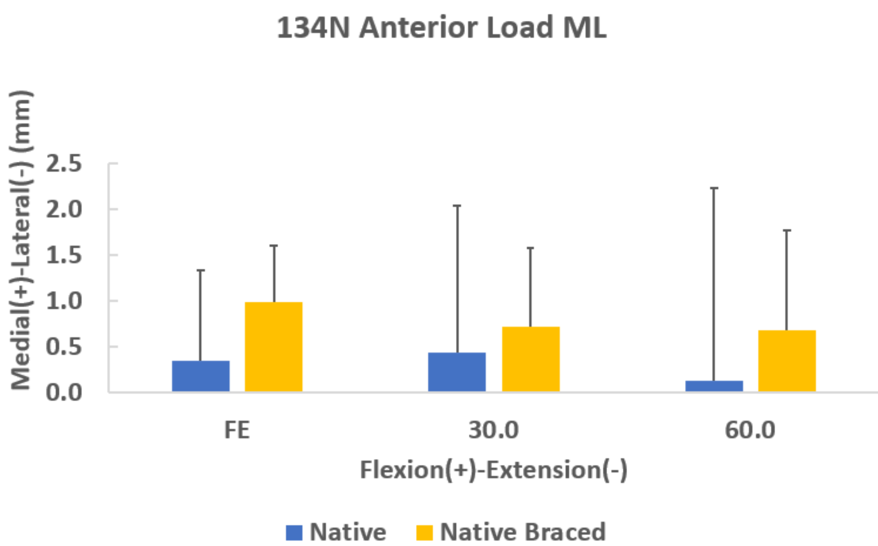
134N Anterior Load ML
Medial(+)-Lateral(-) (mm)
2.5
2.0
1.5
1.0
0.5
0.0
FE
30.0
60.0
Flexion(+)-Extension(-)
Native
Native Braced

C)

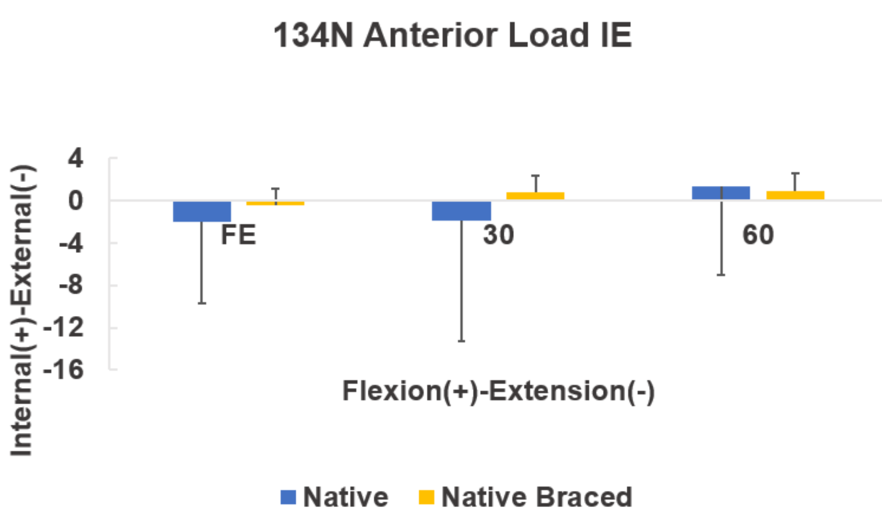
134N Anterior Load IE
Internal(+)-External(-)
4
0
-4
-8
-12
-16
FE
30
60
Flexion(+)-Extension(-)
Native
Native Braced

D)

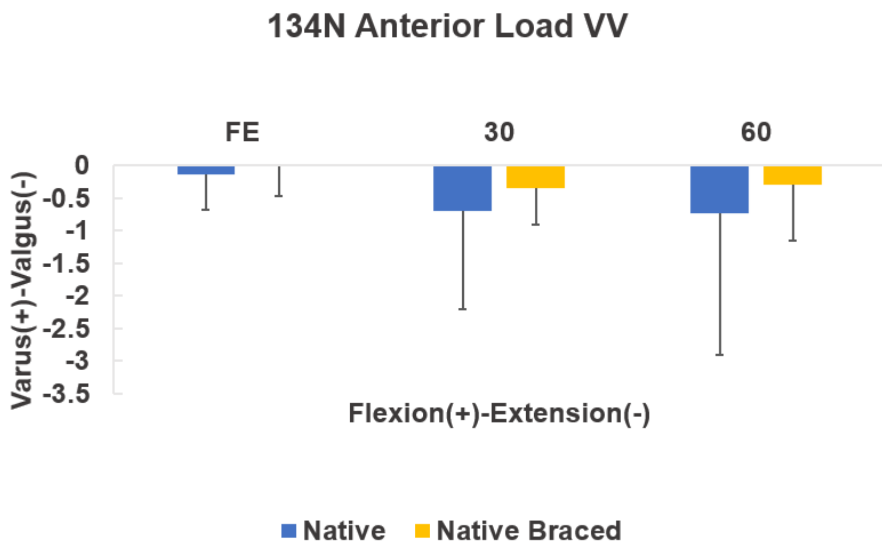

Figure 5.3: Kinematic responses to a 134-N anterior load at each knee state at full extension, 30°, and 60° of flexion: A) anterior-posterior translation, B) medial-lateral translation, C) internal-external rotation, D) varus-valgus rotation. * denotes significantly different from the native state.

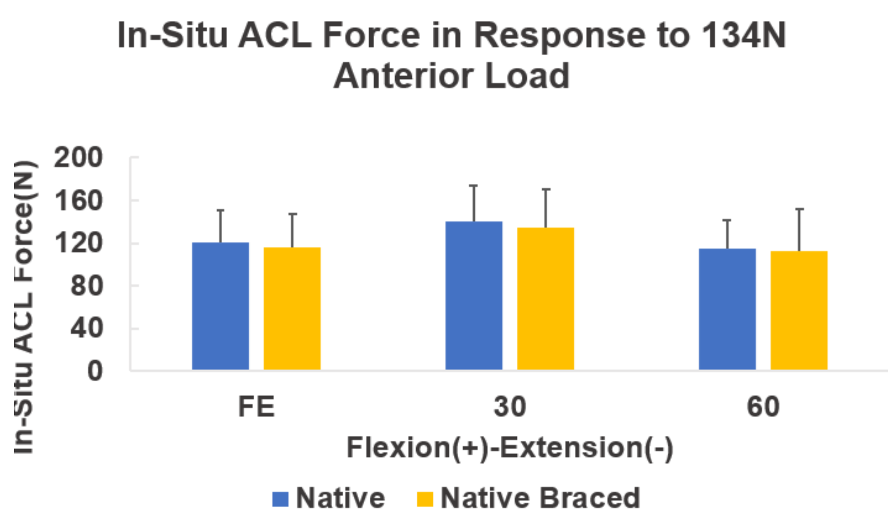

Figure 5.4: In-situ force in the ACL in response to a 134N anterior load at full extension, 30°, and 60° of flexion. * denotes significantly different from the native state.

In response to a 5-Nm internal valgus torques simulating a pivot shift, functional knee brace had no significant effect on anterior translation or lateral translation (Figure 5.5a and 5.5b). In response to the simulated pivot shift, functional knee bracing significantly decreased internal rotation at full extension, 30°, and 60° by 9.3°, 16.7°, and 20.2°, respectively ($p < 0.05$) (Figure 5.5c). The functional knee brace significantly decreased valgus rotation at this loading condition at 60° of flexion by 2.8° ($p < 0.05$) (Figure 5.5d). At full extension and 30° of flexion, the functional knee brace significantly decreased ACL force in response to the simulated pivot shift by 40.2 and 31.8 N, respectively ($p < 0.05$) (Figure 5.6).

A)

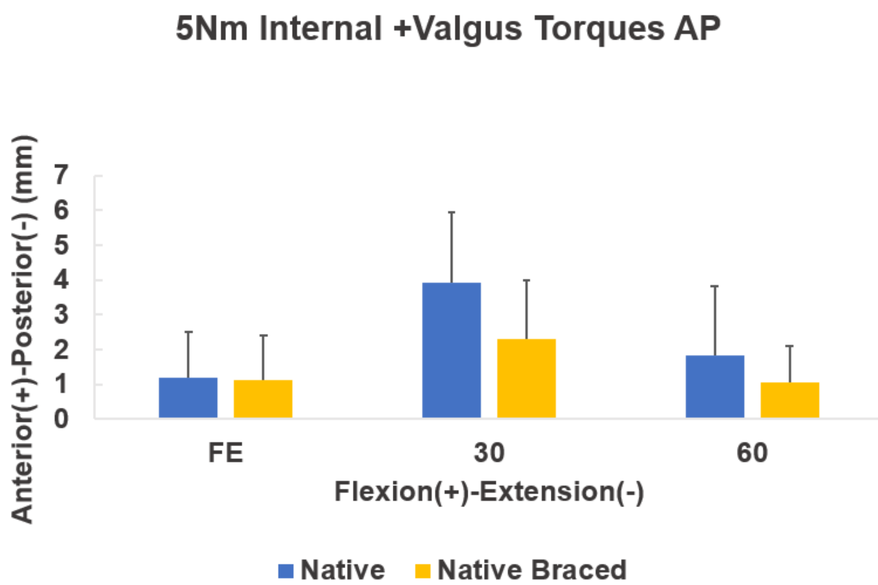
5Nm Internal +Valgus Torques AP
Anterior(+)-Posterior(-) (mm)
7
6
5
4
3
2
1
0
FE
30
60
Flexion(+)-Extension(-)
Native
Native Braced

B)

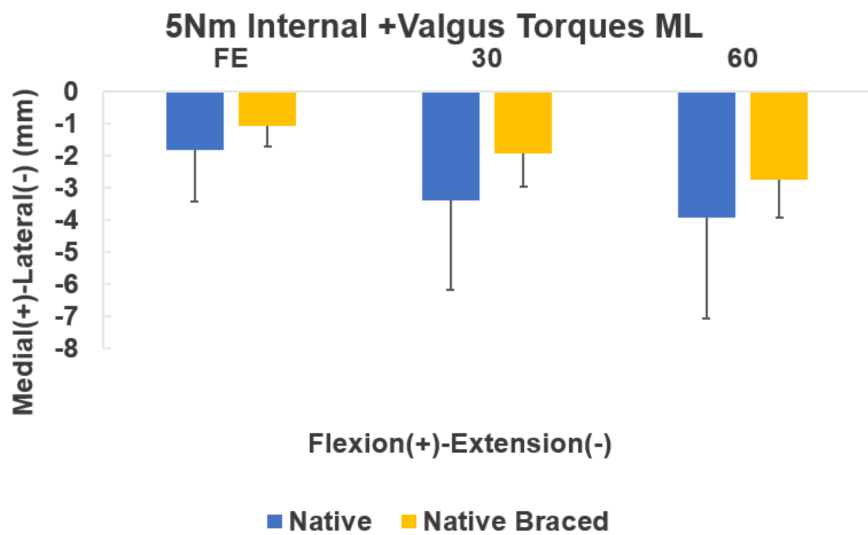
5Nm Internal +Valgus Torques ML
FE
30
60
0
-1
-2
-3
-4
-5
-6
-7
-8
Medial(+)-Lateral(-) (mm)
Flexion(+)-Extension(-)
Native
Native Braced

C)

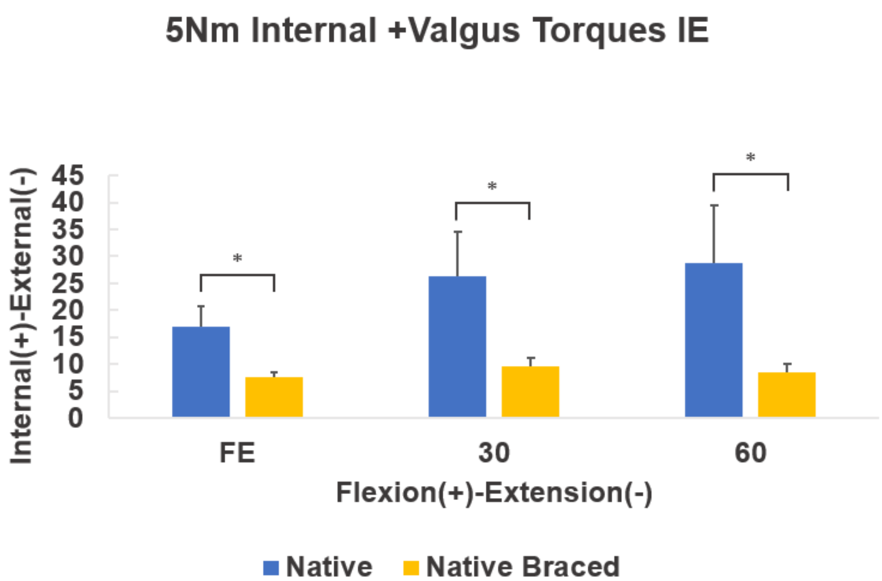

D)

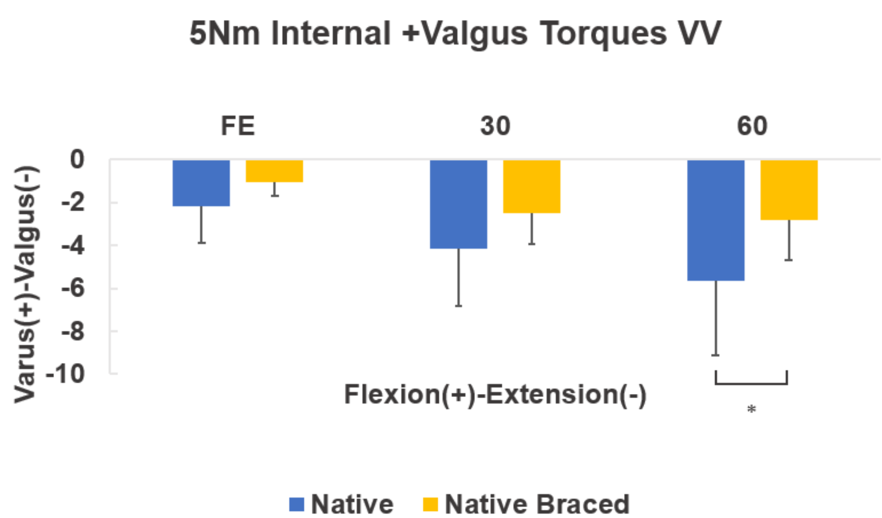

Figure 5.5: Kinematic responses to 5-Nm internal and valgus torques at each knee state at full extension, 30°, and 60° of flexion: A) anterior-posterior translation, B) medial-lateral translation, C) internal-external rotation, D) varus-valgus rotation. * denotes significantly different from the native state.

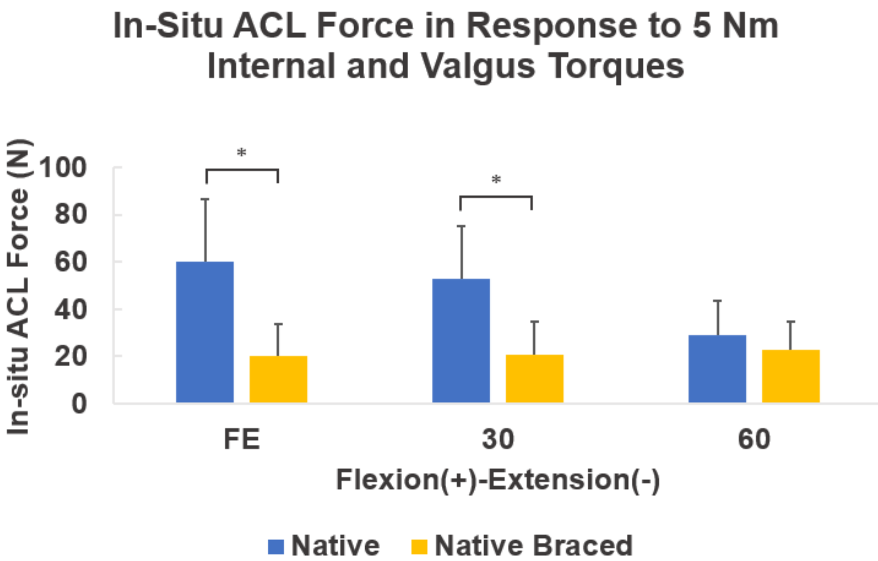

Figure 5.6: In-situ force in the ACL in response to 5-Nm internal and valgus torques at full extension, 30°, and 60° of flexion. * denotes significantly different from the native state.

In response to the 5-Nm external and valgus torque, the functional knee brace had no significant effect on anterior-posterior, medial-lateral translation, and varus/valgus rotation (Figure 5.7a, 5.7b and 5.7d). The functional knee brace significantly decreased external rotation at full extension, 30°, and 60° of flexion by 7.6°, 9.8°, and 9.0°, respectively ($p < 0.05$) (Figure 5.7c). The application of the functional brace significantly decreased the in-situ force in the ACL at full extension by 16.4 N ($p < 0.05$) (Figure 5.8).

A)

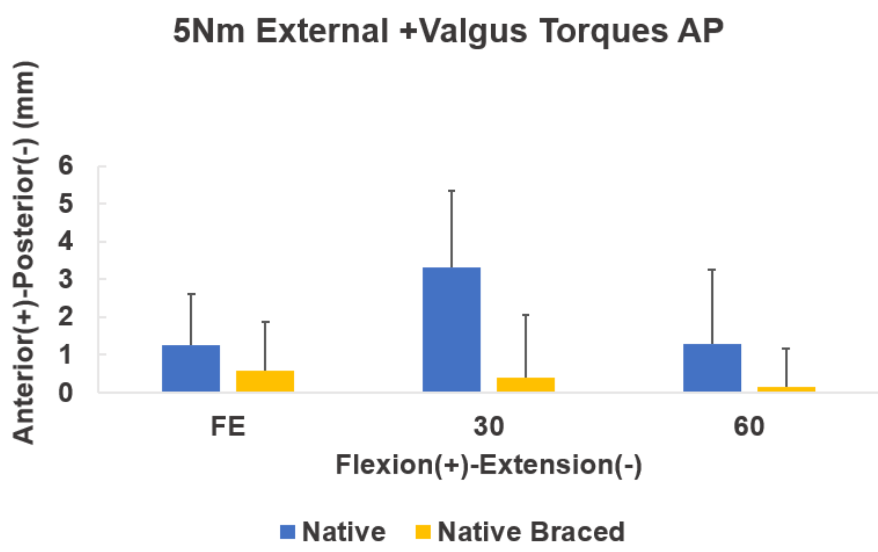

5Nm External +Valgus Torques AP
Anterior(+)-Posterior(-) (mm)
6
5
4
3
2
1
0
FE
30
60
Flexion(+)-Extension(-)
Native
Native Braced

B)

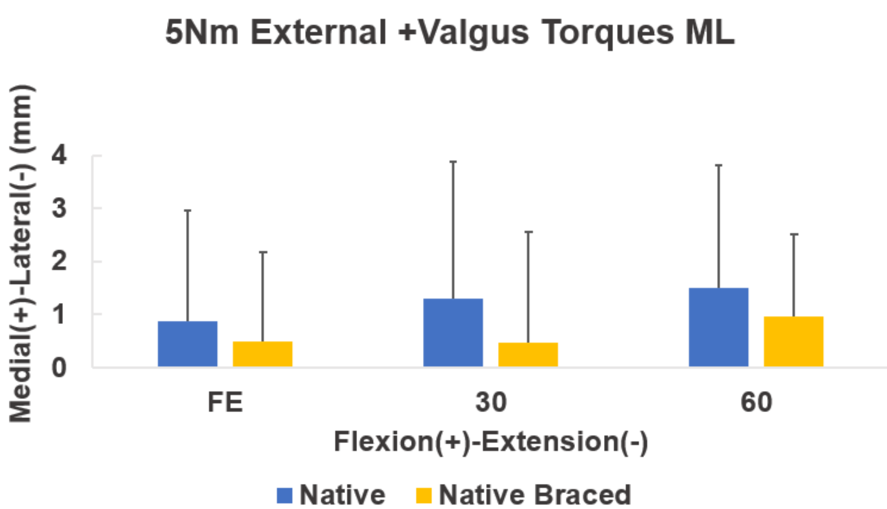

5Nm External +Valgus Torques ML
Medial(+)-Lateral(-) (mm)
4
3
2
1
0
FE
30
60
Flexion(+)-Extension(-)
Native
Native Braced

C)

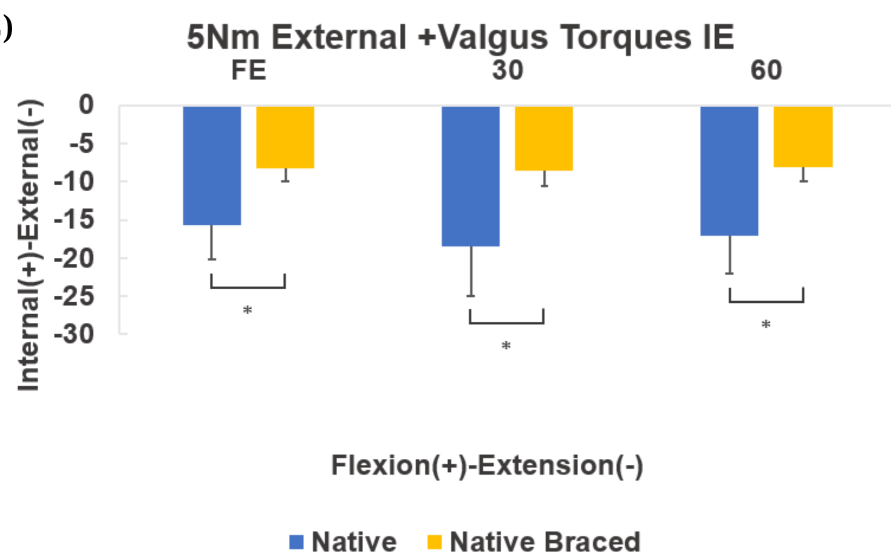

5Nm External +Valgus Torques IE
FE
30
60
Internal(+)-External(-)
0
-5
-10
-15
-20
-25
-30
*
*
*
Flexion(+)-Extension(-)
Native
Native Braced

D)

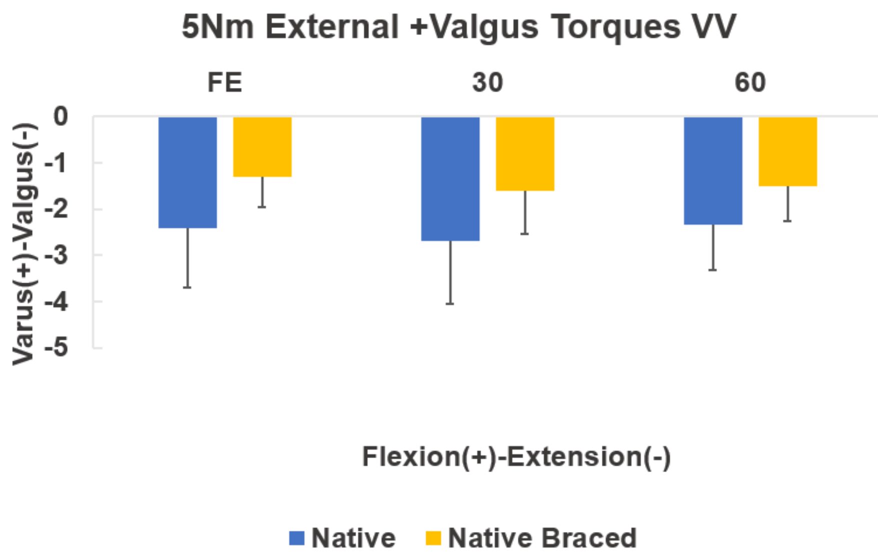

Figure 5.7: Kinematic responses to 5-Nm external and valgus torques at each knee state at full extension, 30°, and 60° of flexion: A) anterior-posterior translation, B) medial-lateral translation, C) internal-external rotation, D) varus-valgus rotation. * denotes significantly different from the native state.

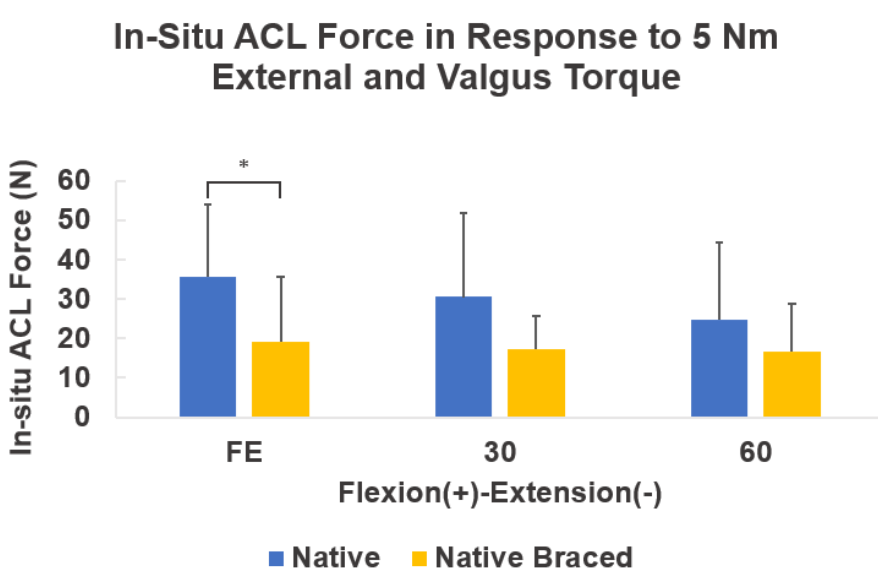

Figure 5.8: In-situ force in the ACL in response to 5-Nm external and valgus torques at full extension, 30°, and 60° of flexion. * denotes significantly different from the native state.

5.1.4 Discussion

The preliminary analysis on brace alignment demonstrated that misalignment of the brace by 5 mm superiorly or inferiorly resulted in deviations less than 1 mm and less than 1 degree which is not clinically significant and thus within acceptable parameters for the research protocol. The primary function of the ACL is to prevent anterior tibial translation, so an anterior drawer is often performed clinically to test the injury status of the ACL. Therefore, a simulated anterior drawer without and without functional bracing was performed on each knee to determine the effectiveness of the brace to prevent anterior translation. The results of this research show that the functional knee brace provides little to no prevention of anterior translation. The statistical analysis of the data determined that the functional brace had a significant effect on anterior translation at full extension and 60° of flexion; however the differences in anterior translation between those braced and unbraced states was less than 2 mm and thus likely not clinically relevant as 3 mm is the side-by-side difference between uninjured contralateral knees that indicates stable knees (Myrer, Schulthies, & Fellingham, 1996). Furthermore, no differences were found in the in-situ forces in the ACL in response to the 134-N anterior load demonstrating that the functional brace had minimal effect on the knee in response to loads in the anterior direction.

A common injury mechanism for ACL injury is a combination of internal and valgus rotation matching the pivot shift, a clinical exam for ACL injuries setting the premise for the second loading condition (Kobayashi et al., 2010; Tanaka et al., 2012). In response to the simulated pivot shift, the functional knee brace provided additional rotatory knee stability. This added stability shows that functional bracing may address the persistent rotatory instability found after ACL injury and subsequent reconstruction. Furthermore, in response to the simulated pivot shift at full extension and 30° of flexion, the functional brace reduced the in-situ force in the ACL up to 66.8%. These results show that while the functional knee brace may do little to prevent anterior translation and possibly anterior subluxation, the added rotatory stability may reduce risk for ACL injury in response to the most common mechanism of injury and also prevent the knee from being in the provocative position that leads to the anterior subluxation that occurs with ACL injury (Boden et al., 2010).

Since MCL injuries are commonly concomitant with ACL injuries and a common mechanism for MCL injury is a combination of valgus and external rotations (Phisitkul, James, Wolf, & Amendola, 2006), a combination of 5-Nm valgus and external torques were applied to the knees with and without functional bracing to determine the effectiveness of the bracing in the injury mechanism. The results of our study show that functional bracing provides additional rotatory stability by reducing the external rotation up to 53.3%. However no significant reduction in the valgus rotation due to the knee brace was determine. Therefore, while the functional knee brace may provide additional rotatory stability in response to external rotation, it may not provide the intended protective effect to the MCL.

The effect of functional knee bracing after superficial MCL injury was originally part of the testing protocol. A 4 cm skin and subcutaneous incision was made distally from the tibia-femoral joint line, in the midline of the posteromedial edge of the tibia and the tibial tubercle. Pes anserinus was found 4-6 cm distal to the tibia-femoral joint line. The interval where the bursa is located between the pes anserinus and the tibia was entered from the superior border of the pes anserinus with the help of surgical scissors. The pes anserinus was preserved with the help of an army-navy retractor and retracted anteriorly. A transverse incision was made 4-5 cm distal to the tibia-femoral joint line. Valgus stress test was performed, and instability was observed. Unfortunately, this injury model failed to create an injury to the superficial MCL in a repeatable manner. Therefore, future research following the workflow laid out in this research with a more consistent injury model would be a substantial contribution to the current body of literature as it would determine the effect of functional knee bracing on the MCL and on the knee after MCL injury as this aim originally aimed to achieve.

The superficial MCL was transected in the correct manner in two of the specimens as well as twice more in pretests. In these pretests, the injury to the superficial MCL resulted in increases in internal and external rotations in response to the combined internal and valgus torques and external and valgus torques, respectively. Little increase in valgus rotation was demonstrated after the superficial MCL injury though. The deep MCL may play a greater role in valgus stability. The functional brace reduced internal and external rotations in our experiment; therefore, a superficial MCL injury may benefit from the added stability of the knee brace.

Several limitations of this research exist. Primarily, the rigid connection between the functional knee brace and the knee does not aptly represent what occurs clinically. However, given that a stiffer connection between the knee brace is desirable as it would theoretically provide more stability than what occurs clinically, the results of this research can be treated as the effect of the "ideal" knee brace which would most likely perform better than experienced in clinical practice. Another limitation of this study is the lack of dynamic loading from the muscles as increasing stabilizing muscle strength is often sought after with conservative injury treatment. The results of this study demonstrate the effect of the functional knee brace on the passive stabilizers in response to external loads and the effect of the dynamic stabilizers on the multifactorial problem that is knee injury treatment should be considered.

The results of this study show that functional knee bracing provides additional rotatory stability in response to rotatory loading conditions. Furthermore, the application of functional knee bracing may reduce the risk of ACL injury through this added rotatory stability and by reducing the force in the ACL in response to a pivot shift motion. However, the effectiveness of the bracing may vary from knee to knee. The results of this research show that the data often had high standard deviations where many comparisons were close to significantly different. These high standard deviations may be explained by the effect of varying tibiofemoral bony morphology that existed in the cohort of knees tested. Two-dimensional features of tibiofemoral bony morphology have already been shown to influence the magnitude of the pivot shift (Musahl et al., 2010). Bony morphology when analyzed 3-dimensionally may reveal more on that influence and the effect of injury and functional bracing.

5.2 Aim 3b: The Effect of Tibiofemoral Bony Morphology on The Effectiveness of Functional Knee Bracing

5.2.1 Introduction

Knee motion is primarily dependent on the bony morphology of the distal femur and proximal tibia (Hoshino et al., 2012a; Ingham, de Carvalho, Abdalla, Fu, & Lovejoy, 2017; D. Lansdown & Ma, 2018). Furthermore, the function of the anterior cruciate ligament (ACL) is dictated by the motion at the knee and thus influenced by the bony morphology. Recently, bony morphology has been shown to contribute to a higher pivot shift grade, which is a clinical exam for ACL injury (Matsumoto, 1990; Musahl et al., 2010). As this dissertation has shown, tibiofemoral morphology influences native knee mechanics. It follows that tibiofemoral bony morphology would influence knee mechanics after injury and treatment. However high standard deviation in kinematics and kinetics after treatment have been shown to occur previously as well as in Aim 3a (Novaretti, Arner, et al., 2020). Variation in bony morphology may help explain these variations and thus help clinicians know which patients might be more receptive to treatment options. However, little is known about the effects of bony morphology on knee kinematics after injury and repair, even though ACL injuries are prevalent among the young athletic population (Hewett et al., 2009).

Non-operatively, functional knee bracing is prescribed to add additional stability (Smith, LaPrade, Jansson, Årøen, & Wijdicks, 2014). Functional knee bracing has been prescribed to provide stability preoperatively to prevent further injury (Logerstedt, Lynch, Axe, & Snyder-Mackler, 2013), postoperatively, to provide additional stability to improve healing environment for the ACL (Beynnon et al., 1992), and as a treatment option to provide mechanical stability without surgery (Kocher, Sterett, Zurakowski, & Steadman, 2003). However, limited research exists showing the mechanical effect of functional bracing on knee function and ligamentous forces. Furthermore, the existing research on knee bracing has shown conflicting results on its effectiveness as no systematic review has shown bracing to reduce risk of ACL injury (E. Alentorn-Geli et al., 2014; Marois et al., 2021). Previous studies have shown with bony morphology affecting pivot shift grades (Musahl et al., 2010); these variations in results may also be influenced by variations in bony morphology.

Therefore, the objective of this aim was to analyze the effect of bony morphology with and without functional bracing on knee kinematics and in-situ forces in the ACL. It was hypothesized that bony morphological risk factors for ACL injury would correlate with greater differences between braced and unbraced kinematics and ligamentous forces in response to external loads.

5.2.2 Methods

The study used eight fresh-frozen cadaveric knees (mean age of 66.4 years; four females, four males) and was tested with a 6 degree-of-freedom robotic testing system that was designed for assessment of knee joint biomechanics (MJT model FRS2010). To provide feedback to the controller, a UFS was used to record the forces the knee joint experiences. External loads were applied to the knee during continuous flexion and allowed unconstrained knee motion utilizing the robotic testing system as described in Aim 3a.

The knees were mounted in the robotic testing system and three loading conditions were applied to each knee at full extension, 30°, 60°, and 90° of flexion and the resulting kinematics which were defined using the Grood-Suntay joint coordinate system were recorded (Grood & Suntay, 1983). The path of passive flexion–extension of the intact knee was then determined from full extension to 90° of flexion while the forces and moments were continuously minimized. The three loading conditions were (1) 134-N of anterior tibial load to simulate an anterior drawer, (2) combined 5-Nm internal and valgus torques to simulate a pivot shift, and (3) combined 5-Nm external and valgus torques at rates of 1.5 mm/s or 1.5 deg/s. The knees were tested at the native and native braced states. Biomechanical testing was performed in the two knee states and kinematics and in-situ force in the ACL were recorded in response to the loading conditions.

A statistical shape model was then created of the cadaveric knees as previously described (S. K. Polamalu et al., 2020). High resolution lower extremity computed tomography (CT) scans (0.625 mm slice thickness, 0.625 mm spacing, 512 x 512 acquisition matrix size, 300 mA at 120 kV, GE LightSpeed 16) were captured for each cadaveric knee. The distal femurs and proximal tibiae were semi-automatically segmented to include a uniform amount of their long axis using Mimics 21 (Materialise NV, Leuven, Belgium). The distal femurs were segmented so that the largest medial-lateral dimension is equal to the distance from the inferior most point to the cut on the long axis of the femur. The proximal tibiae were segmented from the most proximal point to a point distally along the long axis 90% of the largest medial-lateral dimension of the tibial plateau. Including the entire long axis of the tibia would add unwanted variability into the statistical shape model and shift the focus of the analysis. Utilizing Mimics 21 Automatic 3D Calculation function, 3-Dimensional surface models of the distal femur and proximal tibia were created. Anti-aliasing was then performed utilizing a Laplacian filter with a smoothing factor of 0.7 for three iterations. The 3-dimensional models were then exported to 3D Slicer (3D Slicer, 4.10.2, slicer.org). The femur surface models were aligned and preprocessed. The femur and tibia surface models were then exported as binary segmentations to Seg3D (Seg3D 2.2.1, https://www.sci.utah.edu/cibc-software/seg3d.html) to create uniform bounding boxes. Lastly all left femurs and tibiae were reflected as right femurs and tibiae for shape uniformity.

The eight 3-dimensional surface models were imported into Shapeworks (https://www.sci.utah.edu/cibc-software/shapeworks.html) which employs a correspondence method to analyze the variation in 3-dimensional shape (Atkins et al., 2017; Cates et al., 2007). One difficulty of statistical shape modeling is limiting the bias when using bony landmarks to determine particle placement (Chan et al., 2013; Rajamani et al., 2007; Schumann, Tannast, Nolte, & Zheng, 2010). This limitation is avoided through an automatic particle placement using a splitting strategy that randomly chooses a surface location for the first particle which is then split into two particles and repel each other along the surface until a steady state is achieved (Cates et al., 2007). This splitting process was repeated until 2,048 particles were uniformly placed on each bone in the analysis. The uniformity was optimally achieved using a gradient descent approach with a cost function while simultaneously creating a compact distribution of the correspondence of particles on the surface models. A generalized Procrustes analysis was performed throughout to optimize alignment and normalize with respect to scale (Gower, 1975).

A PCA was performed to analyze the variability of the correspondence particle placement in each configuration. The PCA reduces the dimensionality of the correspondence of particles to orthogonal descriptions of the data set while extracting information about independent bony morphological features that describe the cohort of bone shapes (Atkins et al., 2017; Cates et al., 2007). From the PCA, independent bony morphology features can be projected or mapped onto shape variability spectrums called principal components or modes of variation. This mapping called PCA loading values provides a quantitative assessment of the distal femur or proximal tibiae configurations onto each mode of variation. Each mode of variation represents an independent shape feature. The total variation in the data set is described by combining each mode of variation. The largest modes of variation that additively describe 80% of the variation among all the distal femurs or proximal tibiae were correlated with the kinematic and kinetic data from the robotic testing. The modes of variation can be visualized by generating the shape models for ±2 standard deviations for each mode of variation and then creating 3-dimensional topography plots of the differences between the distances of the surfaces when overlaid. Two orthopaedic sports medicine fellows performed an independent analysis to examine these 3-D models through visual inspection and interpret physical representations which were then reviewed by the researcher team. PCA loading values representing quantitative values of shape variation for the cadaveric knee bones on each principal component were correlated with the kinematic and kinetic parameters from the robotic testing system using Spearman's rank correlation coefficient. The kinematic and kinetic parameters of interest were the following: anterior translation in response to the anterior load, internal and valgus rotations in response to the combined internal and valgus torques, external and valgus rotations in response to the combined valgus torques, the in-situ ACL force, and the difference between the corresponding unbraced and braced states in all of the listed parameters at each knee state. Significance was set at $p < 0.05$.

5.2.3 Results

The first three femoral principal components represent greater than 90% of the shape variation in the cohort and correlated with multiple kinematic and kinetic parameters (Table 11-13). The first principal component of the femoral statistical shape model represented normalized medial-lateral width at the epicondyles (Figure 5.9). Note that the unsmooth areas on the bone models are due to noise captured within the correspondence of the statistical shape model and the smaller sample size compared to Aim 1 results in more noise. In response to the 134-N anterior load, this bony morphological feature positively correlated with differences in in-situ ACL force due to the brace at full extension. Furthermore, the normalized medial-lateral width at the epicondyle negatively correlated with anterior translation at the native state at 30° and 60° of flexion. In response to the simulated pivot shift, the normalized medial-lateral width at the femoral epicondyles negatively correlated with in-situ ACL force at the native braced state at full extension. In response to the 5-Nm combined external and valgus torques, no correlations were found.

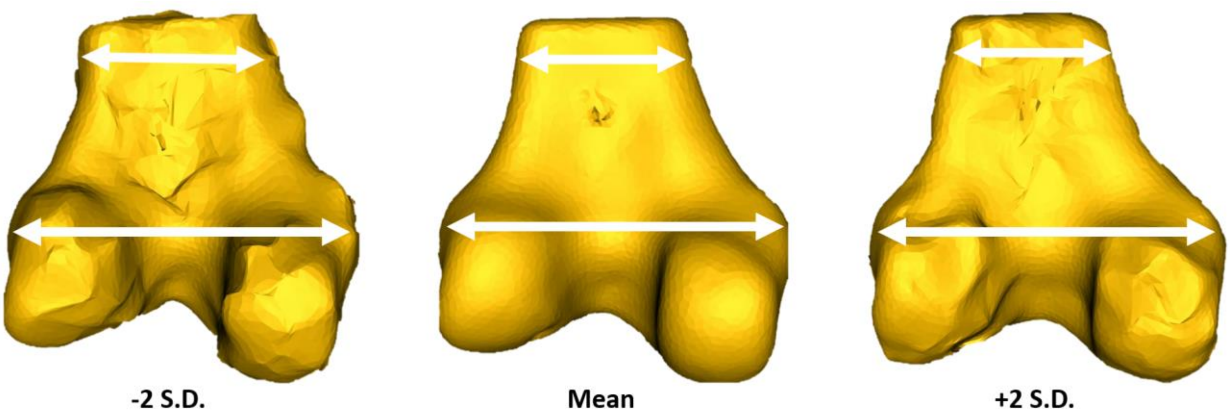

Figure 5.9: Posterior view of the first principal component of the statistical shape model of the femurs represented by 2 standard deviations away from the mean in each direction. This principal component represents variation in the normalized medial-lateral width at the femoral epicondyles.

Table 11: Spearman correlation coefficients between the PC scores associating with normalized medial-lateral width at the femoral epicondyles and kinematic and kinetic parameters from the biomechanical testing on the effect of functional bracing. ATT: anterior tibial translation.

Normalized Medial-Lateral Width at the Femoral Epicondyles			
	Anterior Load	Internal + Valgus Torques	External + Valgus Torques
Full extension	Difference in ACL force from brace, r = 0.76	Native braced ACL force, r = -0.76	N/A
30°	Native ATT, r = 0.76	N/A	N/A
60°	Native ATT, r = -0.71 Native braced ATT, r = -0.86	N/A	N/A

The second femoral principal component associated with anterior height of the lateral femoral condyle (Figure 5.10). In response to the simulated anterior drawer, the lateral femoral condylar did not correlate with any parameter. In response to the simulated pivot shift, the anterior height of the lateral femoral condyle correlated with internal rotation at the unbraced state at full extension as well as with differences of valgus rotation due to functional bracing at full extension and 30° of flexion. In response to the combined external and valgus torques, anterior height lateral femoral condyle correlated with differences in external rotation at the due to the bracing at full extension.

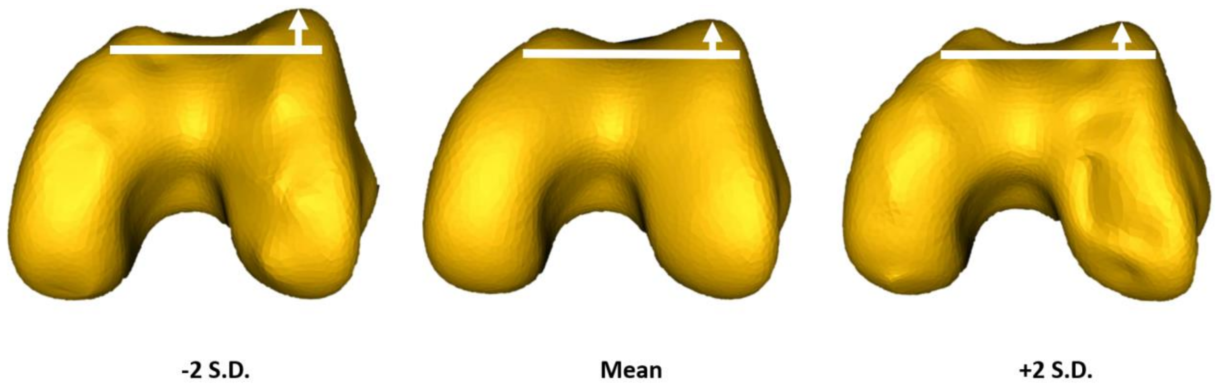

Figure 5.10: Inferior view of the first principal component of the statistical shape model of the femurs represented by 2 standard deviations away from the mean in each direction. This principal component represents variation in the anterior height of the lateral femoral condyle as depicted by the decreasing length from left to right of the arrow that originates parallel to trochlear groove and ends at the lateral femoral condyle.

Table 12: Spearman correlation coefficients between the PC scores associating with lateral femoral condyle height and kinematic and kinetic parameters from the biomechanical testing on the effect of functional bracing. IR: internal rotation, ER: external rotation, Val.R: valgus rotation.

Anterior Height of the Lateral Femoral Condyle			
	Anterior Load	Internal + Valgus Torques	External + Valgus Torques
Full extension	N/A	Native IR, r = -0.79 Difference in Val.R from brace, r = 0.83	Difference in ER from brace, r = -0.74
30°	N/A	Difference in Val.R from brace, r = 0.81	N/A
60°	N/A	N/A	N/A

The third femoral principal component correlated with femoral notch width (Figure 5.11). In response to a simulated anterior drawer, femoral notch width negatively correlated with in-situ ACL force at the native braced state at 30° of flexion and at the native state at 60° of flexion. Furthermore, it negatively correlated with the difference in anterior translation due to the brace at full extension. In response to a simulated pivot shift, the femoral notch width negatively correlated with valgus rotation at the native braced state at full extension and 60° of flexion. In response to combined external and valgus torque, no correlations were found.

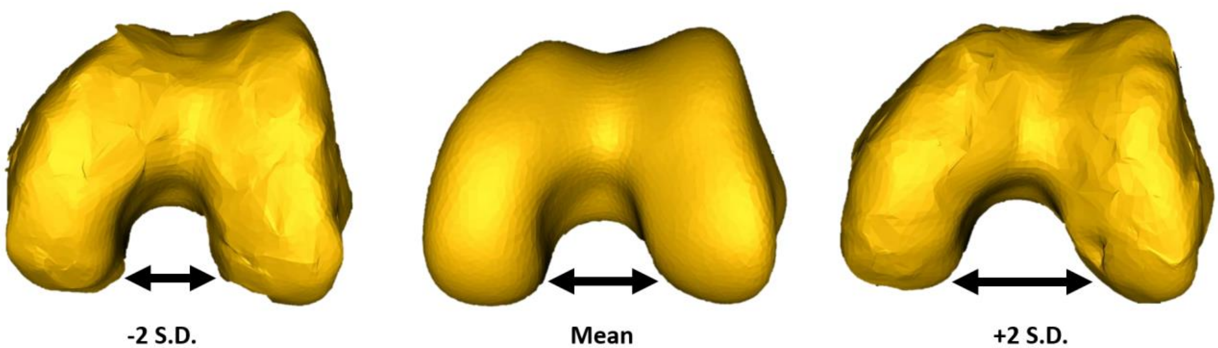

Figure 5.11: Inferior view of the first principal component of the statistical shape model of the femurs represented by 2 standard deviations away from the mean in each direction. This principal component represents variation in the femoral notch width depicted by the increase in length of the black arrow from left to right.

Table 13: Spearman correlation coefficients between the PC scores associating with femoral notch width and kinematic and kinetic parameters from the biomechanical testing on the effect of functional bracing. ATT: anterior tibial translation, Val.R: valgus rotation

Femoral Notch Width			
	Anterior Load	Internal + Valgus Torques	External + Valgus Torques
Full extension	Difference in ATT from brace, r = -0.71	Native braced Val.R, r = -0.83	N/A
30°	Native braced ACL force, r = -0.76	N/A	N/A
60°	Native ACL force, r = -0.76	Native braced Val.R, r = -0.74	N/A

The first three principal components of the statistical shape model of the tibial models represent 90% of the variation in the cohort (Table 14-16). The first tibial principal component represented variation in the tibial plateau width (Figure 5.12). In response to a 134-N anterior load, this width negatively correlated with the in-situ force in the ACL at the native braced state at 30° and 60° of flexion. Furthermore, the tibial plateau width positively correlated with anterior tibial translation at the native state at 60° of flexion. In response to combined 5-Nm internal and valgus torques, the tibial plateau width negatively correlated with valgus rotation at the native state at full extension and 30° of flexion. The tibial plateau width did not correlate with any kinematic or kinetic data from the combined external and valgus torques.

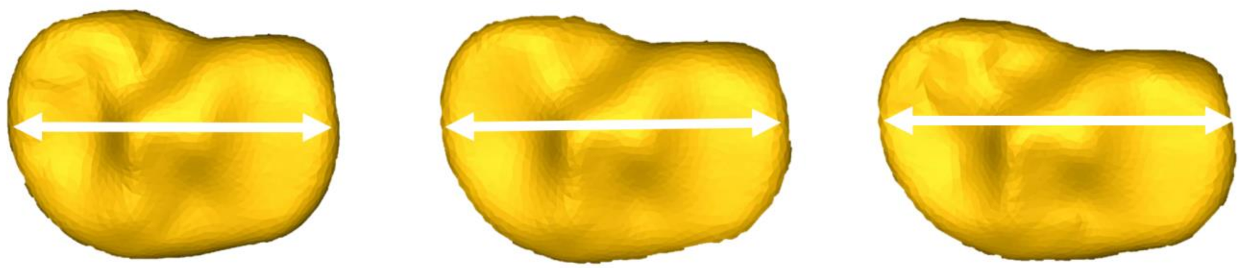

Figure 5.12: Superior view of the first principal component of the statistical shape model represented by 2 standard deviations away from the mean in each direction. This principal component represents variation in the medial-lateral width of the tibial plateau.

Table 14: Spearman correlation coefficients between the PC scores associating with tibial plateau width and kinematic and kinetic parameters from the biomechanical testing on the effect of functional bracing. ATT: anterior tibial translation, Val.R: valgus rotation.

Tibial Plateau Width			
	Anterior Load	Internal + Valgus Torques	External + Valgus Torques
Full extension	N/A	Native Val.R, r = -0.88	N/A
30°	Native braced ACL force, r = -0.71	Native Val.R, r = -0.79	N/A
60°	Native braced ACL force, r = -0.76 Native ATT, r = 0.83	N/A	N/A

The second principal component of the statistical shape model of the tibias represents variation in the tibial slope in the coronal plane (Figure 5.13). In response to a 134-N anterior load, the coronal tibial slope did not correlate with any biomechanical testing data. In response to the combined 5-Nm internal and valgus torques, this slope positively correlated with the force in the ACL at the native state at 30° of flexion. Kinematically, coronal tibial slope positively correlated with internal rotation at the native state at every flexion angle. Furthermore, the coronal tibial slope negatively correlated with the difference in valgus rotation due to the functional brace at every flexion angle. This slope did not correlate with any parameters due to the combined 5-Nm external and valgus torques.

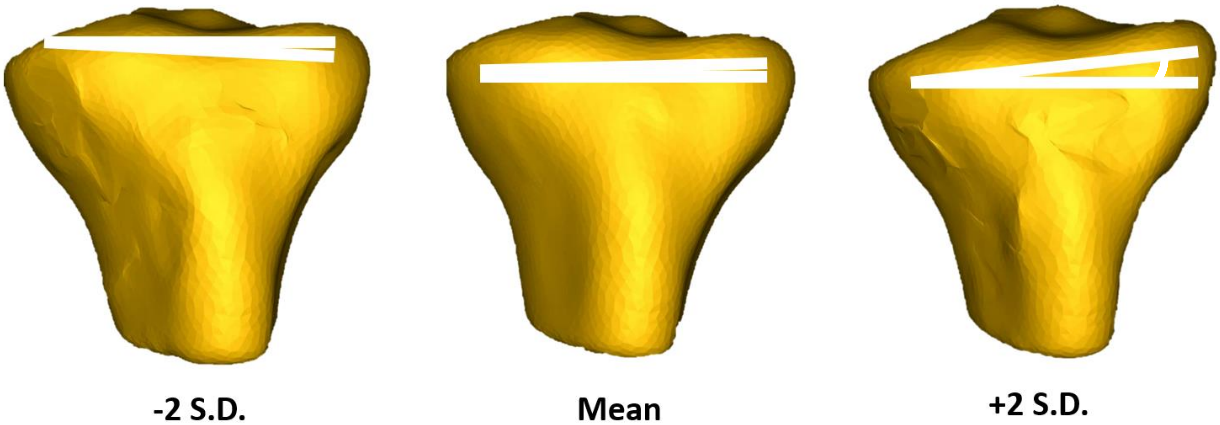

Figure 5.13: Anterior view of the second principal component of the statistical shape model represented by 2 standard deviations away from the mean in each direction. This principal component represents variation in the slope of the tibial plateau in the coronal plane depicted by the incrase in angle between the two white lines from left to right.

Table 15: Spearman correlation coefficients between the PC scores associating with coronal tibial slope and kinematic and kinetic parameters from the biomechanical testing on the effect of functional bracing. IR: internal rotation, Val.R: valgus rotation

Coronal Tibial Slope			
	Anterior Load	Internal + Valgus Torques	External + Valgus Torques
Full extension	N/A	Native IR, r = 0.88 Difference in Val.R from brace, r = -0.81	N/A
30°	N/A	Native ACL force, r = 0.81 Native IR, r = 0.90 Difference in Val.R from brace, r = -0.88	N/A
60°	N/A	Native IR, r = 0.76 Difference in Val.R from brace, r = -0.76	N/A

The third principal component of the statistical shape model of the tibias represents variation in the posterior tibial slope (Figure 5.14). In response to a simulated anterior drawer, the posterior tibial slope positively correlated with the force in the ACL at the native state at full extension and 30° of flexion. In response to a simulated pivot shift, the slope positively correlated with the force in the ACL at the native state at full extension. In response to the external and valgus torques, the posterior tibial slope positively did not correlate with any biomechanical testing data.

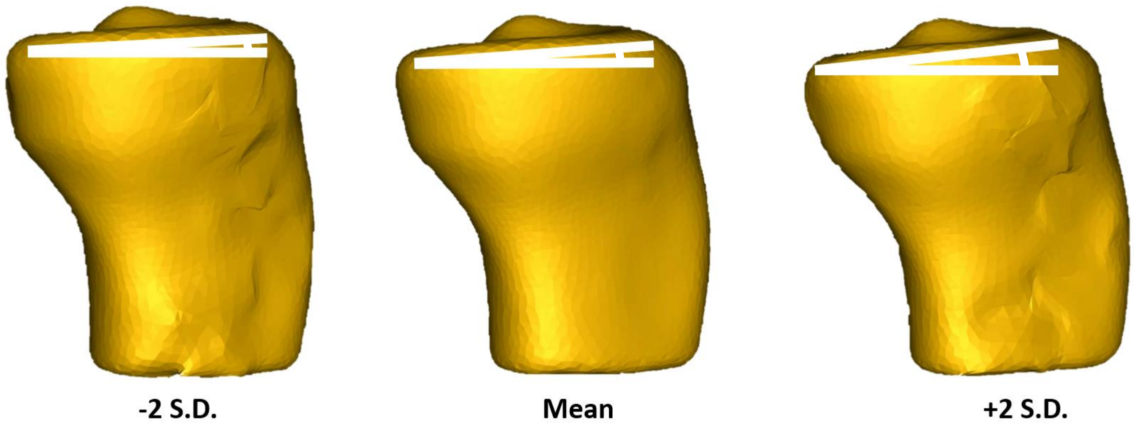

Figure 5.14: Superior view of the first principal component of the statistical shape model represented by 2 standard deviations away from the mean in each direction. This principal component represents variation in the medial-lateral width of the tibial plateau depicted by the incrase in angle between the two white lines from left to right.

Table 16: Spearman correlation coefficients between the PC scores associating with posterior tibial slope and kinematic and kinetic parameters from the biomechanical testing on the effect of functional bracing.

Posterior Tibial Slope			
	Anterior Load	Internal + Valgus Torques	External + Valgus Torques
Full extension	Native ACL force, r = 0.83	Native ACL force, r = 0.88	N/A
30°	Native ACL force, r = 0.86	N/A	N/A
60°	N/A	N/A	N/A

5.2.4 Discussion

A greater normalized medial-lateral width at the femoral epicondyles correlated with greater decreases in the in-situ force in the ACL due to the brace in response to the simulated anterior drawer at the native, unbraced state as well decreased ACL force in the braced at full extension. Furthermore, a greater width correlated with less anterior translation in response to an anterior load at the native, unbraced state and braced state at 30° and 60° of flexion. A greater normalized medial-lateral width at the femoral epicondyle also correlated with decreased ACL force and external rotation in response to the combined external and valgus torques at 30° of flexion. These results demonstrate that a greater medial-lateral width at the femoral epicondyles may have better clinical outcomes when prescribed functional bracing compared to individuals with a smaller width. A smaller normalized medial lateral width at the femoral epicondyle has not been previously described as a risk factor for ACL injury but may be a risk factor for unsuccessful conservative treatment of prescribing a brace to knee injuries.

In response to a simulated anterior drawer, a greater anterior height of the lateral condyle did not correlate with any kinematic or kinetic parameters. In response to the simulated pivot shift, this greater height correlated with greater internal rotation at the native, unbraced state at full extension as well as with decreases in valgus rotation due to functional bracing compared to the smaller anterior height of the lateral femoral condyle. In response to the combined external and valgus torques, greater height of the lateral condyle correlated with greater decreases external rotation due to the bracing at full extension. These results suggest that the greater anterior height of the lateral femoral condyle may have greater rotator stability with functional bracing. Trochlear groove morphology has been shown to associate with ACL injury in skeletally immature patients

(Kwak et al., 2020), and the data in this dissertation suggests that trochlear groove morphology may also influence the effectiveness of functional bracing.

In response to the simulated anterior drawer, a smaller notch width correlated with greater in-situ ACL force at the native braced state at 30° and at the native state at 60° of flexion. Furthermore, a smaller notch width correlated with greater decreases in anterior translation due to the functional brace. In response to a simulated pivot shift, a smaller notch width correlated with greater valgus rotation at the native braced state at full extension and 60° of flexion. These results support previous studies demonstrating that a smaller notch width is a risk factor for ACL injury (Darryl C Whitney et al., 2014), and demonstrate that functional knee bracing may not help knees with smaller notch widths with reducing excess valgus rotation in response to a pivot shift. On the other hand, smaller femoral notch width correlated with a greater decrease in anterior translation due to the brace at full extension. These results demonstrate that a smaller femoral notch width may not be helped by functional bracing, and other additional treatment options or preventative measures should be considered.

In response to a simulated anterior drawer, the wider tibial plateau width correlated with less force in the ACL at the native braced state at 30° and 60°. A smaller tibial width also correlated with less anterior tibial translation at 60° of flexion. In response to a simulated pivot shift, the smaller tibial plateau width correlated with greater valgus rotation at the unbraced state. While previous research found no association between tibial plateau width and ACL injury (van Eck et al., 2016), these results demonstrate that a smaller tibial width may be a risk factor for knee injuries, and functional bracing may not reduce the risk of injury.

A greater coronal tibial slope correlated with greater force in the ACL at 30° and with a greater internal rotation at the native state at every flexion angle in response to a simulated pivot shift. However, a greater coronal tibial slope correlated with less of an effect of functional bracing on valgus rotation. This bony morphological feature did not influence knee mechanics in response to an anterior load or combined external and valgus torques. These results demonstrate that a greater tibial slope may be a risk factor for ACL injury, but functional bracing may not reduce injury risk

A greater posterior tibial slope correlated with greater force in the ACL in response to a simulated anterior drawer and a simulated pivot shift. This greater in-situ force in the ACL supports previous findings that a greater posterior tibial slope is a risk factor for ACL injury (Todd et al., 2010; Zeng et al., 2016). However, posterior tibial slope did not correlate with functional braced mechanics or the effect of functional bracing so no conclusions can be drawn on the effectiveness of functional knee bracing with this bony morphological feature.

Overall, the results of this study demonstrate that tibiofemoral bony morphology influence the effectiveness of functional bracing to provide additional rotatory stability and to reduce the force in the ACL. Armed with this knowledge, clinicians can improve clinical care by prescribing functional bracing to those whose bony morphology would lead to favorable results. Patients with bony morphological features that demonstrated to be less aided by functional bracing can be advised not to rely heavily on the bracing and may need alternative treatment such as strengthen the dynamic stabilizers more than typically prescribed. Furthermore, bracing developers can use these results to try to improve current designs or design individualized bracing based on their bony morphology.

5.3 Aim 3c: The Effect of Tibiofemoral Bony Morphology Effectiveness of Lateral Extraarticular Tenodesis

5.3.1 Introduction

Persistent rotatory knee instability after intra-articular ACL reconstruction may be present in a portion of cases, and some propose that concomitant injury to the anterolateral knee structures is a potential cause (Andrea Ferretti, Monaco, & Vadala, 2014; Hewett et al., 2009; Terry, Norwood, Hughston, & Caldwell, 1993). Lateral extraarticular tenodesis (LET) is performed with ACL reconstruction approximately 10% to address rotatory knee instability; however, increased tibiofemoral contact pressure and overly reduced translations and rotations can occur due to LET procedure (Geeslin et al., 2018; Inderhaug, Stephen, El-Daou, Williams, & Amis, 2017; Nitri et al., 2016; Schon et al., 2016; Sonnery-Cottet et al., 2011). In contrast, it was recently shown that neither increased pressure nor reduced kinematics occurred (Novaretti, Arner, et al., 2020). Rather, large variability existed amongst the data. These large standard deviations in contact pressure and kinematics may be a result of the natural variation in bony morphology amongst the knees examined.

Therefore, the objective of this study was to analyze the effect of bony morphology on knee kinematics, contact pressures, and contact areas in response to external loads before and after anterolateral capsule injury and a type of LET. It was hypothesized that bony morphologic risk factors for ACL injury would correlate with increased knee kinematics and contact pressures and decreased contact areas in response to external loads.

5.3.2 Methods

The study used eight fresh-frozen cadaveric knees (mean age of 66.4 years; four females, four males). Each specimen was examined by a fellowship-trained sports medicine orthopaedic surgeon to exclude specimens with (1) any bony deformities, (2) any ligamentous injuries, (3) any meniscal injuries, (4) osteoarthritis greater than grade 2 as determined by the Kellgren-Lawrence grading scale (Katakura et al., 2019; Novaretti et al., 2021), or (5) chondral injuries greater than grade 2 according to the International Cartilage Repair Society grading system. The femur and the tibia were cut 20 cm from the joint line, and the fibula was fixed to the tibia using a bicortical screw to maintain its anatomic position to allow proper function of the lateral collateral ligament during testing. The femur and the tibia were potted in an epoxy compound (Bondo; 3M, St Paul, MN) and secured within custom-made aluminum clamps.

A 6 degree-of-freedom robotic testing system that was designed for assessment of knee joint biomechanics (MJT model FRS2010) applied loads to the knee during continuous flexion and allowed unconstrained knee motion. To provide feedback to the controller, a universal force-moment sensor (UFS) (ATI Delta IP60, SI-660-60) was used. A LabView Program (Technology Services Inc) was used to control the robotic testing system. The position repeatability of the robotic manipulator was determined to be less than ±0.015 mm and ±0.01°, whereas the measurement uncertainty of the UFS was approximately 1% of full scale (accuracy) (Bell et al., 2015).

The knees were mounted in the robotic testing system and two loading conditions were applied to each knee at full extension, 30°, 60°, and 90° of flexion and the resulting kinematics which were defined using the Grood-Suntay joint coordinate system were recorded (Grood & Suntay, 1983). The path of passive flexion–extension of the intact knee was then determined from full extension to 90° of flexion while the forces and moments were continuously minimized. This passive path was then repeated 5 times to precondition the knee prior mechanical loading (Bell et al., 2015). The two loading conditions were (1) 134-N of anterior tibial load combined with 200-N of axial compression, (2) 7-Nm internal tibial torque combined with 200-N of axial compression at rates of 1.5 mm/s or 1.5 deg/s. A 200-N axial load was applied to the knees to simulate partial weightbearing as performed in previous biomechanical studies (Giffin, Vogrin, Zantop, Woo, & Harner, 2004; Naendrup et al., 2019; Novaretti, Arner, et al., 2020; Novaretti, Lian, et al., 2020). To remove the viscoelastic effects of the soft tissue, the specimens were cycled through the loads five times and the fifth cycle was used for the analysis. After loading the intact knee, anterolateral capsule deficiency was simulated by removing a 2-cm-wide strip from anterior to the lateral collateral ligament to proximal and lateral to the Gerdy's tubercle (Guenther, Irarrázaval, et al., 2017; Guenther et al., 2021) (Figure 5.15), and the loading conditions were applied while the kinematics were simultaneously recorded.

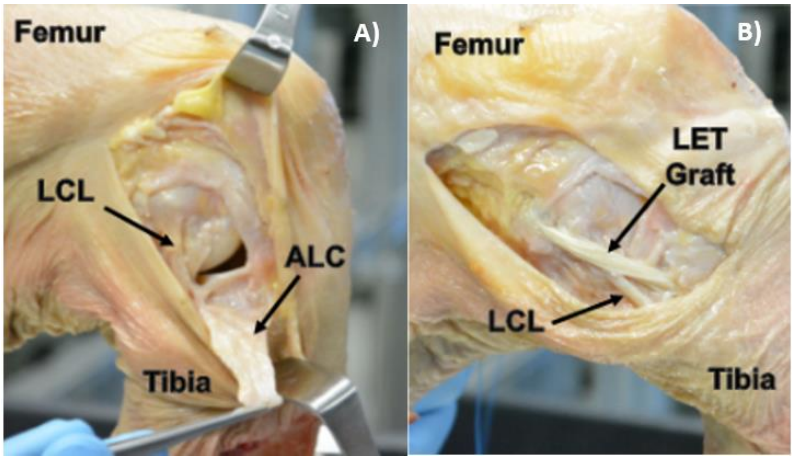

Figure 5.15: Surgical procedure; (A) A 2-cm-wide strip of ALC is removed to simulate ALC deficiency; (B) Lateral extra-articular tenodesis (LET) is performed utilizing a 6-mm semitendinosus graft.

A type of LET was then performed utilizing a 6-mm semitendinosus graft placed according to Kennedy et al's anatomic description of the anterolateral ligament (Kennedy et al., 2015; Rasmussen et al., 2016) and fixed at 30º of knee flexion with interference screws. The graft was tensioned with 20 N as a previous biomechanical study has shown after MacIntosh LET (Inderhaug et al., 2017). Lastly, all soft tissue was removed, and pressure sensors (Model 4000, Tekscan Inc.) were inserted and secured to the tibia to measure tibiofemoral lateral contact pressure and area at each knee state by replaying all previously saved kinematics. The ACL was left intact during testing to simulate an ideal anatomic ACL reconstruction and to isolate the effect of the type of LET procedure performed with a semitendinosus graft, as performed in previous biomechanical studies (Inderhaug et al., 2017).

A statistical shape model was then created of the cadaveric knees as previously described (S. K. Polamalu et al., 2020). High resolution bilateral lower extremity computed tomography (CT) scans (0.625 mm slice thickness, 0.625 mm spacing, 512 x 512 acquisition matrix size, 300 mA at 120 kV, GE LightSpeed 16) were captured for each cadaveric knee. The distal femurs and proximal tibiae were semi-automatically segmented to include a uniform amount of their long axis using Mimics 21 (Materialise NV, Leuven, Belgium). The distal femurs were segmented so that the largest medial-lateral dimension is equal to the distance from the inferior most point to the cut on the long axis of the femur. The proximal tibiae were segmented from the most proximal point to a point distally along the long axis 90% of the largest medial-lateral dimension of the tibial plateau. Including the entire long axis of the tibia would add unwanted variability into the statistical shape model and shift the focus of the analysis. Utilizing Mimics 21 Automatic 3D Calculation function, 3-Dimensional surface models of the distal femur and proximal tibia were created. Anti-aliasing was then performed utilizing a Laplacian filter with a smoothing factor of 0.7 for three iterations.

The 3-dimensional models were then exported to 3D Slicer (3D Slicer, 4.10.2, slicer.org). The femur surface models were rotated so the distal most points were in the same plane for alignment purposes of the bounding boxes. The femur and tibia surface models were then exported as binary segmentations to Seg3D (Seg3D 2.2.1, https://www.sci.utah.edu/cibc-software/seg3d.html) to create uniform bounding boxes. Lastly all left femurs and tibiae were reflected as right femurs and tibiae for shape uniformity.

The 3-dimensional surface models were imported into Shapeworks (https://www.sci.utah.edu/cibc-software/shapeworks.html) which employs a correspondence method to analyze the variation in 3-dimensional shape (Atkins et al., 2017; Cates et al., 2007). One difficulty of statistical shape modeling is limiting the bias when using bony landmarks to determine particle placement (Chan et al., 2013; Rajamani et al., 2007; Schumann et al., 2010). This limitation is avoided through an automatic particle placement using a splitting strategy that randomly chooses a surface location for the first particle which is then split into two particles and repel each other along the surface until a steady state is achieved (Cates et al., 2007). This splitting process was repeated until 2,048 particles were uniformly placed on each bone in the analysis. The uniformity was optimally achieved using a gradient descent approach with a cost function while simultaneously creating a compact distribution of the correspondence of particles on the surface models. A generalized Procrustes analysis was performed throughout to optimize alignment and normalize with respect to scale (Gower, 1975).

A principal component analysis (PCA) was performed to analyze the variability of the correspondence particle placement in each configuration. The PCA reduces the dimensionality of the correspondence of particles to orthogonal descriptions of the data set while extracting information about independent bony morphological features that describe the cohort of bone shapes (Atkins et al., 2017; Cates et al., 2007). From the PCA, independent bony morphology features can be projected or mapped onto shape variability spectrums called principal components or modes of variation. This mapping called PCA loading values provides a quantitative assessment of the distal femur or proximal tibiae configurations onto each mode of variation. Each mode of variation represents an independent shape feature. The total variation in the data set is described by combining each mode of variation. The largest modes of variation that additively describe 80% of the variation among all the distal femurs or proximal tibiae were correlated with the kinematic and contact pressure data from the robotic testing. The modes of variation can be visualized by generating the shape models for ±2 standard deviations for each mode of variation and then creating 3-dimensional topography plots of the differences between the distances of the surfaces when overlaid (Figure 5.16). Two orthopaedic sports medicine fellows performed an independent analysis to examine these 3-D models and interpret physical representations which were then reviewed by the researcher team.

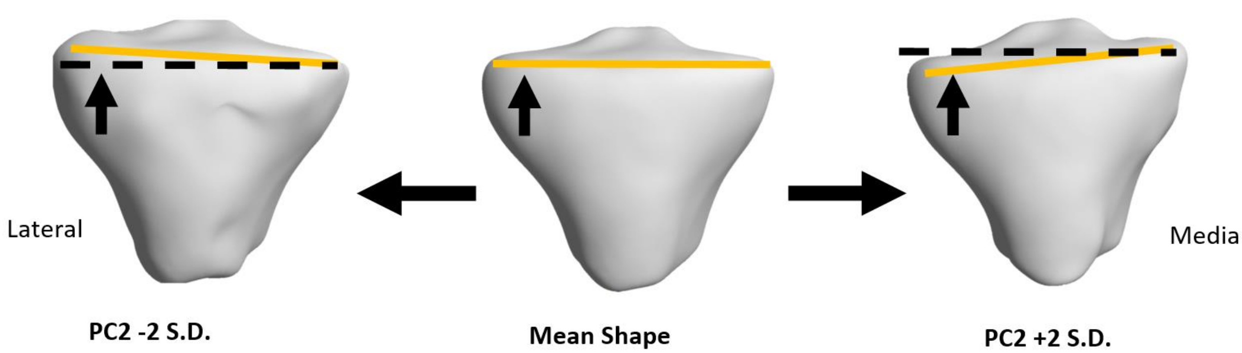

Figure 5.16: Visualization of the tibia from an anterior view demonstrating the variation in the elevation of the lateral tibial plateau as the third tibial principal component from -2 S.D. to +2 S.D. with the mean shape in the middle. The yellow line was added to further define the medial-lateral tibial plateau axis to highlight the variation in the elevation of the lateral tibial plateau.

PCA loading values representing quantitative values of shape variation for the cadaveric knee bones on each principal component were correlated with the kinematic and contact pressure/area parameters from the robotic testing using Pearson’s correlation coefficient. Similarly, the PCA loading values were correlated with various direct measurements that the orthopaedic sports medicine fellows visually determined the principal components might represent bony morphologically. Significance was set at $p < 0.05$. Normality was tested using a Shapiro Wilks W Test. The standard deviations of the modes of variation were determined not to be different to establish homoscedasticity.

5.3.3 Results

The first three femoral principal components represent greater than 90% of the shape variation in the cohort and correlated with multiple kinematic and contact pressure parameters (Table 17-420. The first principal component represented variation in the angle between the femoral long axis and the femoral condyles (Figure 5.17A). However, due to the first principal component encapsulating the greatest amount of bony morphological variation, no relationship was found with a 2-dimensional measurement. The first principal component correlated with mean contact pressure after anterolateral capsule deficiency and a type of LET at full extension in response to an anterior load as well as the difference in anterior tibial translation between the intact state and a type of LET at full extension in response to an internal torque ($p < 0.05$). Furthermore, the first femoral principal component correlated with internal rotation in response to anterior tibial translation at 30° and 60° at only the intact state.

The second femoral principal component represented femoral notch width (Figure 5.17B) ($p < 0.05$) and correlated with lateral tibial translation after anterolateral capsule deficiency and type of LET at every flexion angle in response to an internal torque. It also correlated with contact area after anterolateral capsule deficiency and a type of LET at full extension, 30º, and 60º in response to an anterior load ($p < 0.05$).

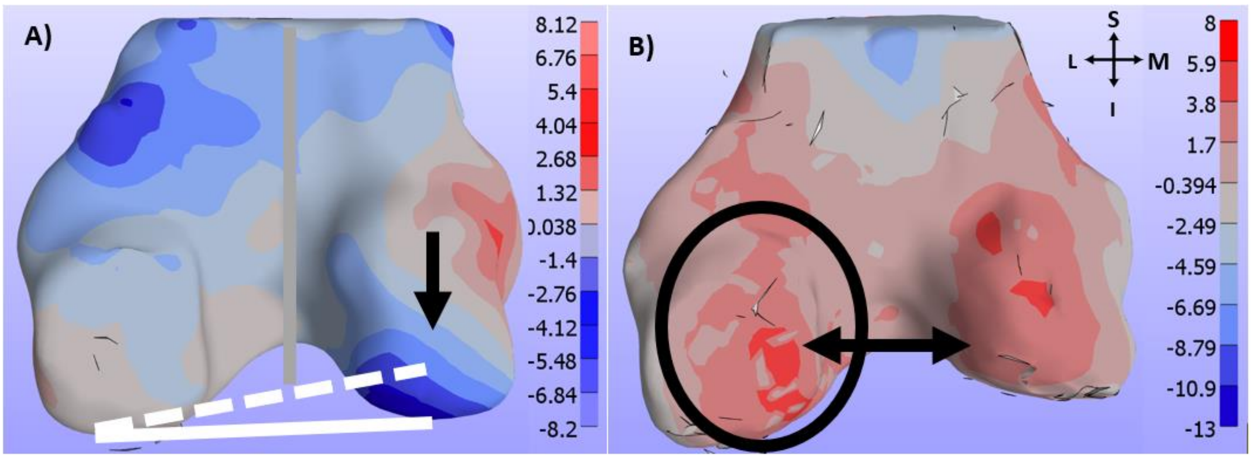

Figure 5.17: Visualizations of A) first and B) second principal component of the distal femur utilizing a 3D distance topography plot showing the distance between +2 SD and -2 SD of the first principal component where red represents outward distance and blue represents inward distance (mm). Posterior view of the 3D visualization of the first mode of variation from the femoral statistical shape model of the cadaveric knees representing variation in the angle between the femoral long axis (gray line) and the femoral condyles (represented by the solid white line, -2SD, and the dashed white line, +2 SD). The second mode of variation from the femoral statistical shape model of the cadaveric knees represents variation in the femoral notch width.

The third femoral principal component represented variation in the anterior medial and lateral condyle heights (Li et al., 2014) (Figure 5.18) ($p < 0.05$) and correlated with anterior tibial translation after a type of LET at full extension in response to an internal torque. It also correlated with the peak contact pressure and mean contact pressure differences between the intact state and after anterolateral capsule deficiency as well as between the intact state and after a type of LET at full extension in response to an anterior load. The third femoral principal component correlated with the difference in internal rotation in response to an internal torque between the anterolateral deficient and a type of LET states at 30º, 60º, and 90º.

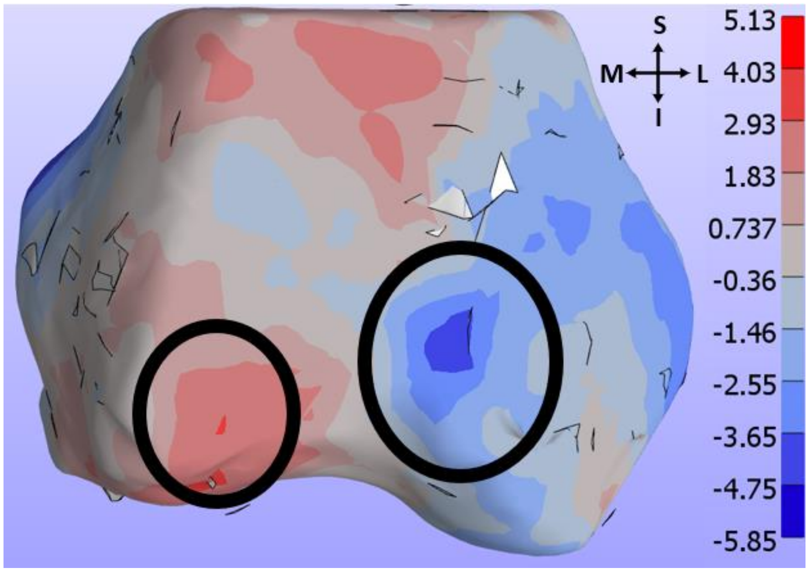

Figure 5.18: Visualizations of third principal component of the distal femurs utilizing a 3D distance topography plots showing the distance between +2 SD and -2 SD of the third principal component where red represents outward distance and blue represents inward distance (mm). Anterior view of the 3D visualization of the first mode of variation from the femoral statistical shape model of the cadaveric knees representing variation in the anterior medial and lateral heights of the distal femur.

The first three tibial principal components represent greater than 90% of the shape variation. The second and third principal components correlated with a kinematic and contact pressure parameters (Table 21). The second tibial principal component represented variation in the angle between the anatomical medial-lateral axis and the functional anterior-posterior axis (Figure 5.19A) ($p < 0.05$). The anatomical-medial lateral axis is defined by the line between the medial most point and the lateral most point of the tibial plateau. The functional anterior-posterior axis is defined by the line between the centroid of the long axis and the tibial tuberosity. Notably, the second tibial principal component correlated with internal rotation at each knee state at 30º, 60º, and 90º in response to an internal torque ($p < 0.05$). In response to an anterior load, the second tibial principal component correlated with contact area in the lateral compartment at full extension, 30º, and 60º for the anterolateral deficient and a type of LET states and at 30º for the intact state.

The third tibial principal component represented variation in lateral tibial plateau elevation (Figure 5.19B) ($p < 0.05$) and correlated with anterior tibial translation for all knee states at 0º and after anterolateral capsule deficiency and a type of LET at 30º, 60º, and 90º in response to an internal torque ($p < 0.05$). The third principal component correlated negatively with anterior tibial translation and all knee states at full extension, with anterior tibial translation for anterolateral capsule deficiency (ACLD) and a type of LET states at 30° and 60° of flexion, and with anterior tibial translation for ALCD state at 90° of flexion. Additionally, in response to an internal torque, the third principal component negatively correlated with internal rotation after ALCD and a type of LET, lateral tibial translation after a type of LET, and valgus rotation for intact and ALCD states at full extension.

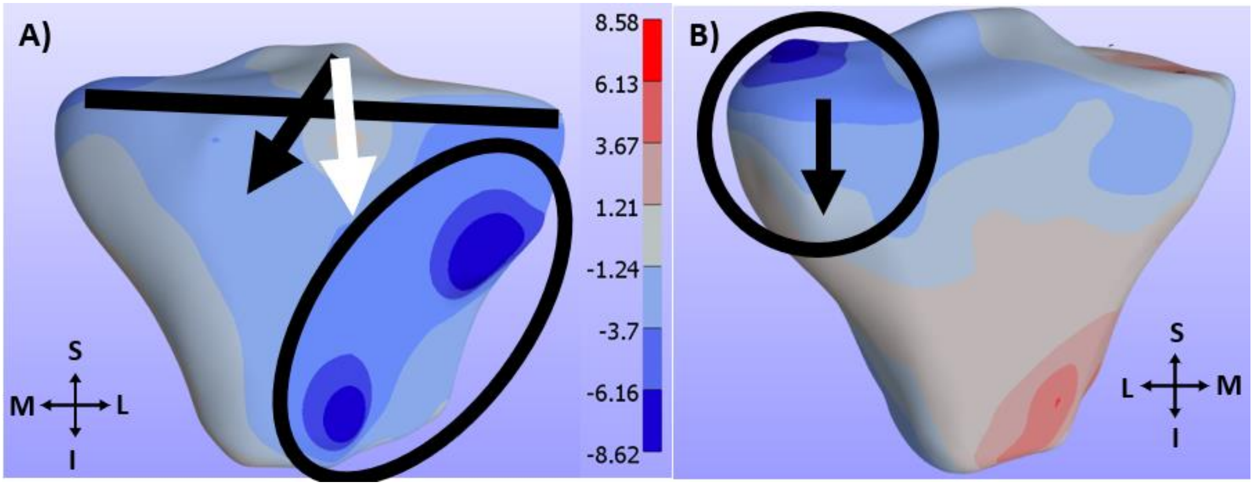

Figure 5.19: Visualizations of second and B) third principal components of the proximal tibiae utilizing 3D distance topography plots showing the distance between +2 SD and -2 SD of the second principal component where red represents outward distance and blue represents inward distance (mm). A) Anterior view of the 3D visualization of the second mode of variation from the tibial statistical shape model of the cadaveric knees representing variation in the angle between the tibial plateau anatomical medial-lateral axis and the functional anterior-posterior axis represented by the black and white line. B) Posterior view of the 3D visualization of the third mode of variation from the statistical shape model of the cadaveric knees representing an increased lateral tibial plateau elevation highlighted by the black circle and arrow.

5.3.4 Discussion

The main finding of this study was that tibiofemoral bony morphology significantly affects knee joint kinematics in response to external loads before and after anterolateral capsule injury and repair differently than the intact state. At full extension, more distal lateral femoral condyle (Figure 5.18A) correlated with decreases in mean contact pressure on the lateral tibial plateau after anterolateral capsule deficiency and a type of LET in response to an external load as well as increased anterior tibial translation after a type of LET in response to an internal torque. The decreased mean contact pressure in the lateral compartment and increased anterior tibial translation may signify that this type of LET may benefit individuals with a greater angle between the femoral long axis and the femoral condyles laterally without the concerns of increased contact pressure and decreased translations while addressing persistent rotatory instability.

A smaller notch width correlated with less lateral tibial translation in response to an internal torque after anterolateral capsule deficiency and a type of LET at all flexion angles as well as decreased contact area on the lateral tibial plateau after anterolateral capsule deficiency and a type of LET at full extension, 30º, and 60º. Less lateral tibial translation may demonstrate that a smaller notch width risks reducing knee motion too much after a type of LET. Less contact area may be the result of smaller and more central femoral condyles demonstrating less of a need for a combined this type of LET and ACL reconstruction after ACL injury.

In response to an internal torque, more anterior medial and lateral condylar heights correlated with greater anterior tibial translation after a type of LET at full extension as well as increases in differences in response to internal rotation between a type of LET and anterolateral capsule deficiency states. Therefore, a greater anterior condyle height may be an indicator for this type of LET successfully returning the knee to intact kinematics after anterolateral capsule deficiency while not being at risk for overly reducing translations after this type of LET. Anterior condylar heights correlated with the difference in internal rotation in response to an internal torque between the anterolateral deficient and LET states at 30º, 60º, and 90º of knee flexion demonstrating this bony morphological feature impacts the effectiveness of this type of LET on rotatory instability when anterolateral injury is present at the flexion angles when the pivot shift occurs. As greater anterior condyle heights were not shown to correlate similarly with the intact knee state, further research needs to be performed to determine if greater anterior condyle heights have a similar effect on ACL reconstruction alone.

For the tibial bony morphology, a greater angle between the anatomical medial-lateral axis of the tibial plateau and the functional anterior-posterior axis correlated with a decreased internal rotation in response to internal torque. As ACL injury is often due to excessive internal rotation, this bony morphological feature may provide clinicians with knowledge on individuals who may be at greater risk for ACL injury. Furthermore, patients with a greater angle between the anatomical medial-lateral axis and the functional anterior-posterior axis may be at risk of over-constraining after this type of LET.

An increased elevation of the lateral tibial plateau correlated with increases in multiple anterior tibial translation, lateral translation, and valgus rotation at multiple flexion angles. An increased elevation of the lateral tibial plateau correlated with an increased anterior tibial translation in response to an internal torque with axial compression for intact, ALCD, and a type of LET states at full extension. This increased elevation also correlated with anterior tibial translation at 30º, 60º, and 90º flexion angles for the ALCD and a type of LET states. Increased elevation of the lateral tibial plateau correlated with an increased valgus knee angles for intact and ALCD states. Additionally, increased lateral tibial translation occurred in knees with greater elevation of the lateral tibial plateau after a type of LET at full extension. These increases in translations and valgus rotation may demonstrate that individuals with greater lateral plateau elevation have more lax knees and may benefit from this type of LET more than others without risk of overly reducing translations and rotations (Geeslin, et al., 2018, Inderhaug et al., 2017, Nitri et al., 2016 Schon et al., 2016).

For many of these bony morphological parameters, correlations were found with kinematics after anterolateral capsule deficiency and a type of LET, but not at the intact state. Therefore, clinicians must consider these as a parameter after anterolateral capsule injury or this type of LET as they significantly influence kinematics in those cases. Furthermore, previous studies that demonstrate bony morphological features effect on knee kinematics do not necessarily impact the knee in the same manner after injury or repair (Hoshino et al., 2012a; Varadarajan, Gill, Freiberg, Rubash, & Li, 2009). This study shows that injury and repair to the knee structures impacts the influence that bony morphological features have on knee function.

There are limitations of this study, the age of the donor specimens (mean age: 66.4 years) was older than the population of individuals at risk for ACL injury and those who typically receive LET procedures. However, a thorough inspection of the tissue and bone quality of each specimen was performed to determine there was no gross degenerative changes in the knees. The ACL was left intact during testing to simulate an ideal anatomic ACL reconstruction and to isolate the effect of a type of LET procedure. However, the ideal ACL reconstruction is probably not possible and exists as a limitation of this research. Another limitation is that the axial compression performed was less than the force generated during walking, so the contact pressures were likely lower than that seen in vivo. Ideally, the research performed in this study would have been performed with a wide range of bony morphology features that increase risk of ACL injury; however, that is not something that can be accounted for before testing. While a post-hoc analysis determined that this research achieved appropriate power, typical power analyses are often ineffective when used with statistical shape modeling due to the high dimensionality. Therefore, the sample size of eight specimens may be a limitation of this data. However, this is a novel methodology correlating kinematic and contact pressure data with bony morphological features from statistical shape modeling and has clinical relevancy even with the possibility of a small sample size. Lastly, each type of LET may have different correlations with tibiofemoral bony morphology and this research may not be translatable to those procedures

The results of this study demonstrate that understanding the effect of tibiofemoral bony morphology on knee function could impact the efficacy of this type of LET procedure. Furthermore, the methodology of this study could lead to further investigation into the effect of bony morphology on various knee injuries and treatment procedures as previous studies have only analyzed the effect of bony morphology on intact knee kinematics. LET has been performed to address persistent rotatory instability often present after treating ACL injury possibly due to injury to the anterolateral complex but has been shown in previous literature to have varying levels of success (Geeslin et al., 2018; Inderhaug et al., 2017; Nitri et al., 2016; Schon et al., 2016). The results of this study demonstrate that tibial bony morphology significantly impacts knee kinematics in response to external loads before and after anterolateral capsule injury and this type of LET differently than the intact knee.

5.3.5 Tables

Table 17: Significant correlation coefficients between the first 3 femoral modes of variation and lateral tibial translation in response to an internal torque. No significant correlations were found in response to an anterior load. Correlations that were not significant are denoted with n.s.. (ALCD: anterolateral capsule deficiency, LET: lateral extra-articular tenodesis)

		Internal Torque		
	Flexion	Intact	ALCD	LET
PC0	0	n.s.	n.s.	n.s.
	30	n.s.	n.s.	n.s.
	60	n.s.	n.s.	n.s.
	90	n.s.	n.s.	n.s.
PC1	0	n.s.	0.82	0.79
	30	n.s.	0.83	0.82
	60	n.s.	0.72	0.79
	90	n.s.	0.75	0.83
PC2	0	n.s.	n.s.	n.s.
	30	n.s.	n.s.	n.s.
	60	-0.72	n.s.	n.s.
	90	-0.74	n.s.	n.s.

Table 18: Significant correlation coefficients (bolded font) between the first femoral mode of variation and kinematic data in response to an internal torque. Correlations that were not significant are denoted with n. s.. The table can be read as the following: Applied load, kinematic/contact pressure data, knee state, flexion angle. If the kinematic/contact pressure data includes the word difference, then the correlated value is the difference between the two knee states listed kinematic/contact pressure data. (ALCD: anterolateral capsule deficiency, ATT: anterior tibial translation, LET: lateral extra-articular tenodesis).

Internal torque, ATT, intact, 30 degrees	-0.83
Internal torque, ATT, intact, 60 degrees	-0.75
Anterior load, internal rotation, intact, 90 degrees	-0.92
Anterior load, mean pressure, ALCD, 0 degrees	-0.78
Anterior load, mean pressure, LET, 0 degrees	-0.72
Internal torque, ATT difference, Intact and LET, 0 degrees	0.83
Internal torque, peak pressure difference, intact and ALCD, 60 degrees	0.72
Internal torque, peak pressure difference, intact and ALCD, 90 degrees	0.73
Internal torque, mean pressure difference, intact and LET, 60 degrees	0.71
Anterior load, mean pressure difference, intact and LET, 30 degrees	0.71

Table 19: Significant correlation coefficients (bolded font) between the second femoral mode of variation and kinematic data in response to an internal torque. Correlations that were not significant are denoted with n. s.. The table can be read as the following: Applied load, kinematic/contact pressure data, knee state, flexion angle. If the kinematic/contact pressure data includes the word difference, then the correlated value is the difference between the two knee states listed kinematic/contact pressure data. (ALCD: anterolateral capsule deficiency, ATT: anterior tibial translation, LET: lateral extra-articular tenodesis, LTT: lateral tibial translation).

Anterior load, contact area, ACLD, 0 degrees	0.73
Anterior load, contact area, LET, 0 degrees	0.72
Anterior load, contact area, intact, 30 degrees	0.72
Anterior load, contact area, ACLD, 30 degrees	0.78
Anterior load, contact area, LET, 30 degrees	0.78
Anterior load, contact area, ACLD, 60 degrees	0.71
Anterior load, contact area, LET, 60 degrees	0.75
Internal torque, ATT difference, ALCD and LET, 60 degrees	0.76
Internal rotation, internal rotation difference, intact and ALCD, 30 degrees	-0.71
Internal torque, LTT difference, Intact and ALCD, 60 degrees	0.72
Internal torque, varus-valgus difference, intact and ALCD, 60 degrees	-0.76
Internal torque, varus-valgus difference, intact and ALCD, 90 degrees	-0.79
Internal torque, contact area difference, intact and LET, 0 degrees	0.75
Internal torque, contact area difference, intact and LET, 0 degrees	0.75
Anterior load, contact area difference, intact and LET, 0 degrees	0.73

Table 20: Significant correlation coefficients (bolded font) between the third femoral mode of variation and kinematic data in response to an internal torque. The table can be read as the following: Applied load, kinematic/contact pressure data, knee state, flexion angle. If the kinematic/contact pressure data includes the word difference, then the correlated value is the difference between the two knee states listed kinematic/contact pressure data. (ALCD: anterolateral capsule deficiency, ATT: anterior tibial translation, LET: lateral extra-articular tenodesis, LTT: lateral tibial translation).

Internal torque, ATT, LET, 0 degrees	-0.87
Internal torque, ATT, LET, 90 degrees	-0.73
Internal torque, varus-valgus, intact, 60 degrees	0.79
Internal torque, varus-valgus, intact, 90 degrees	0.85
Anterior load, peak, pressure, intact, 0 degrees	0.76
Internal torque, internal rotation difference, ALCD and LET, 30 degrees	-0.73
Internal torque, internal rotation difference, ALCD and LET, 60 degrees	-0.84
Internal torque, internal rotation difference, ALCD and LET, 90 degrees	-0.92
Internal torque, varus-valgus difference, ALCD and LET, 60 degrees	-071
Internal torque, varus-valgus difference, ALCD and LET, 90 degrees	-0.95
Anterior load, peak pressure difference, intact and ALCD, 0 degrees	-0.72
Anterior load, peak pressure difference, intact and LET, 0 degrees	-0.76
Anterior load, peak mean difference, intact and ALCD, 0 degrees	-0.73
Anterior load, peak mean difference, intact and LET, 0 degrees	-0.72

Table 21: Significant correlation coefficients (bolded font) between the second and third tibial modes of variation and kinematic data in response to an internal torque. Correlations that were not significant are denoted with n. s.. (ALCD: anterolateral capsule deficiency, ATT: anterior tibial translation, IR: internal rotation, LET: lateral extra-articular tenodesis, LTT: lateral tibial translation, VR: valgus rotation).

		PC2			PC3		
	Flexion	Intact	ALCD	LET	Intact	ALCD	LET
ATT	0	n. s.	n. s.	n. s.	-0.78	-0.92	-0.88
	30	n. s.	n. s.	n. s.	n. s.	-0.8	-0.8
	60	n. s.	n. s.	n. s.	n. s.	-0.77	-0.74
	90	n. s.	n. s.	n. s.	n. s.	-0.75	n. s.
IR	0	n. s.	n. s.	n. s.	n. s.	-0.78	-0.83
	30	0.97	0.93	0.9	n. s.	n. s.	n. s.
	60	0.96	0.92	0.9	n. s.	n. s.	n. s.
	90	0.96	0.91	0.88	n. s.	n. s.	n. s.
LTT	0	n.s.	n.s.	n.s.	n.s.	n.s.	0.75
VR	0	n.s.	n.s.	n.s.	-0.77	-0.77	n.s.

6.0 Discussion

6.1.1 Relationship of Findings Between Aims

The three specific aims of this dissertation provide detailed investigations on the intertwined relationship between tibiofemoral bony morphology, ACL injury, and ACL injury care. Distinct 3-dimensional bony morphological features of the tibiofemoral joint associated with ACL injury compared to uninjured controls. These morphological features include a smaller anterior-posterior length of the tibial plateau, a greater angle between the femoral long axis and femoral condylar axis, and a more lateral mechanical axis of the distal femur. These bony morphological features resulted in variation in the forces in the AM and PL bundles when modeled as non-linear springs in response to a 134-N anterior load displacement. These variations combined with previous studies demonstrating that tibiofemoral bony morphology influences knee kinematics (Hoshino et al., 2012a; D. Lansdown & Ma, 2018; D. A. Lansdown et al., 2017), show that tibiofemoral bony morphology influence knee mechanics and thus influence ACL injury mechanics. The results in this dissertation also show that tibiofemoral morphology influence is the effectiveness of treatment options as demonstrated by a smaller coronal tibial slope having a greater reduction in valgus rotation due to the functional brace compared to tibias with a greater coronal tibial slope, for example. Clinicians should consider these bony morphological features and their impact when treating patients at an individualized level.

Additionally functional knee bracing was shown to provide additional rotatory stability to the knee by reducing tibial rotations and reducing the in-situ ACL force in response to rotatory loads. Previous biomechanical studies have shown that knee bracing reduces valgus angulation and increases knee flexion angle of ACL reconstructed knees when jumping (R. J. Butler et al., 2014; Gentile et al., 2021). However, no systematic review has shown evidence of functional bracing reducing risk of ACL injury (E. Alentorn-Geli et al., 2014; Gentile et al., 2021; Pietrosimone, Grindstaff, Linens, Uczekaj, & Hertel, 2008). These results conflicting between the experimental biomechanical outcomes and the observed clinical outcomes

The biomechanical effect of functional knee bracing was previously underexplored and conflicting results on its effectiveness to provide stability and reduce risk of injury exist (Gentile et al., 2021; Hinterwimmer, Graichen, Baumgart, & Plitz, 2004; Yang, Feng, He, Wang, & Hu, 2019). Similarly, conflicting results regarding the effectiveness of the LET have been shown (Geeslin et al., 2018; Novaretti, Arner, et al., 2020). Our hypothesis was that the large standard deviations in kinematics and kinetics after these treatment options can be attributed to variation in tibiofemoral bony morphology. The results of Aim 3 support this hypothesis by demonstrating that tibiofemoral bony morphology influences the impact of injury and effectiveness of these treatment options. The results of Aim 3 expand upon this demonstrating the effect of tibiofemoral bony morphology after injury and treatment. Bony morphology was shown to influence kinematics, arthrokinematics, and kinetics differently after injury and additional treatment (LET and functional bracing). A decreased lateral tibial plateau elevation correlated with greater internal rotation and anterior tibial translation after anterolateral capsule deficiency and LET. Decreased notch width correlated with decreased contact area after anterolateral capsule deficiency and LET demonstrating it as a risk factor for ACL injury (Sene K Polamalu, Novaretti, Musahl, & Debski, 2021). This was further supported by decreased notch width that correlated with greater in-situ force in the ACL. However, a smaller femoral notch width correlated with greater decreases in forces in the ACL due the functional bracing which may indicate that patients with smaller notch widths may have better clinical outcomes from functional bracing compared to patients with larger notch widths.

Previously described relationships between tibiofemoral bony morphology and uninjured knee mechanics must be reconsidered after accounting for the changes due to injury or treatment. Overall, tibiofemoral bony morphology plays a large role in the mechanisms behind ACL injury and the effectiveness of ACL injury treatment options through its influence on the ACL function due to the bone-to-bone articulation. The intertwined relationship between tibiofemoral bony morphology on knee motion through its direct influence on arthrokinematics and thus the function of the ACL before and after injury and treatment Figure (6.1). The impact of tibiofemoral morphology on knee mechanics should be considered by clinicians in order to improve individualized patient care for and to prevent these injuries by considering how the bony morphological features investigated in this dissertation impacted knee mechanics after the two different treatment options.

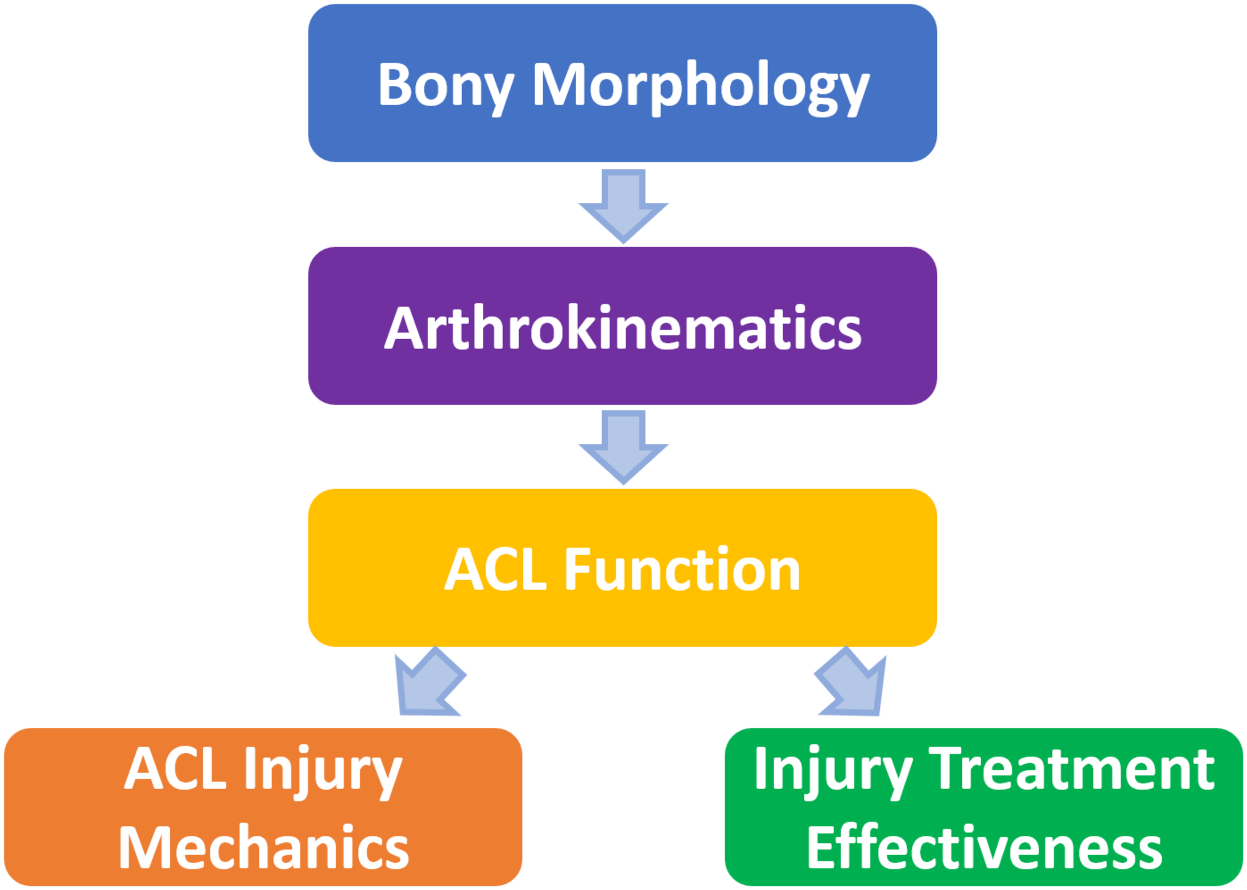

Figure 6.1: Overview of the effect of tibiofemoral bony morphology on ACL function and subsequently ACL injury mechanics and injury treatment effectiveness.

6.1.2 Future Directions

The work in this dissertation demonstrates the influence of bony morphology on the biomechanical factors of the complex environment of ACL injury and care. Improving the understanding of the relationships between tibiofemoral bony morphology and the other aspects of the multifaceted problem that is ACL injury treatment and prevention would further improve the individualized treatment and prevention of these injuries. Furthermore, addressing several limitations found throughout this work should also lead to new findings, research directions, and improved clinical care.

The workflow and protocol from Aim 1 to create statistical shape models to distinguish bony morphological features between an injured group and an uninjured group could be expanded to other injuries like meniscal tears or other joints like rotator cuff tears at the shoulder. This protocol can also be used to try to determine differences between injured groups with varying severity such as isolated ACL injuries and combined MCL and ACL injuries to determine if any bony morphological factors could predispose individuals to greater risk for combined injury. Furthermore, factors can be taken accounted for such as age and level of activity. Expanding the protocol in this research to include those factors could determine how bony morphology may change with age or due to greater levels of activity such as in high level athletes. Expanding the protocol of this research to analyze how tibial and femoral morphological features occur in the same patients by analyzing the paired variation across the joint utilizing a multi-surface statistical shape model would provide even more information to clinicians. Knowing which tibial bony morphologies frequently occur with certain femoral bony morphologies would allow clinicians to better predict which treatment options would be optimal as well as allow for better individualization of treatment options and possibly customization of bracing in the future by modifying the brace to account for the influence of both the patient’s tibial and femoral morphology.

Longitudinal studies on the effect of various levels of activity (high level running sport, high-level non-running sport, and control) on tibiofemoral bony morphology would provide clinicians, coaches, physical therapists, and athletes themselves pertinent information on how their daily training regimens affect their knee joint. Bony morphology is typically considered innate and unmodifiable, however various studies have shown that to not be true (Crockett et al., 2002; Reagan et al., 2002; Zhong et al., 2019). Increased humeral head retroversion has been shown between the throwing arm of a pitcher and their contralateral arm (Crockett et al., 2002; Reagan et al., 2002). No differences existed between the non-dominant arms of throwers and non-throwers. Therefore, it is reasonable to assume that the repetitive loading that the throwing shoulder undergoes, alters the bone shape over time. In addition, stress distribution was found to vary across athletes from different sports (Zhong et al., 2019). Since athletes undergo intense training regimens, bone shape adaptations may develop. Determining which knee bone shapes are common among high level athletes compared to more sedentary populations would help surgeons optimize treatment. Furthermore, longitudinal studies on the effect of ACL injury as well as ACL reconstruction on tibiofemoral bony morphology using an animal model study would provide valuable information as well as it could tell surgeons of possible variations that could occur if there is a certain amount of time between injury and reconstruction.

The research of Aim 2 can be expanded upon to have better accuracy of what is occurring at different individuals' knees. The model was designed to be purely comparative, but changes/additions can be made to improve the accuracy of the findings. Determining the force in each bundle of the ACL for each subject using the same protocol would allow for correlating those forces with the statistical shape modeling results possibly supporting the validity of Aim 2's protocol of using the geometries from 2 standard deviations along each principal component. A force driven model instead of a displacement driven model may more accurately represent what would occur at each joint by simulating the effect of the bony morphological feature on joint's response to external loads. Modeling the ACL as continuum elements instead of springs may provide a better representation of the forces in the ACL and specifically may allow differentiation of the stresses throughout different regions of the ACL. Including contact mechanics between the ACL and the condyle may also improve the model to allow wrapping mechanics that occur at greater flexion angles (Song et al., 2004). Furthermore, including the mechanics and material properties of the insertion sites may increase the accuracy of what occurs at the different bony morphologies. Including these changes and additions may paint a better picture of the effect of tibiofemoral bony morphology on the forces in the ACL and lead to new understandings of the ACL injury care. However, the comparative nature of the study design in Aim 2 still demonstrates the isolated effect of the tibiofemoral bony morphological features on the force in the ACL and the previously noted adjustments may lead to the same conclusions.

The research performed in Aim 3 leads to various avenues of research that can be performed. The effect of functional bracing on knee mechanics can be advanced further to determine the effect of isolated ACL injury or to compare the effect of different braces. Adjustments to the braces can be made and then tested to try to improve the current braces. One aspect that could be adjusted would be the stiffness of the brace construct. The stiffness of the brace could be determined, and adjustments could be made to make the brace stiffer in more desirable degrees of freedom. This research has shown the brace's ability to reduce internal and external tibial rotation but may benefit from preventing valgus rotations and anterior translations more to prevent ACL injuries and the results from Aim 3 demonstrate that the brace may be less stiff in these two degrees of freedom.

The workflow combining statistical shape modeling and kinematic/kinetic/arthrokinematics data leads to countless study designs as it can be a secondary study for any research performed with robotic testing or even in addition to studies with in-vivo motion capturing.

6.1.3 Summary

The key finding from Aim 1 is that certain 3-dimensional bony morphological features associate with ACL injured knees compared to uninjured knees. Those features are a smaller anterior-posterior length of the tibial plateau, a greater angle between the femoral long axis and the femoral condylar axis, and a more lateral mechanical axis of the distal femur. Furthermore, no differences were found between the injured knee and the contralateral knee of the injured subjects meaning that both knees are at equal risk for ACL injury. These findings expand upon the current literature describing bony morphological risk factors ACL injury.

The key finding of Aim 2 is that the bony morphological features that associate with ACL injury resulted in different forces in the ACL in response to an anterior load displacement compared to the features that associated the uninjured subjects. The smaller anterior-posterior length of the tibial plateau and the more lateral mechanical axis resulted in greater forces than their uninjured counterparts. However, the greater angle between the femoral long axis and the femoral condylar axis had a smaller ACL force compared to its uninjured counterpart emphasizes the multifaceted nature of ACL injury in that alignment and kinematics play a role.

The results of Aim 3a demonstrate the impact of functional knee bracing on knee mechanics. Functional knee bracing was shown to decrease tibial rotations and decrease the in-situ force in the ACL in response to rotatory loads. However, the functional knee bracing did not reduce anterior translation in response to an anterior load. These findings show that functional knee bracing may provide additional rotatory stability and provide a protective effect on the ACL in response to rotatory loads. The lack of anterior translation prevention should be noted though as the functional knee brace may not help prevent anterior subluxation that commonly occurs with

ACL injury outside of possibly preventing the knee from being in positions that are at risk subluxation.

The results of Aim 3b underscore the connection between tibiofemoral bony morphology and the effectiveness of functional bracing to provide additional rotatory stability and prevent injury. Certain bony morphological features correlated with a greater effect of functional bracing. Similarly, results of Aim 3c demonstrate that tibiofemoral bony morphology influences the effect of anterolateral capsule injury and LET on knee mechanics. A better understanding of the effect of tibiofemoral bony morphology on ACL function can lead to improvements in individualized treatment and prevention of ACL injuries. Specifically knowing which bony morphological features associate with ACL injuries and how they affect knee mechanics before and after injury and treatment, will allow clinicians to create better injury prevention programs by knowing who is at risk and individualize their treatment options by knowing how the patient's bony morphology will influence the effectiveness of each option. Ultimately, defining the parameters that of the patient's ACL injury environment will improve individualized care and thus clinical outcomes.

Bibliography

Abdi, H., & Williams, L. J. (2010). Principal component analysis. *Wiley interdisciplinary reviews: computational statistics, 2*(4), 433-459.

Albright, J. P., Powell, J. W., Smith, W., Martindale, A., Crowley, E., Monroe, J., . . . Miller, D. (1994). Medial collateral ligament knee sprains in college football: effectiveness of preventive braces. *The American journal of sports medicine, 22*(1), 12-18.

Alentorn-Geli, E., Mendiguchía, J., Samuelsson, K., Musahl, V., Karlsson, J., Cugat, R., & Myer, G. D. (2014). Prevention of non-contact anterior cruciate ligament injuries in sports. Part II: systematic review of the effectiveness of prevention programmes in male athletes. *Knee Surg Sports Traumatol Arthrosc, 22*(1), 16-25. doi:10.1007/s00167-013-2739-x

Alentorn-Geli, E., Myer, G. D., Silvers, H. J., Samitier, G., Romero, D., Lázaro-Haro, C., & Cugat, R. (2009). Prevention of non-contact anterior cruciate ligament injuries in soccer players. Part 1: Mechanisms of injury and underlying risk factors. *Knee Surgery, Sports Traumatology, Arthroscopy, 17*(7), 705-729.

Anderson, A. F., Lipscomb, A. B., Liudahl, K. J., & Addlestone, R. B. (1987). Analysis of the intercondylar notch by computed tomography. *The American journal of sports medicine, 15*(6), 547-552.

Andrade, R., Vasta, S., Sevivas, N., Pereira, R., Leal, A., Papalia, R., . . . Espregueira-Mendes, J. (2016). Notch morphology is a risk factor for ACL injury: a systematic review and meta-analysis. *Journal of ISAKOS: Joint Disorders & Orthopaedic Sports Medicine, 1*(2), 70-81.

Arendt, E., & Dick, R. (1995). Knee injury patterns among men and women in collegiate basketball and soccer: NCAA data and review of literature. *The American journal of sports medicine, 23*(6), 694-701.

Atkins, P. R., Elhabian, S. Y., Agrawal, P., Harris, M. D., Whitaker, R. T., Weiss, J. A., . . . Anderson, A. E. (2017). Quantitative comparison of cortical bone thickness using correspondence-based shape modeling in patients with cam femoroacetabular impingement. *Journal of orthopaedic research, 35*(8), 1743-1753.

Baldwin, M. A., Langenderfer, J. E., Rullkoetter, P. J., & Laz, P. J. (2010). Development of subject-specific and statistical shape models of the knee using an efficient segmentation and mesh-morphing approach. *Computer methods and programs in biomedicine, 97*(3), 232-240.

Bell, K. M., Arilla, F. V., Rahnemai-Azar, A. A., Fu, F. H., Musahl, V., & Debski, R. E. (2015). Novel technique for evaluation of knee function continuously through the range of flexion. *Journal of biomechanics, 48*(13), 3728-3731.

Beynnon, B., POPE, D. M., Wertheimer, C., Johnson, R., Fleming, B., Nichols, C., & Howe, J. (1992). The effect of functional knee-braces on strain on the anterior cruciate ligament in vivo. *The Journal of bone and joint surgery. American volume, 74*(9), 1298.

Biau, D. J., Katsahian, S., Kartus, J., Harilainen, A., Feller, J. A., Sajovic, M., . . . Nizard, R. (2009). Patellar tendon versus hamstring tendon autografts for reconstructing the anterior cruciate ligament: a meta-analysis based on individual patient data. *The American journal of sports medicine, 37*(12), 2470-2478.

Blanke, F., Paul, J., Haenle, M., Sailer, J., Pagenstert, G., von Wehren, L., . . . Majewski, M. (2017). Results of a new treatment concept for concomitant lesion of medial collateral ligament in patients with rupture of anterior cruciate ligament. *The journal of knee surgery, 30*(07), 652-658.

Boden, B. P., Dean, G. S., Feagin, J. A., & Garrett, W. E. (2000). Mechanisms of anterior cruciate ligament injury. In: SLACK Incorporated Thorofare, NJ.

Boden, B. P., Sheehan, F. T., Torg, J. S., & Hewett, T. E. (2010). Non-contact ACL injuries: mechanisms and risk factors. *The Journal of the American Academy of Orthopaedic Surgeons, 18*(9), 520.

Bradley, J. P., Klimkiewicz, J. J., Rytel, M. J., & Powell, J. W. (2002). Anterior cruciate ligament injuries in the National Football League: epidemiology and current treatment trends among team physicians. *Arthroscopy, 18*(5), 502-509. doi:10.1053/jars.2002.30649

Branch, T., Siebold, R., Freedberg, H., & Jacobs, C. (2011). Double-bundle ACL reconstruction demonstrated superior clinical stability to single-bundle ACL reconstruction: a matched-pairs analysis of instrumented tests of tibial anterior translation and internal rotation laxity. *Knee Surgery, Sports Traumatology, Arthroscopy, 19*(3), 432-440.

Brophy, R. H., Silvers, H. J., & Mandelbaum, B. R. (2010). Anterior cruciate ligament injuries: etiology and prevention. *Sports medicine and arthroscopy review, 18*(1), 2-11.

Butler, D. L., Guan, Y., Kay, M. D., Cummings, J. F., Feder, S. M., & Levy, M. S. (1992). Location-dependent variations in the material properties of the anterior cruciate ligament. *Journal of biomechanics, 25*(5), 511-518.

Butler, R. J., Dai, B., Garrett, W. E., & Queen, R. M. (2014). Changes in landing mechanics in patients following anterior cruciate ligament reconstruction when wearing an extension constraint knee brace. *Sports Health, 6*(3), 203-209.

Cates, J., Elhabian, S., & Whitaker, R. (2017). Shapeworks: particle-based shape correspondence and visualization software. In *Statistical Shape and Deformation Analysis* (pp. 257-298): Elsevier.

Cates, J., Fletcher, P. T., Styner, M., Shenton, M., & Whitaker, R. (2007). *Shape modeling and analysis with entropy-based particle systems.* Paper presented at the Biennial International Conference on Information Processing in Medical Imaging.

Cawley, P. W., France, E. P., & Paulos, L. E. (1989). Comparison of rehabilitative knee braces: A biomechanical investigation. *The American journal of sports medicine, 17*(2), 141-146.

Chan, E. F., Farnsworth, C. L., Koziol, J. A., Hosalkar, H. S., & Sah, R. L. (2013). Statistical shape modeling of proximal femoral shape deformities in Legg–Calvé–Perthes disease and slipped capital femoral epiphysis. *Osteoarthritis and cartilage, 21*(3), 443-449.

Checa, S., Taylor, M., & New, A. (2008). Influence of an interpositional spacer on the behaviour of the tibiofemoral joint: a finite element study. *Clinical biomechanics, 23*(8), 1044-1052.

Cherian, J. J., Kapadia, B. H., Banerjee, S., Jauregui, J. J., Issa, K., & Mont, M. A. (2014). Mechanical, anatomical, and kinematic axis in TKA: concepts and practical applications. *Current reviews in musculoskeletal medicine, 7*(2), 89-95.

Claes, S., Vereecke, E., Maes, M., Victor, J., Verdonk, P., & Bellemans, J. (2013). Anatomy of the anterolateral ligament of the knee. *Journal of anatomy, 223*(4), 321-328.

Clarke, K. S., & Buckley, W. E. (1980). Women's injuries in collegiate sports. A preliminary comparative overview of three seasons. *Am J Sports Med, 8*(3), 187-191. doi:10.1177/036354658000800308

Crockett, H. C., Gross, L. B., Wilk, K. E., Schwartz, M. L., Reed, J., O'Mara, J., . . . Andrews, J. R. (2002). Osseous adaptation and range of motion at the glenohumeral joint in professional baseball pitchers. *Am J Sports Med, 30*(1), 20-26. doi:10.1177/03635465020300011701

Dai, B., Herman, D., Liu, H., Garrett, W. E., & Yu, B. (2012). Prevention of ACL injury, part I: injury characteristics, risk factors, and loading mechanism. *Research in sports medicine, 20*(3-4), 180-197.

Dedinsky, R., Baker, L., Imbus, S., Bowman, M., & Murray, L. (2017). Exercises that facilitate optimal hamstring and quadriceps co-activation to help decrease ACL injury risk in healthy females: A systematic review of the literature. *International journal of sports physical therapy, 12*(1), 3.

Duthon, V. B., Magnussen, R. A., Servien, E., & Neyret, P. (2013). ACL reconstruction and extra-articular tenodesis. *Clinics in sports medicine, 32*(1), 141-153.

Ferretti, A., Conteduca, F., De Carli, A., Fontana, M., & Mariani, P. (1991). Osteoarthritis of the knee after ACL reconstruction. *International orthopaedics, 15*(4), 367-371.

Ferretti, A., Monaco, E., Fabbri, M., Maestri, B., & De Carli, A. (2017). Prevalence and classification of injuries of anterolateral complex in acute anterior cruciate ligament tears. *Arthroscopy: The Journal of Arthroscopic & Related Surgery, 33*(1), 147-154.

Ferretti, A., Monaco, E., & Vadala, A. (2014). Rotatory instability of the knee after ACL tear and reconstruction. *Journal of Orthopaedics and Traumatology, 15*(2), 75-79.

Focke, A., Steingrebe, H., Möhler, F., Ringhof, S., Sell, S., Potthast, W., & Stein, T. (2020). Effect of Different Knee Braces in ACL-Deficient Patients. *Frontiers in bioengineering and biotechnology, 8*, 964.

Friel, N. A., & Chu, C. R. (2013). The role of ACL injury in the development of posttraumatic knee osteoarthritis. *Clinics in sports medicine, 32*(1), 1-12.

Fujie, H., Livesay, G. A., Woo, S. L., Kashiwaguchi, S., & Blomstrom, G. (1995). The use of a universal force-moment sensor to determine in-situ forces in ligaments: a new methodology. *Journal of biomechanical engineering, 117*(1), 1-7.

Gabriel, M. T., Wong, E. K., Woo, S. L. Y., Yagi, M., & Debski, R. E. (2004). Distribution of in situ forces in the anterior cruciate ligament in response to rotatory loads. *Journal of orthopaedic research, 22*(1), 85-89.

Galbusera, F., Freutel, M., Dürselen, L., D'Aiuto, M., Croce, D., Villa, T., . . . Innocenti, B. (2014). Material models and properties in the finite element analysis of knee ligaments: a literature review. *Frontiers in bioengineering and biotechnology, 2*, 54.

Geeslin, A. G., Moatshe, G., Chahla, J., Kruckeberg, B. M., Muckenhirn, K. J., Dornan, G. J., . . . Godin, J. A. (2018). Anterolateral knee extra-articular stabilizers: a robotic study comparing anterolateral ligament reconstruction and modified Lemaire lateral extra-articular tenodesis. *The American journal of sports medicine, 46*(3), 607-616.

Gentile, J. M., O'Brien, M. C., Conrad, B., Horodyski, M., Bruner, M. L., & Farmer, K. W. (2021). A biomechanical comparison shows no difference between two knee braces used for medial collateral ligament injuries. *Arthroscopy, Sports Medicine, and Rehabilitation, 3*(3), e901-e907.

Giesche, F., Niederer, D., Banzer, W., & Vogt, L. (2020). Evidence for the effects of prehabilitation before ACL-reconstruction on return to sport-related and self-reported knee function: A systematic review. *Plos one, 15*(10), e0240192.

Giffin, J. R., Vogrin, T. M., Zantop, T., Woo, S. L., & Harner, C. D. (2004). Effects of increasing tibial slope on the biomechanics of the knee. *The American journal of sports medicine, 32*(2), 376-382.

Golan, E. J., Tisherman, R., Byrne, K., Diermeier, T., Vaswani, R., & Musahl, V. (2019). Anterior cruciate ligament injury and the anterolateral complex of the knee—importance in rotatory knee instability? *Current reviews in musculoskeletal medicine, 12*(4), 472-478.

Görmeli, C. A., Görmeli, G., Öztürk, B. Y., Özdemir, Z., Kahraman, A. S., Yıldırım, O., & Gözükarab, H. (2015). The effect of the intercondylar notch width index on anterior cruciate ligament injuries: a study on groups with unilateral and bilateral ACL injury. *Acta Orthop Belg, 81*(2), 240-244.

Gower, J. C. (1975). Generalized procrustes analysis. *Psychometrika, 40*(1), 33-51.

Griffin, L. Y., Albohm, M. J., Arendt, E. A., Bahr, R., Beynnon, B. D., DeMaio, M., . . . Hannafin, J. A. (2006). Understanding and preventing noncontact anterior cruciate ligament injuries: a review of the Hunt Valley II meeting, January 2005. *The American journal of sports medicine, 34*(9), 1512-1532.

Griffin, L. Y., Albohm, M. J., Arendt, E. A., Bahr, R., Beynnon, B. D., Demaio, M., . . . Yu, B. (2006). Understanding and preventing noncontact anterior cruciate ligament injuries: a review of the Hunt Valley II meeting, January 2005. *Am J Sports Med, 34*(9), 1512-1532. doi:10.1177/0363546506286866

Grood, E. S., & Suntay, W. J. (1983). A joint coordinate system for the clinical description of three-dimensional motions: application to the knee. *Journal of biomechanical engineering, 105*(2), 136-144.

Guenther, D., Irarrázaval, S., Bell, K. M., Rahnemai-Azar, A. A., Fu, F. H., Debski, R. E., & Musahl, V. (2017). The role of extra-articular tenodesis in combined ACL and anterolateral capsular injury. *JBJS, 99*(19), 1654-1660.

Guenther, D., Pfeiffer, T., Petersen, W., Imhoff, A., Herbort, M., Achtnich, A., . . . Akoto, R. (2021). Treatment of Combined Injuries to the ACL and the MCL Complex: A Consensus Statement of the Ligament Injury Committee of the German Knee Society (DKG). *Orthopaedic Journal of Sports Medicine, 9*(11), 23259671211050929.

Guenther, D., Rahnemai-Azar, A. A., Bell, K. M., Irarrazaval, S., Fu, F. H., Musahl, V., & Debski, R. E. (2017). The anterolateral capsule of the knee behaves like a sheet of fibrous tissue. *The American journal of sports medicine, 45*(4), 849-855.

Hagino, T., Ochiai, S., Senga, S., Yamashita, T., Wako, M., Ando, T., & Haro, H. (2015). Meniscal tears associated with anterior cruciate ligament injury. *Archives of orthopaedic and trauma surgery, 135*(12), 1701-1706.

Hanzlíková, I., Richards, J., Hébert-Losier, K., & Smékal, D. (2019). The effect of proprioceptive knee bracing on knee stability after anterior cruciate ligament reconstruction. *Gait & posture, 67*, 242-247.

Hewett, T. E., Torg, J. S., & Boden, B. P. (2009). Video analysis of trunk and knee motion during non-contact anterior cruciate ligament injury in female athletes: lateral trunk and knee abduction motion are combined components of the injury mechanism. *British journal of sports medicine, 43*(6), 417-422.

Hewison, C. E., Tran, M. N., Kaniki, N., Remtulla, A., Bryant, D., & Getgood, A. M. (2015). Lateral extra-articular tenodesis reduces rotational laxity when combined with anterior cruciate ligament reconstruction: a systematic review of the literature. *Arthroscopy: The Journal of Arthroscopic & Related Surgery, 31*(10), 2022-2034.

Hinterwimmer, S., Graichen, H., Baumgart, R., & Plitz, W. (2004). Influence of a mono-centric knee brace on the tension of the collateral ligaments in knee joints after sectioning of the anterior cruciate ligament—an in vitro study. *Clinical biomechanics, 19*(7), 719-725.

Hoshino, Y., Wang, J. H., Lorenz, S., Fu, F. H., & Tashman, S. (2012a). The effect of distal femur bony morphology on in vivo knee translational and rotational kinematics. *Knee Surgery, Sports Traumatology, Arthroscopy, 20*(7), 1331-1338.

Hoshino, Y., Wang, J. H., Lorenz, S., Fu, F. H., & Tashman, S. (2012b). Gender difference of the femoral kinematics axis location and its relation to anterior cruciate ligament injury: a 3D-CT study. *Knee Surgery, Sports Traumatology, Arthroscopy, 20*(7), 1282-1288.

Ihara, H., & Kawano, T. (2017). Influence of age on healing capacity of acute tears of the anterior cruciate ligament based on magnetic resonance imaging assessment. *Journal of computer assisted tomography, 41*(2), 206.

Inderhaug, E., Stephen, J. M., El-Daou, H., Williams, A., & Amis, A. A. (2017). The effects of anterolateral tenodesis on tibiofemoral contact pressures and kinematics. *The American journal of sports medicine, 45*(13), 3081-3088.

Ingham, S. J. M., de Carvalho, R. T., Abdalla, R. J., Fu, F. H., & Lovejoy, C. O. (2017). Bony morphology: comparative anatomy and its importance for the anterior cruciate ligament. *Operative Techniques in Orthopaedics, 27*(1), 2-7.

Ireland, M. L. (2002). The female ACL: why is it more prone to injury? *Orthopedic Clinics, 33*(4), 637-651.

Jung, H.-J., Fisher, M. B., & Woo, S. L. (2009). Role of biomechanics in the understanding of normal, injured, and healing ligaments and tendons. *BMC Sports Science, Medicine and Rehabilitation*, *1*(1), 1-17.

Kaeding, C. C., Pedroza, A. D., Reinke, E. K., Huston, L. J., Consortium, M., & Spindler, K. P. (2015). Risk factors and predictors of subsequent ACL injury in either knee after ACL reconstruction: prospective analysis of 2488 primary ACL reconstructions from the MOON cohort. *The American journal of sports medicine, 43*(7), 1583-1590.

Kamath, G. V., Murphy, T., Creighton, R. A., Viradia, N., Taft, T. N., & Spang, J. T. (2014). Anterior cruciate ligament injury, return to play, and reinjury in the elite collegiate athlete: analysis of an NCAA Division I cohort. *The American journal of sports medicine, 42*(7), 1638-1643.

Kanamori, A., Woo, S. L., Ma, C. B., Zeminski, J., Rudy, T. W., Li, G., & Livesay, G. A. (2000). The forces in the anterior cruciate ligament and knee kinematics during a simulated pivot shift test: a human cadaveric study using robotic technology. *Arthroscopy: The Journal of Arthroscopic & Related Surgery, 16*(6), 633-639.

Kannus, P., & Järvinen, M. (1987). Conservatively treated tears of the anterior cruciate ligament. Long-term results. *JBJS, 69*(7), 1007-1012.

Katakura, M., Koga, H., Nakamura, T., Araki, D., Nagai, K., Nishida, K., . . . Muneta, T. (2019). Biomechanical effects of additional anterolateral structure reconstruction with different femoral attachment sites on anterior cruciate ligament reconstruction. *The American journal of sports medicine, 47*(14), 3373-3380.

Kennedy, M. I., Claes, S., Fuso, F. A. F., Williams, B. T., Goldsmith, M. T., Turnbull, T. L., . . . LaPrade, R. F. (2015). The anterolateral ligament: an anatomic, radiographic, and biomechanical analysis. *The American journal of sports medicine, 43*(7), 1606-1615.

Kernkamp, W. A., van de Velde, S. K., Bakker, E. W., & van Arkel, E. R. (2015). Anterolateral extra-articular soft tissue reconstruction in anterolateral rotatory instability of the knee. *Arthroscopy techniques, 4*(6), e863-e867.

Kessler, M., Behrend, H., Henz, S., Stutz, G., Rukavina, A., & Kuster, M. (2008). Function, osteoarthritis and activity after ACL-rupture: 11 years follow-up results of conservative versus reconstructive treatment. *Knee Surgery, Sports Traumatology, Arthroscopy, 16*(5), 442-448.

Kobayashi, H., Kanamura, T., Koshida, S., Miyashita, K., Okado, T., Shimizu, T., & Yokoe, K. (2010). Mechanisms of the anterior cruciate ligament injury in sports activities: a twenty-year clinical research of 1,700 athletes. *Journal of sports science & medicine, 9*(4), 669.

Kocher, M. S., Sterett, W. I., Zurakowski, D., & Steadman, J. R. (2003). Effect of Functional Bracing on Subsequent Knee Injury in ACL-Deficient Professional Skiers. *The journal of knee surgery, 16*, 87-92.

Kohn, L., Rembeck, E., & Rauch, A. (2020). Anterior cruciate ligament injury in adults: Diagnostics and treatment. *Der Orthopade, 49*(11), 1013-1028.

Krosshaug, T., Nakamae, A., Boden, B. P., Engebretsen, L., Smith, G., Slauterbeck, J. R., . . . Bahr, R. (2007). Mechanisms of anterior cruciate ligament injury in basketball: video analysis of 39 cases. *The American journal of sports medicine, 35*(3), 359-367.

Kwak, Y. H., Nam, J.-H., Koh, Y.-G., Park, B.-K., Hong, K.-B., & Kang, K.-T. (2020). Femoral trochlear morphology is associated with anterior cruciate ligament injury in skeletally immature patients. *Knee Surgery, Sports Traumatology, Arthroscopy, 28*(12), 3969-3977.

Lansdown, D., & Ma, C. B. (2018). The Influence of Tibial and Femoral Bone Morphology on Knee Kinematics in the ACL Injured Knee. *Clinics in sports medicine, 37*(1), 127.

Lansdown, D. A., Pedoia, V., Zaid, M., Amano, K., Souza, R. B., Li, X., & Ma, C. B. (2017). Variations in knee kinematics after ACL injury and after reconstruction are correlated with bone shape differences. *Clinical Orthopaedics and Related Research®, 475*(10), 2427-2435.

Leblanc, M.-C., Kowalczuk, M., Andruszkiewicz, N., Simunovic, N., Farrokhyar, F., Turnbull, T. L., . . . Ayeni, O. R. (2015). Diagnostic accuracy of physical examination for anterior knee instability: a systematic review. *Knee Surgery, Sports Traumatology, Arthroscopy, 23*(10), 2805-2813.

Limbert, G., Middleton, J., & Taylor, M. (2004). Finite element analysis of the human ACL subjected to passive anterior tibial loads. *Computer methods in biomechanics and biomedical engineering, 7*(1), 1-8.

Logerstedt, D., Lynch, A., Axe, M. J., & Snyder-Mackler, L. (2013). Symmetry restoration and functional recovery before and after anterior cruciate ligament reconstruction. *Knee Surgery, Sports Traumatology, Arthroscopy, 21*(4), 859-868.

Luc, B., Gribble, P. A., & Pietrosimone, B. G. (2014). Osteoarthritis prevalence following anterior cruciate ligament reconstruction: a systematic review and numbers-needed-to-treat analysis. *J Athl Train, 49*(6), 806-819. doi:10.4085/1062-6050-49.3.35

Lucidi, G. A., Agostinone, P., Grassi, A., Di Paolo, S., Dal Fabbro, G., Bonanzinga, T., & Zaffagnini, S. (2022). Do Clinical Outcomes and Failure Rates Differ in Patients With Combined ACL and Grade 2 MCL Tears Versus Isolated ACL Tears?: A Prospective Study With 14-Year Follow-up. *Orthopaedic Journal of Sports Medicine, 10*(1), 23259671211047860.

Marois, B., Tan, X. W., Pauyo, T., Dodin, P., Ballaz, L., & Nault, M.-L. (2021). Can a Knee Brace Prevent ACL Reinjury: A Systematic Review. *International Journal of Environmental Research and Public Health, 18*(14), 7611.

Marom, N., Jahandar, H., Fraychineaud, T. J., Zayyad, Z. A., Ouanezar, H., Hurwit, D., . . . Imhauser, C. W. (2021). Lateral Extra-articular Tenodesis Alters Lateral Compartment Contact Mechanics under Simulated Pivoting Maneuvers: An In Vitro Study. *The American journal of sports medicine, 49*(11), 2898-2907.

Marshall, J., Wang, J., Furman, W., Girgis, F., & Warren, R. (1975). The anterior drawer sign: what is it? *The Journal of sports medicine, 3*(4), 152-158.

Marshall, N. E., Keller, R. A., Dines, J., Bush-Joseph, C., & Limpisvasti, O. (2019). Current practice: postoperative and return to play trends after ACL reconstruction by fellowship-trained sports surgeons. *Musculoskelet Surg, 103*(1), 55-61. doi:10.1007/s12306-018-0574-4

Mather, R. C., 3rd, Koenig, L., Kocher, M. S., Dall, T. M., Gallo, P., Scott, D. J., . . . Spindler, K. P. (2013). Societal and economic impact of anterior cruciate ligament tears. *J Bone Joint Surg Am, 95*(19), 1751-1759. doi:10.2106/jbjs.L.01705

Matsumoto, H. (1990). Mechanism of the pivot shift. *The Journal of bone and joint surgery. British volume, 72*(5), 816-821.

McLean, S. G., Huang, X., & Van Den Bogert, A. J. (2005). Association between lower extremity posture at contact and peak knee valgus moment during sidestepping: implications for ACL injury. *Clinical biomechanics, 20*(8), 863-870.

Medina McKeon, J. M., & Hertel, J. (2009). Sex differences and representative values for 6 lower extremity alignment measures. *Journal of athletic training*, *44*(3), 249-255.

Mohtadi, N. G., Webster-Bogaert, S., & Fowler, P. J. (1991). Limitation of motion following anterior cruciate ligament reconstruction: a case-control study. *The American journal of sports medicine*, *19*(6), 620-625.

Moon, J., Kim, H., Lee, J., & Panday, S. B. (2018). Effect of wearing a knee brace or sleeve on the knee joint and anterior cruciate ligament force during drop jumps: A clinical intervention study. *The Knee, 25*(6), 1009-1015.

Muneta, T., Takakuda, K., & Yamamoto, H. (1997). Intercondylar notch width and its relation to the configuration and cross-sectional area of the anterior cruciate ligament: a cadaveric knee study. *The American journal of sports medicine, 25*(1), 69-72.

Murray, M. M., Martin, S., Martin, T., & Spector, M. (2000). Histological changes in the human anterior cruciate ligament after rupture. *JBJS, 82*(10), 1387.

Musahl, V., Ayeni, O. R., Citak, M., Irrgang, J. J., Pearle, A. D., & Wickiewicz, T. L. (2010). The influence of bony morphology on the magnitude of the pivot shift. *Knee Surgery, Sports Traumatology, Arthroscopy, 18*(9), 1232-1238.

Musahl, V., Getgood, A., Neyret, P., Claes, S., Burnham, J. M., Batailler, C., . . . Zaffagnini, S. (2017). Contributions of the anterolateral complex and the anterolateral ligament to rotatory knee stability in the setting of ACL Injury: a roundtable discussion. *Knee Surgery, Sports Traumatology, Arthroscopy, 25*(4), 997-1008.

Myer, G. D., Ford, K. R., & Hewett, T. (2006). Preventing ACL injuries in women. *JOURNAL OF MUSCULOSKELETAL MEDICINE, 23*(1), 12.

Myrer, J. W., Schulthies, S. S., & Fellingham, G. W. (1996). Relative and absolute reliability of the KT-2000 arthrometer for uninjured knees: testing at 67, 89, 134, and 178 N and manual maximum forces. *The American journal of sports medicine, 24*(1), 104-108.

Naendrup, J.-H., Pfeiffer, T. R., Chan, C., Nagai, K., Novaretti, J. V., Sheean, A. J., . . . Musahl, V. (2019). Effect of meniscal ramp lesion repair on knee kinematics, bony contact forces, and in situ forces in the anterior cruciate ligament. *The American journal of sports medicine, 47*(13), 3195-3202.

Negrin, R., Uribe-Echevarria, B., & Reyes, N. (2017). Do knee braces prevent ski knee injuries? *Asian journal of sports medicine, 8*(4).

Nessler, T., Denney, L., & Sampley, J. (2017). ACL injury prevention: what does research tell us? *Current reviews in musculoskeletal medicine, 10*(3), 281-288.

Nicholls, M., Ingvarsson, T., & Briem, K. (2021). Younger age increases the risk of sustaining multiple concomitant injuries with an ACL rupture. *Knee Surgery, Sports Traumatology, Arthroscopy*, 1-8.

Niki, Y., Hakozaki, A., Iwamoto, W., Kanagawa, H., Matsumoto, H., Toyama, Y., & Suda, Y. (2012). Factors affecting anterior knee pain following anatomic double-bundle anterior cruciate ligament reconstruction. *Knee Surgery, Sports Traumatology, Arthroscopy, 20*(8), 1543-1549.

Nitri, M., Rasmussen, M. T., Williams, B. T., Moulton, S. G., Cruz, R. S., Dornan, G. J., . . . LaPrade, R. F. (2016). An in vitro robotic assessment of the anterolateral ligament, part 2: anterolateral ligament reconstruction combined with anterior cruciate ligament reconstruction. *The American journal of sports medicine, 44*(3), 593-601.

Novaretti, J. V., Arner, J. W., Chan, C. K., Polamalu, S., Harner, C. D., Debski, R. E., & Lesniak, B. P. (2020). Does lateral extra-articular tenodesis of the knee affect anterior cruciate ligament graft in situ forces and tibiofemoral contact pressures? *Arthroscopy: The Journal of Arthroscopic & Related Surgery, 36*(5), 1365-1373.

Novaretti, J. V., Herbst, E., Chan, C. K., Debski, R. E., & Musahl, V. (2021). Small lateral meniscus tears propagate over time in ACL intact and deficient knees. *Knee Surgery, Sports Traumatology, Arthroscopy, 29*(9), 3068-3076.

Novaretti, J. V., Lian, J., Patel, N. K., Chan, C. K., Cohen, M., Musahl, V., & Debski, R. E. (2020). Partial lateral meniscectomy affects knee stability even in anterior cruciate ligament-intact knees. *JBJS, 102*(7), 567-573.

Novaretti, J. V., Lian, J., Sheean, A. J., Chan, C. K., Wang, J. H., Cohen, M., . . . Musahl, V. (2019). Lateral meniscal allograft transplantation with bone block and suture-only techniques partially restores knee kinematics and forces. *The American journal of sports medicine, 47*(10), 2427-2436.

O'Connor, D. P., Laughlin, M. S., & Woods, G. W. (2005). Factors related to additional knee injuries after anterior cruciate ligament injury. *Arthroscopy: The Journal of Arthroscopic & Related Surgery, 21*(4), 431-438.

Patel, N. K., Chan, C., Murphy, C. I., Debski, R. E., Musahl, V., & Hogan, M. V. (2020). Hybrid fixation restores tibiofibular kinematics for early weightbearing after syndesmotic injury. *Orthopaedic Journal of Sports Medicine, 8*(9), 2325967120946744.

Paterno, M. V. (2017). Non-operative care of the patient with an ACL-deficient knee. *Current reviews in musculoskeletal medicine, 10*(3), 322-327.

Paterno, M. V., Rauh, M. J., Schmitt, L. C., Ford, K. R., & Hewett, T. E. (2012). Incidence of contralateral and ipsilateral anterior cruciate ligament (ACL) injury after primary ACL reconstruction and return to sport. *Clinical journal of sport medicine: official journal of the Canadian Academy of Sport Medicine, 22*(2), 116.

Pedoia, V., Lansdown, D. A., Zaid, M., McCulloch, C. E., Souza, R., Ma, C. B., & Li, X. (2015). Three-dimensional MRI-based statistical shape model and application to a cohort of knees with acute ACL injury. *Osteoarthritis and cartilage, 23*(10), 1695-1703.

Perrone, G. S., Webster, K. E., Imbriaco, C., Portilla, G. M., Vairagade, A., Murray, M. M., & Kiapour, A. M. (2019). Risk of secondary ACL injury in adolescents prescribed functional bracing after ACL reconstruction. *Orthopaedic Journal of Sports Medicine, 7*(11), 2325967119879880.

Petersen, W., & Zantop, T. (2007). Anatomy of the anterior cruciate ligament with regard to its two bundles. *Clinical Orthopaedics and Related Research (1976-2007), 454,* 35-47.

Pfeiffer, T. R., Herbst, E., Kanakamedala, A. C., Naendrup, J.-H., Debski, R. E., & Musahl, V. (2018). The use of fluoroscopy leads to improved identification of the femoral lateral collateral ligament origin site when compared with traditional tactile techniques. *Arthroscopy: The Journal of Arthroscopic & Related Surgery, 34*(8), 2487-2493. e2481.

Pfeiffer, T. R., Naendrup, J. H., Chan, C., Nagai, K., Novaretti, J. V., Debski, R., & Musahl, V. (2018). Effect of meniscal ramp repair on knee kinematics, ACL in situ force and bony contact forces-a biomechanical study. *Orthopaedic Journal of Sports Medicine, 6*(7_suppl4), 2325967118S2325900157.

Phisitkul, P., James, S. L., Wolf, B. R., & Amendola, A. (2006). MCL injuries of the knee: current concepts review. *The Iowa orthopaedic journal, 26*, 77.

Pietrosimone, B. G., Grindstaff, T. L., Linens, S. W., Uczekaj, E., & Hertel, J. (2008). A systematic review of prophylactic braces in the prevention of knee ligament injuries in collegiate football players. *J Athl Train, 43*(4), 409-415. doi:10.4085/1062-6050-43.4.409

Polamalu, S. K., Musahl, V., & Debski, R. E. (2020). Tibiofemoral bony morphology features associated with ACL injury and sex utilizing three-dimensional statistical shape modeling. *J Orthop Res*. doi:10.1002/jor.24952

Polamalu, S. K., Novaretti, J., Musahl, V., & Debski, R. E. (2021). Tibiofemoral bony morphology impacts the knee kinematics after anterolateral capsule injury and lateral extraarticular tenodesis differently than intact state. *Journal of biomechanics*, 110857.

Racine, J., & Aaron, R. K. (2014). Post-traumatic osteoarthritis after ACL injury. *RI Med J, 97*(11), 25-28.

Rajamani, K. T., Styner, M. A., Talib, H., Zheng, G., Nolte, L. P., & Ballester, M. A. G. (2007). Statistical deformable bone models for robust 3D surface extrapolation from sparse data. *Medical image analysis, 11*(2), 99-109.

Rao, C., Fitzpatrick, C. K., Rullkoetter, P. J., Maletsky, L. P., Kim, R. H., & Laz, P. J. (2013). A statistical finite element model of the knee accounting for shape and alignment variability. *Medical engineering & physics, 35*(10), 1450-1456.

Rasmussen, M. T., Nitri, M., Williams, B. T., Moulton, S. G., Cruz, R. S., Dornan, G. J., . . . LaPrade, R. F. (2016). An in vitro robotic assessment of the anterolateral ligament, part 1: secondary role of the anterolateral ligament in the setting of an anterior cruciate ligament injury. *The American journal of sports medicine, 44*(3), 585-592.

Reagan, K. M., Meister, K., Horodyski, M. B., Werner, D. W., Carruthers, C., & Wilk, K. (2002). Humeral retroversion and its relationship to glenohumeral rotation in the shoulder of college baseball players. *Am J Sports Med, 30*(3), 354-360. doi:10.1177/03635465020300030901

Renstrom, P., Ljungqvist, A., Arendt, E., Beynnon, B., Fukubayashi, T., Garrett, W., . . . Krosshaug, T. (2008). Non-contact ACL injuries in female athletes: an International Olympic Committee current concepts statement. *British journal of sports medicine, 42*(6), 394-412.

Rishiraj, N., Taunton, J. E., Lloyd-Smith, R., Woollard, R., Regan, W., & Clement, D. (2009). The potential role of prophylactic/functional knee bracing in preventing knee ligament injury. *Sports Medicine, 39*(11), 937-960.

Schon, J. M., Moatshe, G., Brady, A. W., Serra Cruz, R., Chahla, J., Dornan, G. J., . . . LaPrade, R. F. (2016). Anatomic anterolateral ligament reconstruction of the knee leads to overconstraint at any fixation angle. *The American journal of sports medicine, 44*(10), 2546-2556.

Schumann, S., Tannast, M., Nolte, L.-P., & Zheng, G. (2010). Validation of statistical shape model based reconstruction of the proximal femur—a morphology study. *Medical engineering & physics, 32*(6), 638-644.

Selmi, T. A. S., Fithian, D., & Neyret, P. (2006). The evolution of osteoarthritis in 103 patients with ACL reconstruction at 17 years follow-up. *The Knee, 13*(5), 353-358.

Shelbourne, K. D., Davis, T. J., & Klootwyk, T. E. (1998). The relationship between intercondylar notch width of the femur and the incidence of anterior cruciate ligament tears. *The American journal of sports medicine, 26*(3), 402-408.

Shelbourne, K. D., & Kerr, B. (2001). The relationship of femoral intercondylar notch width to height, weight, and sex in patients with intact anterior cruciate ligaments. *The American journal of knee surgery, 14*(2), 92-96.

Shelbourne, K. D., & Porter, D. A. (1992). Anterior cruciate ligament-medial collateral ligament injury: nonoperative management of medial collateral ligament tears with anterior cruciate ligament reconstruction: a preliminary report. *The American journal of sports medicine, 20*(3), 283-286.

Silvers, H. J., & Mandelbaum, B. R. (2011). ACL injury prevention in the athlete. *Sport-Orthopädie-Sport-Traumatologie-Sports Orthopaedics and Traumatology, 27*(1), 18-26.

Simon, R., Everhart, J., Nagaraja, H., & Chaudhari, A. (2010). A case-control study of anterior cruciate ligament volume, tibial plateau slopes and intercondylar notch dimensions in ACL-injured knees. *Journal of biomechanics, 43*(9), 1702-1707.

Singer, J. C., & Lamontagne, M. (2008). The effect of functional knee brace design and hinge misalignment on lower limb joint mechanics. *Clinical biomechanics, 23*(1), 52-59.

Skutek, M., Elsner, H.-A., Slateva, K., Mayr, H.-O., Weig, T.-G., van Griensven, M., . . . Bosch, U. (2004). Screening for arthrofibrosis after anterior cruciate ligament reconstruction: analysis of association with human leukocyte antigen. *Arthroscopy: The Journal of Arthroscopic & Related Surgery, 20*(5), 469-473.

Slette, E. L., Mikula, J. D., Schon, J. M., Marchetti, D. C., Kheir, M. M., Turnbull, T. L., & LaPrade, R. F. (2016). Biomechanical results of lateral extra-articular tenodesis procedures of the knee: a systematic review. *Arthroscopy: The Journal of Arthroscopic & Related Surgery, 32*(12), 2592-2611.

Smith, S. D., LaPrade, R. F., Jansson, K. S., Årøen, A., & Wijdicks, C. A. (2014). Functional bracing of ACL injuries: current state and future directions. *Knee Surgery, Sports Traumatology, Arthroscopy, 22*(5), 1131-1141.

Song, Y., Debski, R. E., Musahl, V., Thomas, M., & Woo, S. L.-Y. (2004). A three-dimensional finite element model of the human anterior cruciate ligament: a computational analysis with experimental validation. *Journal of biomechanics, 37*(3), 383-390.

Sonnery-Cottet, B., Archbold, P., Zayni, R., Bortolletto, J., Thaunat, M., Prost, T., . . . Chambat, P. (2011). Prevalence of septic arthritis after anterior cruciate ligament reconstruction among professional athletes. *The American journal of sports medicine, 39*(11), 2371-2376.

Sousa, P. L., Krych, A. J., Cates, R. A., Levy, B. A., Stuart, M. J., & Dahm, D. L. (2017). Return to sport: Does excellent 6-month strength and function following ACL reconstruction predict midterm outcomes? *Knee Surg Sports Traumatol Arthrosc, 25*(5), 1356-1363. doi:10.1007/s00167-015-3697-2

Starman, J. S., VanBeek, C., Armfield, D. R., Sahasrabudhe, A., Baker, C. L., Irrgang, J. J., & Fu, F. H. (2007). Assessment of normal ACL double bundle anatomy in standard viewing planes by magnetic resonance imaging. *Knee Surgery, Sports Traumatology, Arthroscopy, 15*(5), 493-499.

Sutton, K. M., & Bullock, J. M. (2013). Anterior cruciate ligament rupture: differences between males and females. *J Am Acad Orthop Surg, 21*(1), 41-50. doi:10.5435/jaaos-21-01-41

Takeda, Y., Xerogeanes, J. W., Livesay, G. A., Fu, F. H., & Woo, S. L. (1994). Biomechanical function of the human anterior cruciate ligament. *Arthroscopy: The Journal of Arthroscopic & Related Surgery, 10*(2), 140-147.

Tanaka, M., Vyas, D., Moloney, G., Bedi, A., Pearle, A., & Musahl, V. (2012). What does it take to have a high-grade pivot shift? *Knee Surgery, Sports Traumatology, Arthroscopy, 20*(4), 737-742.

Terry, G. C., Norwood, L. A., Hughston, J. C., & Caldwell, K. M. (1993). How iliotibial tract injuries of the knee combine with acute anterior cruciate ligament tears to influence abnormal anterior tibial displacement. *The American journal of sports medicine, 21*(1), 55-60.

Todd, M. S., Lalliss, S., Garcia, E. S., DeBerardino, T. M., & Cameron, K. L. (2010). The relationship between posterior tibial slope and anterior cruciate ligament injuries. *The American journal of sports medicine, 38*(1), 63-67.

Uhorchak, J. M., Scoville, C. R., Williams, G. N., Arciero, R. A., Pierre, P. S., & Taylor, D. C. (2003). Risk factors associated with noncontact injury of the anterior cruciate ligament. *The American journal of sports medicine, 31*(6), 831-842.

Uhorchak, J. M., Scoville, C. R., Williams, G. N., Arciero, R. A., St Pierre, P., & Taylor, D. C. (2003). Risk factors associated with noncontact injury of the anterior cruciate ligament: a prospective four-year evaluation of 859 West Point cadets. *Am J Sports Med, 31*(6), 831-842. doi:10.1177/03635465030310061801

van der List, J. P., Hagemans, F. J., Hofstee, D. J., & Jonkers, F. J. (2020). The role of patient characteristics in the success of nonoperative treatment of anterior cruciate ligament injuries. *The American journal of sports medicine, 48*(7), 1657-1664.

van Diek, F. M., Wolf, M. R., Murawski, C. D., van Eck, C. F., & Fu, F. H. (2014). Knee morphology and risk factors for developing an anterior cruciate ligament rupture: an MRI comparison between ACL-ruptured and non-injured knees. *Knee Surgery, Sports Traumatology, Arthroscopy, 22*(5), 987-994.

van Eck, C., Azar, A., Yaseen, Z., Irrgang, J., Fu, F., & Musahl, V. (2016). Increased lateral tibial plateau slope predisposes male college football players to ACL injury. *Arthroscopy, 32*(6), e7-e8.

Varadarajan, K. M., Gill, T. J., Freiberg, A. A., Rubash, H. E., & Li, G. (2009). Gender differences in trochlear groove orientation and rotational kinematics of human knees. *Journal of orthopaedic research, 27*(7), 871-878.

Webster, K. E., & Feller, J. A. (2016). Exploring the high reinjury rate in younger patients undergoing anterior cruciate ligament reconstruction. *The American journal of sports medicine, 44*(11), 2827-2832.

Whitney, D. C., Sturnick, D. R., Vacek, P. M., DeSarno, M. J., Gardner-Morse, M., Tourville, T. W., . . . Shultz, S. J. (2014). Relationship between the risk of suffering a first-time noncontact ACL injury and geometry of the femoral notch and ACL: a prospective cohort study with a nested case-control analysis. *The American journal of sports medicine, 42*(8), 1796-1805.

Whitney, D. C., Sturnick, D. R., Vacek, P. M., DeSarno, M. J., Gardner-Morse, M., Tourville, T. W., . . . Beynnon, B. D. (2014). Relationship Between the Risk of Suffering a First-Time Noncontact ACL Injury and Geometry of the Femoral Notch and ACL: A Prospective Cohort Study With a Nested Case-Control Analysis. *Am J Sports Med, 42*(8), 1796-1805. doi:10.1177/0363546514534182

Wilson, D. R., Feikes, J., Zavatsky, A., & O'connor, J. (2000). The components of passive knee movement are coupled to flexion angle. *Journal of biomechanics, 33*(4), 465-473.

Woo, S. L., Debski, R. E., Wong, E. K., Yagi, M., & Tarinelli, D. (1999). Use of robotic technology for diathrodial joint research. *Journal of Science and Medicine in Sport, 2*(4), 283-297.

Yang, X.-g., Feng, J.-t., He, X., Wang, F., & Hu, Y.-c. (2019). The effect of knee bracing on the knee function and stability following anterior cruciate ligament reconstruction: a systematic review and meta-analysis of randomized controlled trials. *Orthopaedics & Traumatology: Surgery & Research, 105*(6), 1107-1114.

Yu, B., Herman, D., Preston, J., Lu, W., Kirkendall, D. T., & Garrett, W. E. (2004). Immediate effects of a knee brace with a constraint to knee extension on knee kinematics and ground reaction forces in a stop-jump task. *The American journal of sports medicine, 32*(5), 1136-1143.

Yu, C.-H., Walker, P. S., & Dewar, M. E. (2001). The effect of design variables of condylar total knees on the joint forces in step climbing based on a computer model. *Journal of biomechanics, 34*(8), 1011-1021.

Zantop, T., Herbort, M., Raschke, M. J., Fu, F. H., & Petersen, W. (2007). The role of the anteromedial and posterolateral bundles of the anterior cruciate ligament in anterior tibial translation and internal rotation. *The American journal of sports medicine, 35*(2), 223-227.

Zantop, T., Petersen, W., & Fu, F. H. (2005). Anatomy of the anterior cruciate ligament. *Operative Techniques in Orthopaedics, 15*(1), 20-28.

Zeng, C., Yang, T., Wu, S., Gao, S.-g., Li, H., Deng, Z.-h., . . . Lei, G.-h. (2016). Is posterior tibial slope associated with noncontact anterior cruciate ligament injury? *Knee Surgery, Sports Traumatology, Arthroscopy, 24*(3), 830-837.

Zhong, Q., Pedoia, V., Tanaka, M., Neumann, J., Link, T. M., Ma, B., . . . Li, X. (2019). 3D bone-shape changes and their correlations with cartilage T1ρ and T2 relaxation times and patient-reported outcomes over 3-years after ACL reconstruction. *Osteoarthritis and cartilage, 27*(6), 915-921.